Metal nanoparticles as catalysts for oxidation reactions

Dissertation submitted to the University of Madeira in order to obtain the degree of Master in Nanochemistry and Nanomaterials

By Ying Yu

Work developed under the supervision of
Prof. Lu ísa Margarida D.R.S. Martins and co-supervised by
Prof. Jo ão Manuel Cunha Rodrigues

Faculdade de Ci ências Exatas e de Engenharia,
Centro de Qu ímica da Madeira,
Campus Universit ário da Penteada, 9000-390 Funchal, Portugal

November 2016

Declaration

I hereby declare that this thesis is the result of my own work, is original and was written by me. I also declare that its reproduction and publication by Madeira University will not break any third party rights and that I have not previously (in its entirety or in part) submitted it elsewhere for obtaining any qualification or degree. Furthermore, I certify that all the sources of information used in the thesis were properly cited.

Lisbon, November 2016

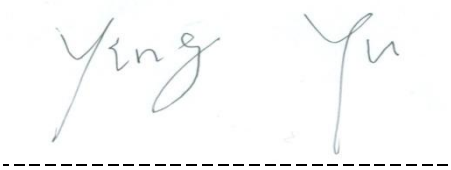

Conference contributions

May 2016

Poster Presentation in *10º Encontro Nacional de Catálise e Materiais Porosos (X ENCMP).*

Ying Yu, Ana P.C. Ribeiro, Sónia A.C. Carabineiro, Armando J.L. Pombeiro, João Rodrigues, Miguel Avalos-Borja, Josephus G. Buijnsters, José L. Figueiredo, Luísa M.D.R.S. Martins, *Au NPs@ carbon materials as catalysts for MW-assisted solvent free oxidation of alcohols*, 10ºEncontro Nacional de Catálise e Materiais Porosos, Instituto Superior Técnico, Portugal, 2016, p. 27.

Acknowledgements

I would like to express my special thanks of gratitude to my supervisors, Professor João Rodrigues and Professor Luísa Margarida Martins, who gave me the opportunity to do the project in the field of nanoscience, which also helped me in doing a lot of research, therefore I came to know so many new things, which enrich my knowledge and expand my horizon.

Secondly, I would also like to thank my tutor, Dr. Ana Paula Ribeiro, for her valuable advice and assistance in keeping my project on schedule. Her willingness to sacrifice her time to help me has been very much appreciated.

I would also like to extend my thanks to the Group 5 of CQE, which offered all the resources in running my project, all the group members who helped me a lot in finding the reagents and handing the instruments. Especially my colleagues in the lab, Inês Matias, Marta Mendes, Emmanuele Fontolan, Jiawei Wang, Yuyu Cheng, Goncalo Tiago, Tiago Duarte, Anup Paul, are to be greatly gratitude to enrich my knowledge, also make my learning experience interesting and grateful.

I would like to acknowledge the Portuguese Foundation for Science and Technology (FCT) for funding my work through project UID/QUI/00100/2013.

Finally, I wish to thank my parents for their support and encouragement throughout my study. They provided a great source of moral support and motivation and was reminded how lucky I am to have so many supportive people in my life.

Abstract

Gold catalysts are currently a “hot topic” of research, as they show application in many reactions of industrial and environmental importance. The catalytic activity of gold nanoparticles supported on different carbon materials, as heterogeneous catalysts, was tested for the microwave-assisted solvent-free oxidation of 1-phenylethanol by *tert*-butyl hydroperoxide (TBHP). The catalytic performance was related to the support interaction, reaction time and temperature, quantity of catalyst, presence of additives, and other parameters. The possibility of recycling the catalysts was also investigated.

Gold nanoparticles (1 wt. %) supported on a variety of carbon materials (activated carbon, graphite, silicon carbide, carbon xerogel, nanodiamonds, and microdiamonds), by two different methods (colloidal method and double impregnation), were used as catalysts for the oxidation of 1-phenylethanol. A maximum yield of acetophenone (99.9%) was obtained with Au nanoparticles supported on microdiamonds by colloidal method, while Au nanoparticles supported on silicon carbide by double impregnation method led to the minimum yield of 27.1%. Moreover, catalyst recyclability was tested up to six consecutive cycles at the optimized conditions for each catalyst, and it was observed that the catalytic activity of gold nanoparticles supported on microdiamonds, prepared by the colloidal method, maintains higher activity when compared with other catalysts after several reaction cycles.

In addition, copper nanoparticles supported on carbon nanotubes were tested for degradation of dyes. However, the obtained results were not suitable to be presented and therefore are compiled in appendix.

Keywords： gold nanoparticles, carbon materials, heterogeneous catalyst, oxidation.

Resumo

Os catalisadores de ouro são actualmente um "hot topic" de investigação, uma vez que têm aplicação em muitas reacções de importância industrial e ambiental. Neste projecto foi testada a actividade catalítica de nanopartículas de ouro suportadas em diferentes materiais de carbono, como catalisadores heterogéneos, para a oxidação assistida por microondas e isenta de solventes, por hidroperóxido de *terc*-butilo (TBHP). O desempenho catalítico foi relacionado com a interacção com o suporte, tempo e temperatura reaccionais, quantidade de catalisador, presença de aditivos e outros parâmetros. A possibilidade de reciclagem dos catalisadores foi também investigada.

As nanopartículas de ouro (1% p/p) suportadas numa variedade de materiais de carbono (carvão activado, grafite, carboneto de silício, xerogel de carbono, nanodiamantes e microdiamantes), por dois métodos diferentes (método coloidal e impregnação dupla), foram usadas como catalisadores para a oxidação de 1-feniletanol. Foi obtido um rendimento máximo de acetofenona (99.9%) na presença de nanopartículas de Au suportadas em microdiamantes pelo método coloidal, enquanto que as nanopartículas de Au suportadas em carboneto de silício por dupla impregnação conduziram a um rendimento mínimo de 27.1%.

Além disso, para cada catalisador, foi testada, nas condições previamente optimizadas, a sua possibilidade de reciclagem até seis ciclos catalíticos consecutivos. Foi observado que a actividade catalítica das nanopartículas de ouro suportadas em microdiamantes, preparadas pelo método coloidal, se mantém mais elevada, quando comparada com a dos outros catalisadores, após vários ciclos catalíticos.

Adicionalmente, nanopartículas de cobre suportadas em nanotubos de carbono foram testadas para a degradação de corantes. No entanto, os resultados obtidos não se afiguram adequados para serem apresentados nesta dissertação e consequentemente são compilados em anexo.

Palavras chave: nanopartículas de ouro, materiais de carbono, catalisadores heterogéneos, oxidação.

Index

List of Figures

List of Schemes

List of Tables

List of acronyms, abbreviations, and symbols

AC	Activated carbon
BJH	Barrett Joyner Halenda
CX	Carbon xerogel (pH=6)
CXL	Carbon xerogel (pH=5.5)
GR	Graphite
GC	Gas Chromatography
GC-MS	Gas Chromatography-Mass Spectrometry
MD	Microdiamonds
MWCNT	Multiwalled Carbon Nanotubes
MW	Microwave
NDLIQ	Nanodiamonds (liquid)
NDPW	Nanodiamonds (powder)
SC	Silicon carbide
TBHP	Tert-butyl hydroperoxide
TEMPO	2,2,6,6-tetramethyl-1-piperidinyloxy radical
UV-Vis	Ultraviolet-Visible spectroscopy

Gold nanoparticles supported on carbon materials for MW-assisted solvent free oxidation of 1-phenylethanol

1. Introduction

1.1 Gold nanoparticles

Gold (bulk) have been considered as an inactive catalyst for a long time[1]. It is not easily oxidized; moreover, the surface of gold does not absorb most of the molecules from the gas state[2]. However, Haruta[3] and his co-workers found that when gold nanoparticles (2-5 nm) are deposited on a Fe_2O_3 support, prepared by co-precipitation and deposition-precipitation methods, present unpredictable high catalytic activity regarding oxidation reaction of CO to CO_2 at room temperature or even at low temperature such as -76 ℃, which demonstrates that supported gold nanoparticles are extremely active catalysts for the oxidation of CO even at low temperature. Since then, supported gold catalysts have attracted much more attention by scientists and engineers to discover the potential application of Au catalysts. Many researchers began to study Au nanoparticles deposited on different kinds of support (metal oxides, carbon xerogels, graphite, etc.)[4-6]. They can be applied for oxidation reactions such as selective oxidation of alcohols[7-9], cycloalkanes[10], etc.

Nanoparticles are defined as particles with sizes between 1 and 100 nm[11]. Compared with bulk materials, nanoparticles with small dimensions exhibit different physical and chemical properties[12]. Additionally, gold nanoparticles are widely used in the biological field[13]. They can be coupled with different kinds of macromolecules, which avoid breaking the bioactivity; so many researchers found that they can be used as agents for drug delivery[14, 15], biological imaging[16], and diagnosis of diseases[17]. Nowadays, the major attention attracted by gold nanoparticles is their application in catalytic systems; they can be applied as catalysts for a variety of chemical reactions, such as reduction[18] and oxidation reactions[19]. Moreover, the catalytic properties are related to three crucial elements： contact structure[20], support selection[21], and the particle size[22]. The first factor is the most important, since the perimeter interfaces around gold nanoparticles provide the site for reaction.

1.2 Heterogeneous catalysis

Both homogeneous and heterogeneous gold catalysts present interesting activity among various reaction such as alkynes and alkenes selective hydrogenations and oxidations [23].

Generally speaking, homogeneous catalysts react in the same phase during the reaction process, while heterogeneous catalysts operate in a different phase when the reaction occurs. The main difference between them is that every single catalytic entity can act as a unique site in homogeneous catalysts, which makes homogenous catalysts inherently more selective and active in contrast to the conventional heterogeneous ones. The crucial advantage of a heterogeneous catalyst, when compared with a homogenous one, is that the separation and recycling process of a heterogeneous catalyst is much more simple and cheap than of a homogeneous catalyst, when possible[24].

For an extended period of time, the preparations of heterogeneous catalysts have many challenges, i.e., the development of heterogeneous catalysts was regarded more like alchemy than science. However, it began to develop in the 1970s when the concept of the scientific basis for the preparation of the catalysts has arisen[25].

There are a variety of methods for heterogeneous catalysts preparation, including deposition-precipitation method, sol-gel technique, and hydrothermal approach, etc.

Deposition-precipitation[26] can be used to deposit gold with high dispersion on metal oxides such as MgO, TiO_2, and Al_2O_3. Iwasawa[27] and co-workers have found that the reaction between $[Au(PPh_3)](NO_3)$ and OH groups from the metal hydroxides supplied well-dispersed gold catalysts, and this method is the most efficient way to synthesize Au/Mn_xO_y (MnO, Mn_3O_4, Mn_5O_8, Mn_2O_3, MnO_2), which showed high catalytic activity for CO oxidation in air.

Sol-gel technique[28] has been regarded as an attractive method to prepare heterogeneous catalysts, and the texture, composition and structural properties can be tuned by changing the parameters of the preparation process, thus making accessible the production of tailored materials, for example, well-dispersed metals and

chemically modified supports. Wang and colleagues[29] have been used the sol-gel method to synthesize MWCNT-TiO_2 material as catalysts. The surface area of the catalyst can be increased in this case, the solid state UV-Vis spectra indicated that the absorption increased with increasing the MWNT/TiO_2 ratio from 1 to 40% of the catalyst; the reason is that MWCNT in the complex material can be embedded in the TiO_2 substrate, thus to alleviate the agglomeration of TiO_2 particles, so that the surface area of the catalyst increased.

Typically, a heterogeneous metal catalyst is made of three parts：active metal part, activators and a support material. Under some circumstances, the metallic state forms the active component by itself[30]. Nevertheless, this situation is mostly restricted to noble metals and some basic metals used under specific conditions. Polymers can be provided as stabilizers for metal nanoparticles (NPs) while binding weakly to the surface of NP; their function is as ligands. Toshima[31] and co-workers used PVP to stabilize bimetallic core-shell gold-palladium nanoparticles (Au-PdNPs) (core-Au; shell-Pd), and it was demonstrated that the catalytic activity of bimetallic Au-Pd core-shell nanoparticles is much higher than the simple PVP stabilized PdNPs, thus the Au core increases the catalytic performance of PdNPs at the PdNPs surface[32]. However, the catalytic performances are different when reverses the core−shell formation (Pd core, Au shell); which can be used for methylacrylate hydrogenation. There are other solid supports which stabilized the metal nanoparticles widely used in recent years, such as carbonaceous materials and metal oxides (*e.g.* SiO_2 and Fe_3O_4).

1.3 Carbon supports

Carbon is regarded as a universal material which can be used for various technological processes; that is mainly because carbon atoms can bond to each other in different ways such as linear, planar and tetrahedral bonding settings, therefore producing materials with a variety of performances[33]. Electro-conductibility[34], porosity[35] and surface area[36] and other physicochemical properties could be modified for desired applications. In generally, carbon catalysts with large surface

area and well developed porosity can avoid sintering as much as possible with high metal loadings[37], and the distribution of pore size can be switched to apply to different reactions[38]. When applied for heterogeneous catalysis, carbon materials used as individual catalyst supports, not only permit the interaction with the active phase, but also act as catalysts or catalyst poisons directly.

Moreover, the surface chemistry is related to the performance of carbon materials when used as catalysts and catalysts supports[39]. Typically, carbon materials are hydrophobic, have low affinity to polar solvents such as water, but show high affinity to solvents such as acetone. While the hydrophobic property may influence the distribution of the active phase beyond the carbon support, the surface chemistry performance can be modified easily for carbon materials; oxidation is an effective way to enhance the hydrophilic performance[40]. The surface groups influence the acidity or alkalinity of the carbon surface; moreover, a few inorganic groups from the organic precursor (coal or wood) could exist on carbon materials, and it is extremely important for their performance, especially when they are used as catalysts supports.

Carbon materials, such as activated carbon, carbon xerogels, graphite and others have been applied for heterogeneous catalysis[41-44], as well as catalyst supports for catalytic reactions for a long time. The majority of the catalysts are metals, or metallic compounds supported on carbon materials[45]. The advantages of carbon materials are not only to provide a well-developed dispersion phase, but also influence the catalytic activity of the catalysts, which means that it may participate in any steps of the reaction, or favor the mutual effect between active phase and support.

Activated carbon (AC) is known for its rich surface chemistry properties; it is also a well-developed porosity material, and it has many advantages over other carbon materials, such as high adsorption capacity[46] and convenient disposal.

Carbon xerogels (CX) are mesoporous polymer based carbon materials with large surface area (400-1100 m^2/g), where the textural performance can be changed by adjusting the parameters during the preparation process[47, 48], and present applications such as super capacitors, filters, and catalyst supports**.** Rodrigues[49] and–co-workers found in the glycerol oxidation, Au/5CX ($d_{Barrett\ Joyner\ Halenda\ (BJH)}$ =5 nm) catalyst

prefers the formation of glyceric acid (GLYCEA) ((selectivity：48%； $X_{Glycerol\ (GLY)}$：90%)，and Au/20CX (d_{BJH}=20 nm) catalyst favors the formation of formic acid (FORMA) as the main product (selectivity: 42%; X_{GLY}： 90%)[50]； which means that the pore size of carbon xerogels determines the products of glycerol oxidation.

Graphite (GR) is an allotrope of carbon element, but either the natural graphite or the manufactured graphite is rarely applied to catalyst supports. The main reason is that the surface area of graphite is very low (10-50 m^2/g). However, graphite materials can produce graphite intercalated materials, which can develop a higher surface area (100-300 m^2/g). Additionally, the high surface area can be formed by high energy ball-milling method with a sharply growth of surface area from 10 to 600 m^2/g[51], and they can be used in different reactions, such as NO reduction[52], hydrogenation[53], etc.

Silicon carbide (SC) is known as carborundum, is an inert, semiconductor, abrasive material[54]**.** It is a material with excellent thermal conductivity[55], high radiation resistance[56] and high breakdown voltage[57], which is appropriate for demanding application under specific conditions. It can be used for light emitters[58], high power microwave equipment[59], and micro-electromechanical system (MEMS) mechanics[60].

Carbon nanotubes (CNT) are filamentous materials with a hollow cavity; consist of several layers of concentric graphite[61] (typically synthesized by catalytic decomposition of specific hydrocarbons), which present superiority over traditional supports, such as high purity which can avoid self-poisoning. Moreover, they have extraordinary mechanical properties, for instance, high electro-conductibility[62] and thermo-stability. They provide the potential of adjusting specific metal-support interaction, in the case to influence the catalytic selectivity. There also have different approaches regarding the decoration of CNT[63]. Efforts have been done to decorate CNT with various organic materials by the covalent attachment, and processing with the surfactant by non-covalent attachment. Moreover, a lot of inorganic materials have been coated on the surface of carbon nanotubes, and they have applications such as sensors[64], solar cells and magnetic apparatuses**.** Hernadi[65] and coworkers obtained

multi-walled carbon nanotubes (MWCNT) with a variety of inorganic materials such as alumina and silica, which supplied a beneficial surface wettability for dispersion.

Nanodiamonds (ND) are monocrystalline diamond molecules generated from an explosion process[66]. Normally, ND has small primary particle sizes (4-5 nm) with narrow size distribution, with the extremely high surface area.

On the other side, microdiamonds (MD) have particle sizes from 1 to 2.5 μm, which are extracted from rock samples by drill core or outcrop, and they are used in grinding and abrasive technology. When compared with MD, ND has a smaller particle size (4-5 nm) and higher surface area (BET surface area approximately 300 m^2/g for ND, and 5 m^2/g for MD), which promotes the generation of a great amount of surface reactive chemical functional groups[67]. It is expected that the individual properties of ND will be applied for the exploitation of therapeutic agents for gene treatment, antiviral, antibacterial therapy[68], and tissue scaffolds[69]. It was reported that Amanee[70] and coworkers had used polycaprolactone nanodiamonds composite scaffolds with an electrostatic spinning method for bone tissue engineering.

In the next table, is shown the description of the carbon materials used in this work, which characterization has been done previously.

Table 1-1 Characterization of (powder) carbon samples obtained by adsorption of N_2 at -196 ℃, and amounts of CO and CO_2 desorbed, as determined by TPD[71].

Sample designation	Sample material	*S_{BET} (m^2/g)	*V_p (cm^3/g)	*L (nm)	*V_{micro} (cm^3/g)	*$S_{external}$ (m^2/g)	CO (μmol/g)	CO_2 (μmol/g)
AC	Activated carbon	974	0.67	-	0.348	260	740	205
CNT	Carbon nanotubes	257	2.89	-	~0	257	194	70
NDPW	Nanodiamonds	295	1.08	10.6	~0	295	780	260
MD	Microdiamonds	4	0.01	3.8	~0	4	51	25
CX	Xerogel (pH=6)	611	0.90	13.6	~0	611	564	156
CXL	Xerogel (pH=5.5)	614	1.29	32.3	0.012	538	379	125
GR	Graphite	5	0.02	4.5	~0	5	40	21
SC	Silicon carbide	~0	~0	-	~0	~0	-	-

*Surface area (S_{BET}), total pore volume (V_p), average mesopore width (L), micropore volume (V_{micro}), external area ($S_{external}$).

1.4 Gold heterogenization methods

There are different methods to load gold on various supports, such as deposition-precipitation method, sol-gel technique and hydrothermal approach, which were mentioned in section **1.2**. In our case, gold was loaded on the carbon supports by two different methods：colloidal (COL) and double impregnation (DIM) method.

COL method[72] refers to the simple and well known wet chemistry precipitation approach, the solutions of diverse ions are mixed under specific temperature and pressure to form insoluble precipitates. The COL method has proven to be specifically appropriate to obtain nanoparticles with controlled morphologies and prominent catalytic performance[73].

DIM preparation[74] is the procedure that the reaction between chloroauric acid and a base (Na_2CO_3) produce the precipitation of gold hydroxide within the pores of the catalyst. The chemical mechanism for the enhanced activity of such catalyst owes to the formation of $Au(OH)_3$ during the Au deposition process, not as gold chloride (Cl). Since the Cl is not bonded with the Au, is removed by the washing process. So it could be a more active catalyst. The reason is that the chlorine may poison reaction sites in the catalyst. Moreover, the gold nanoparticles can be easily sintered in the presence of chloride[75].

The sizes of gold nanoparticles also play an important role that influences the catalytic activity of such nanoparticles[76]. Britt[77] and co-workers have explained the relationship between gold nanoparticles size, and chemical activity through the origin of the effect; suggesting that the active sites of gold nanoparticles are the corners and edges, and the catalytic activity can be explained by quantum size effects[78], support-induce strain[79], and the function of low-coordinated Au atoms scales in nanoparticles[80]. Zhou[81] and colleagues have used single-molecule microscopy of fluorogenic reactions to study the catalytic activity influenced by gold nanoparticles size. It can be observed that when decreased particle size; the substrate binding affinity reduced, in the meanwhile, the catalytic conversion increased per surface area. On the contrary, the product binding affinity increased when the particle size

decreased.

Normally, the catalytic activity increased when the gold nanoparticles size decreased, but in some conditions, there are optimized particle sizes for the catalytic systems. For example, Valden[82] and co-workers have done the investigation about dispersing Au NPs (1 to 6 nm) on single-crystalline TiO_2 surfaces, and they found that when the gold particle size was between 2 and 4 nm, the highest catalytic activity was obtained in the CO oxidation. The **Table 1-2** presents a summary of the values of the gold nanoparticles size and dispersion of the catalysts used in the present work.

Table 1-2 Average gold nanoparticle size, range and dispersion calculated from HRTEM/HAADF measurements[71].

Sample	Au average size (nm)	Au range (nm)	Metal dispersion (%)
Au@AC (COL)	6.8±1.5	1-20	16.9
Au@NDPW (COL)	7.6±1.4	2-18	15.1
Au@NDLIQ (COL)	8.2±1.4	1-20	14.0
Au@MD (COL)	8.2±1.4	1-20	14.0
Au@CX(COL)	4.4±1.0	1-14	26.2
Au@CXL(COL)	4.4±1.0	1-14	26.2

The characterization of gold nanoparticle sizes has been done previously[71]. The **Figure 1-1** shows HAADF micrographs and HRTEM images of gold nanoparticles on CNT, AC, MD, NDPW, NDLIQ, CX, and CXL, respectively. The first technique allows detection of the gold particles through the Z-contrast micrographs, as they are seen as bright spots, while on HRTEM images gold nanoparticles are visible as darker areas.

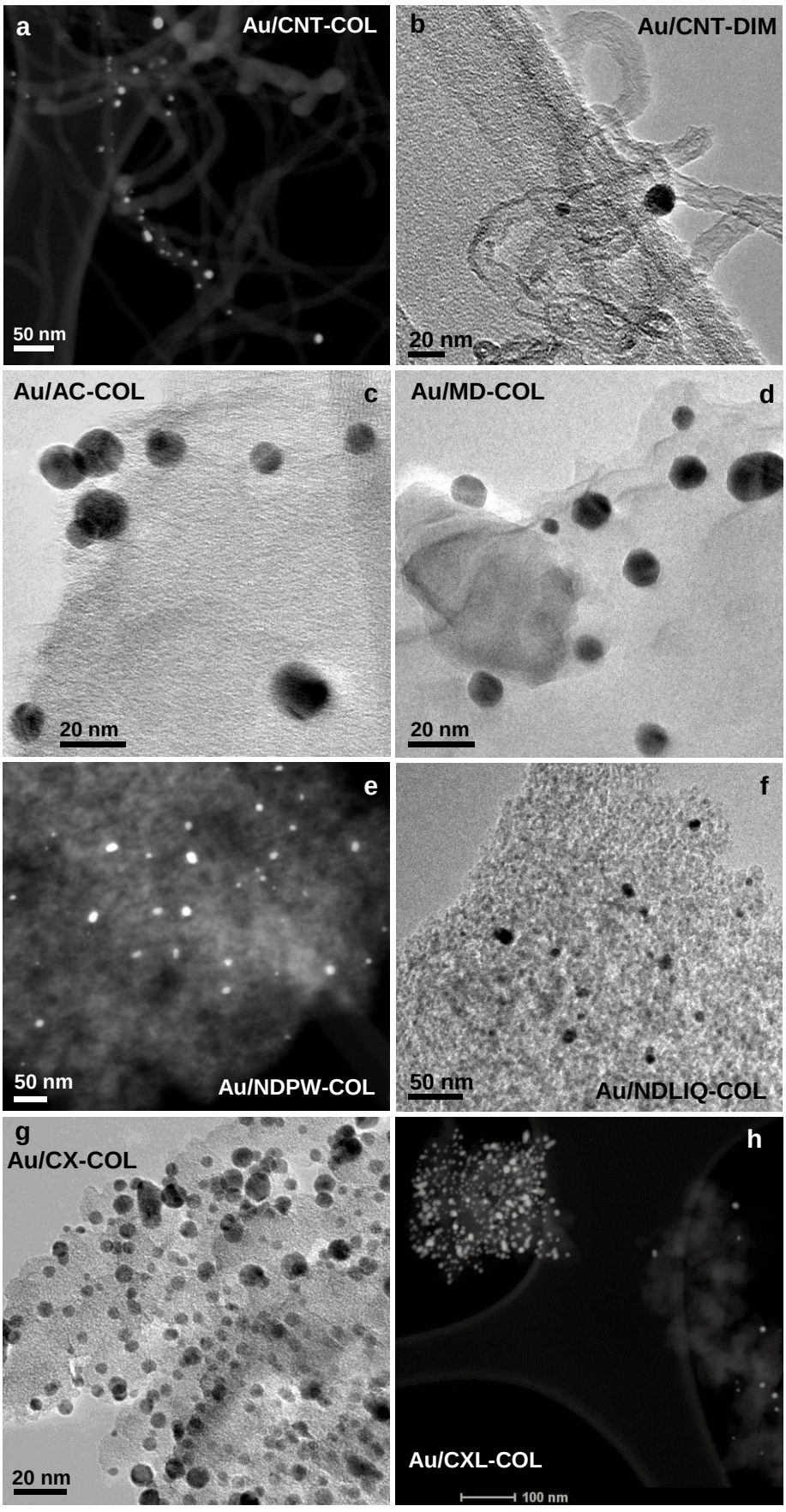

Figure 1-1 HAADF micrograph of Au/CNT-COL (a). HRTEM images of

Au/CNT-DIM (b). Au/AC-COL (c) and Au/MD-COL (d). HAADF micrograph of Au/NDPW-COL (e). HRTEM images of Au/NDLIQ-COL (f) and Au/CX-COL (g). HAADF micrograph of Au/CXL-COL (h). Gold nanoparticles are seen as darker spots on HRTEM images and as bright spots on HAADF micrographs**[69]**.

1.5 Reactions catalyzed by supported gold nanoparticles

Supported gold nanoparticles have been attracted much attention because of their unique and superior catalytic properties[83-85]. The application of gold supported on different materials in various reactions is presented in **Table 1-3**. Moreover, the aerobic oxidations of alcohols primarily to carbonyl and carboxylic compounds catalyzed by gold have been widely investigated in organic synthesis[92]. Benzyl alcohol is one of the most attractive substrates, and when substituted benzyl alcohols contain electron-donating groups (CH_3, OCH_3 or OH groups), are much more easily oxidized compared with those without electron-donating groups. The catalyst $Au/Ga_3Al_3O_9$ was very efficient and active on the benzyl alcohol oxidation at room temperature. Moreover, $Au/Ga_3Al_3O_9$ catalyst produced extremely high turnover frequency (TOF) of 25000 h^{-1} under the temperature at 160 ℃ and solvent-free conditions[93]. Additionally, the bimetallic Au-Pd catalysts with the ceria support ($scCeO_2$) supercritically prepared at 140 ℃, in the absence of O_2 and in the solvent-free conditions, showed high activity and selectivity for benzaldehyde (91%). The other products were benzyl benzoate (3%), benzoic acid (2%) and toluene (3%). The catalytic activity of Au-Pd supported on supercritically prepared ceria material (Au-Pd/$scCeO_2$) was almost 4 times more active than Au-Pd supported on standard ceria material (Au-Pd/$unCeO_2$)[94]. The catalyst morphology from high angle annular dark field (HAADF) imaging, scanning transmission electron microscopy and X-ray energy dispersive spectrometry (STEM-XEDS) mapping and X-ray photoelectron spectroscopy (XPS) presented that both Au and Pd metallic constituents were well mixed and consistently dispersed on the nanocrystalline CeO_2 support. Furthermore, Mertens[95] and co-workers have found that polyvinylpyrrolidone stabilized gold-palladium clusters (ca. 1.9 nm) under solvent free conditions showed high activity (TOF of 22500 h^{-1} for benzyl alcohol, 59000 h^{-1} for 1-phenylethanol), and the

recyclability rate was more than 97% in the fourth oxidation run during the recycling experiments. Takato[96] and co-workers observed that a hydrotalcite-supported nanoparticle (Au/HT) was an efficient heterogeneous catalyst for the oxidation of 1-phenylethanol under mild conditions. Therefore, the turnover number (TON) and TOF were 200000 and 8300 h^{-1}, respectively. Moreover, the catalyst can be easily filtrated and recycled without loss of activity and selectivity. Furthermore, Ji[97] and colleagues have reported an efficient H_2O_2-Au approach for the oxidation of 1-phenylethanol under solvent free conditions, which was regarded as a green oxidation of heterogeneous metal complexes. For instance, the catalyst gold supported on TiO_2 obtained a conversion of 99%, and the yield of acetophenone was between 98 and 100%, which means that the well-dispersed gold nanoparticles in association with a beneficial interaction with TiO_2 support is the major factor for obtaining high activity in the H_2O_2 mediated oxidation of 1-phenylethanol.

Table 1-3 Assay conditions for various reactions catalyzed by gold catalyst on different supports.

Catalyst	Conditions	Y(%)/C(%)/S(%)[a]	Ref.
Au@anion-exchange resin	oxidation of glucose to gluconic acid; 60 ℃, 2h, pO_2=0.1 MPa.	Y:98	86
Au@polystyrene copolymer	oxidation of 1-phenylethanol to acetophenone; 160 ℃, 0.5h, pO_2=0.1 MPa.	Y:6	87
1%Au@TiO_2	epoxidation of propene in the presence of dihydrogen; 50 ℃	C: 1.1; S: PO[b] (＞ 99)	88
1%Au@TiO_2	epoxidation of propene in the presence of dihydrogen; 80 ℃	C:0.8; S: C_3H_8 (＜ 10), CO_2 (＞70)	88
5%Au@CeO_2	n-heptanal air oxidation; 50 ℃, 3.9mmol of aldehyde, 3.5g of acetonitrile, 0.05g of catalyst, 3.5h	Y: 93.6	89
5%Au@CeO_2	n-heptanal air oxidation; 25 ℃ 3.9mmol of aldehyde, 3.5g of acetonitrile, 0.05g of catalyst, 3.5h	Y:78.1	89
1%Au@Chitosan@SiO_2	hydroamination of aniline with 1-octyne in toluene. 50 ℃, 2h	C: 100%; Y: 99%; S: Imine: Ketone: 55:45.	90

Table 1-3 Assay conditions for various reactions catalyzed by gold catalyst on different supports (cont).

1%Au@SiO_2	hydroamination of aniline with 1-octyne in toluene. 50 ℃, 2h	C: 68%; Y: 64%; S: Imine: Ketone: 88:12.	90
0.5%Au@CeO_2	Oxidation of 3-octanol to 3-octanone. 80 ℃, 3.5h	C: 97; S: ＞99	91

[a] Y: Yield; S: Selectively; C: Conversion. [b] PO: propene oxide.

1.6 Present work

In this work, the catalytic activity of gold supported on different kinds of carbon materials (activated carbon, silicon carbide, graphite, carbon xerogels, multi-walled carbon nanotubes, nanodiamonds and microdiamonds) was studied for the oxidation reaction of 1-phenylethanol to acetophenone, in the presence of aqueous *tert*-butyl hydroperoxide (TBHP, ^{t}BuOOH) as oxidizing agent, under several reaction conditions (such as different temperature, different reaction times, different amounts of TBHP and TEMPO additive), with the assistance of microwave irradiation (MW).

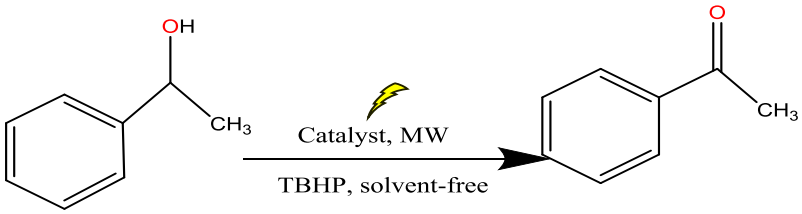

Scheme 1-1 MW-assisted oxidation of 1-phenylethanol to acetophenone.

The oxidation of 1-phenylethanol was selected as the model reaction since it is regarded as a very important reaction in organic chemistry[98]. Although the selectivity and efficiency are high in traditional oxidation reactions, normally they use toxic oxidants and solvents. A large amount of waste is produced during those reactions. Thus, green oxidants such as hydrogen peroxide (H_2O_2) or TBHP are more suitable oxidants and should be used. TBHP was selected as an efficient oxidant with high stability for the oxidation of 1-phenylethanol. Moreover, the microwave irradiation method is regarded as much more effective when compared with conventional heating;

usually, similar yields can be achieved in a shorter time[99].

2. Experimental

2.1 Materials

Eight different kinds of carbon materials were used as supports for the gold nanoparticles：activated carbon (AC) from Sigma-Aldrich Norit® ROX 0.8, silicon carbide (SC) from VWR®, carbon xerogel (CX) synthesized by polycondensation of resorcinol and formaldehyde at pH=6, CXL (carbon xerogel with larger width) prepared at pH=5.5, graphite powder (GR) supplied by Sigma-Aldrich®, multi-walled carbon nanotubes (CNT) from Nanocyl™ NC3100, nano-sized diamonds (powder, NDPW) from Sigma-Aldrich®, and nanodiamonds (aqueous, NDLIQ) supplied by NanoAmando®.

The preparation of the used gold catalysts was as follows[71]. Gold (1 wt. %) was loaded on the carbon supports by two different methods：colloidal methods (COL) and double impregnation (DIM).

The first procedure consists in dissolving the gold precursor, $HAuCl_4 \cdot 3H_2O$ (Alfa Aesar), in water, adding polyvinyl alcohol (Aldrich) and $NaBH_4$ (Aldrich), resulting in a ruby red sol to which the powder support is added under stirring (in the case of NDLIQ, the ND suspension was added to the solution). After a few days, the solution starts to lose color, as Au is deposited on the support. The colorless solution is filtered, the catalyst washed thoroughly with distilled water until the filtrate is free of chloride and dried at 110 ℃ overnight. The organic scaffold is removed from the support by a heat treatment under nitrogen flow for 3 h at 350 ℃ (showed by elemental analysis to be efficient for this purpose), and then, the catalyst is activated by future treatment under hydrogen flow for 3 h also at 350 ℃.

The DIM method consists in impregnating the support with an aqueous solution of gold precursor and then with a solution of Na_2CO_3 (Sigma-Aldrich), followed by washing with water and drying. This step removes chloride, which is well known to cause sintering of Au particles, thus turning them inactive.

1-Phenylethanol (98%), *tert*-butyl hydroperoxide (TBHP, 70%, aq. solution), 2,2,6,6-tetramethyl-1-piperidinyloxy radical (98%, TEMPO) and acetophenone (99%) were obtained from Sigma-Aldrich, nitromethane (≥ 99%) from ACROS, and the acetonitrile (99.99%) from Fisher Scientific, UK.

2.2 Instruments

The catalytic activity was tested using microwave (MW) irradiation equipment. It contains a Anton Paar Monwave 300 microwave reactor, which is suitable for a rotational system and an IR temperature detector, applying a 10 mL reaction tube with a 13 mm internal diameter, and the centrifuge (speed of 10000 rmp; 1.5 mL × 8 PCR tube) from Millipore Instrument.

Gas chromatographic (GC) analysis was performed at a Fisons gas chromatograph (GC) 8000 instrument, using DB-642 (J&W) capillary column (DB-WAX,column length: 30 m, internal diameter: 0.32mm), FID detecor, and the Jasco-Borwin v.1.50 software.

GC-MS were carried out at a Perkin Elmer Clarus 600C facility (He as the carrier gas). The ionization voltage was 70 eV. Gas chromatography was applying a SGE BPX5 column (30 m × 0.25 mm ×0.25 μm) as the temperature programme. The products were identified by comparison of the retention time regarding the reference compounds.

2.3 Experimental procedure

2.3.1 MW-assisted oxidation of 1-phenylethanol

The catalytic procedure was as follows: the catalyst (Au, loading 1 to 5 μmol), 2.5 mmol of 1-phenylethanol and TBHP (70% aqueous solution) were added to a MW G10 vessel. The mixture was stirred at 600 rmp at 10 W power MW, at different temperatures (50 to 150 ℃) for different times (30 to 720 min) in the microwave reactor. As the boiling point of TBHP (aq. 70%) is 160 ℃, for safety reasons. the reaction temperature should below 160 ℃. The conditions are presented in **Table 1-4**.

Table 1-4 Assay conditions for the oxidation of 1-phenylethanol catalyzed by gold nanoparticles supported on different carbon materials.

Entry	Catalyst	TBHP (mmol)	Au (μmol)	T (℃)	t (min)
1	1%Au@AC(DIM)	5-10	1-5	50-150	30-120
2	1%Au@AC(COL)	5-10	1-5	50-150	30-120
3	1%Au@SC(DIM)	5-10	1-5	50-150	30-720
4	1%Au@SC(COL)	5-10	1-5	50-150	30-120
5	1%Au@GR(DIM)	5-10	1-5	50-150	30-120
6	1%Au@GR(COL)	5-10	1-5	50-150	30-120
7	1%Au@CX(DIM)	5-10	1-5	50-150	30-120
8	1%Au@CX(COL)	5-10	1-5	50-150	30-720
9	1%Au@CXL(COL)	5-10	1-5	50-150	30-120
10	1%Au@NDLIQ(DIM)	5-10	1-5	50-150	30-120
11	1%Au@NDLIQ(COL)	5-10	1-5	50-150	30-120
12	1%Au@NDPW(COL)	5-10	1-5	50-150	30-120
13	1%Au@MD(DIM)	5-10	1-5	50-150	30-120
14	1%Au@MD(COL)	5-10	1-5	50-150	30-120
15	AC	5	1	50-100	120
16	SC	5	1	50-100	120
17	GR	5	1	50-100	120
18	CX	5	1	50-110	120
19	CXL	5	1	60-100	120
20	MD	5	5	110	120
21[a]	1%Au@AC(COL)	10	5	110	120
22[a]	1%Au@SC(DIM)	5	5	110	120
23[a]	1%Au@GR(COL)	10	5	110	120
24[a]	1%Au@CX(COL)	5	5	110	120
25[a]	1%Au@CXL(COL)	10	5	110	120
26[a]	1%Au@NDLIQ(DIM)	10	5	110	120

[a]In the presence of 2.5mol% of TEMPO.

2.3.2 Products detection by GC analysis

After the reaction using microwave irradiation, the mixture needed to cool down to room temperature. Then 50 μL of nitromethane (internal standard) was added. The obtained mixture was stirred for *ca.* 15 min, therefore 1μL of the sample was taken from the mixture, analyzed by GC after centrifuge (5000 rpm 5 min). The GC temperature program used was as follows: the temperature of injection was 120 ℃. After the injection, the reaction temperature was held at 120 ℃ for 1 min, then raised the temperature, by 10 ℃/min, either to 200 ℃ and maintained at this temperature for

1 min. Helium was used as the carrier gas. The products were identified by comparison of their retention times with known reference compounds.

2.3.3 Recycling procedure

Recycling of the catalysts was tested up to 6 consecutive cycles. In each cycle, the method for recycling started by collecting the reaction solution from the G10 vessel, the catalyst was separated using centrifuge (5000 rpm, 5 min), and then wash the catalysts with acetonitrile (repeated at least 2 times), dried under compressed air at room temperature. Afterward, the catalysts were reused for the 1-phenylethanol oxidation experiments, while the molar ratio of substrate to catalyst remained constant.

Table 1-5 Assay conditions for the oxidation of 1-phenylethanol catalyzed by recycled Au NPs supported on different carbon materials.

Entry	Catalyst	TBHP(mmol)	Au (μmol)	T (℃)	t (min)
1	1%Au@AC(COL)	10	3.25-5	110	120
2	1%Au@SC(DIM)	5	4.5-5	110	120
3	1%Au@GR(COL)	10	3-5	110	120
4	1%Au@CX(COL)	5	4-5	110	120
5	1%Au@CXL(COL)	10	1.5-5	110	120
6	1%Au@NDLIQ(DIM)	10	4-5	110	120
7	1%Au@MD(COL)	10	2-5	110	120

2.3.4 Calibration curves for the internal standard method

In this procedure, solutions with 4 different concentrations of substrate and product were prepared, each solution contained 1-phenylethanol (substrate), and nitromethane (internal standard), TBHP (oxidant) and acetonitrile (solvent). Only the amount of nitromethane remained the same (50 μL). The prepared samples are presented in **Table 1-6**. Then the prepared solution was injected in GC instrument, and the area of each compound was recorded and used to calculate the calibration curve.

Table 1-6 Assay conditions for calibration curve calculations using 4 concentrations of solutions.

Entry	1-Phenylethanol (µL)	Acetophenone (µL)	TBHP (µL)	Acetonitrile (µL)	Nitromethane (µL)
1	50	50	50	800	50
2	100	100	100	650	50
3	150	150	150	500	50
4	200	200	200	350	50

The calibration curves are presented in **Figures 1-2** and **1-3**. **Figure 1-2** is the calibration curve for acetophenone, **Figure 1-3** is the calibration curve for 1-phenylethanol.

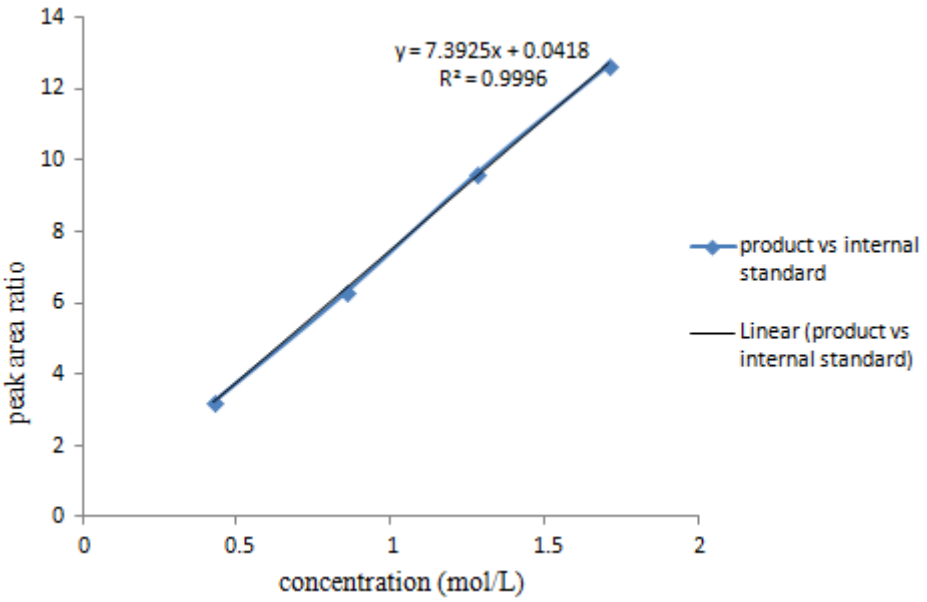

Figure 1-2 Calibration curve of acetophenone. Peak area ratio of acetophenone/nitromethane *vs.* concentration of nitromethane.

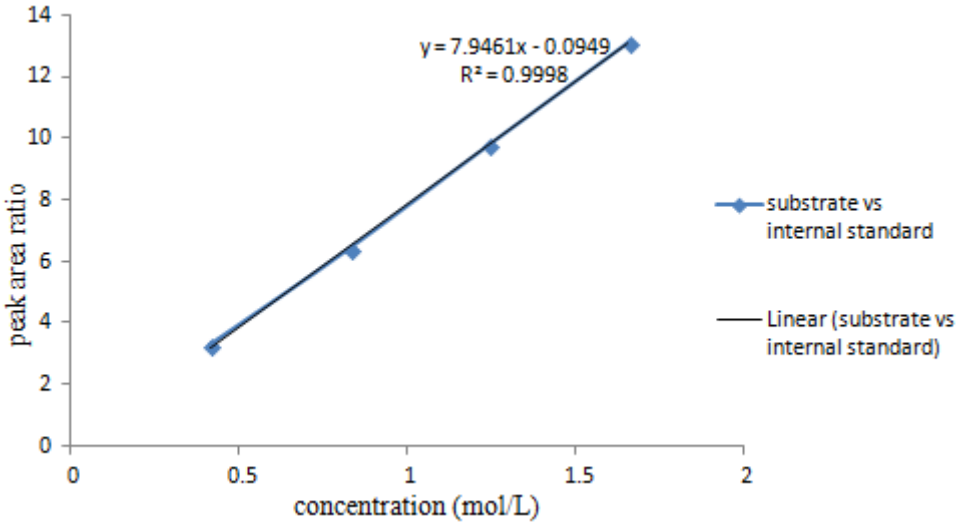

Figure 1-3 Calibration curve of 1-phenylethanol. Peak area ratio of 1-phenylethanol/nitromethane *vs.* concentration of nitromethane.

From **Figures 1-2** and **1-3,** it can be seen that the coefficient is 7.39 and 7.95, respectively, and the R^2 is 0.9996 and 0.9998, while R^2 is a statistical measure that how close the data are to the fitted regression line, it is between 0 and 100%, so the parameters explain we obtain higher variability to the response data.

3. Results and Discussion

3.1 Oxidation of 1-phenylethanol catalyzed by Au@AC

1% Au NPs supported on activated carbon (AC) was tested as a heterogeneous catalyst for the microwave-assisted solvent-free oxidation of 1-phenylethanol by ^{t}BuOOH. The influence of several catalytic parameters such as temperature and reaction time was investigated and is presented as follows.

3.1.1 Influence of temperature

A series of experiments have been done to prove that different temperatures influence on the yields of acetophenone, with the different gold loading methods: colloidal method (COL) and double impregnation (DIM). The results are presented in

Figures 1-4 to **1-6**.

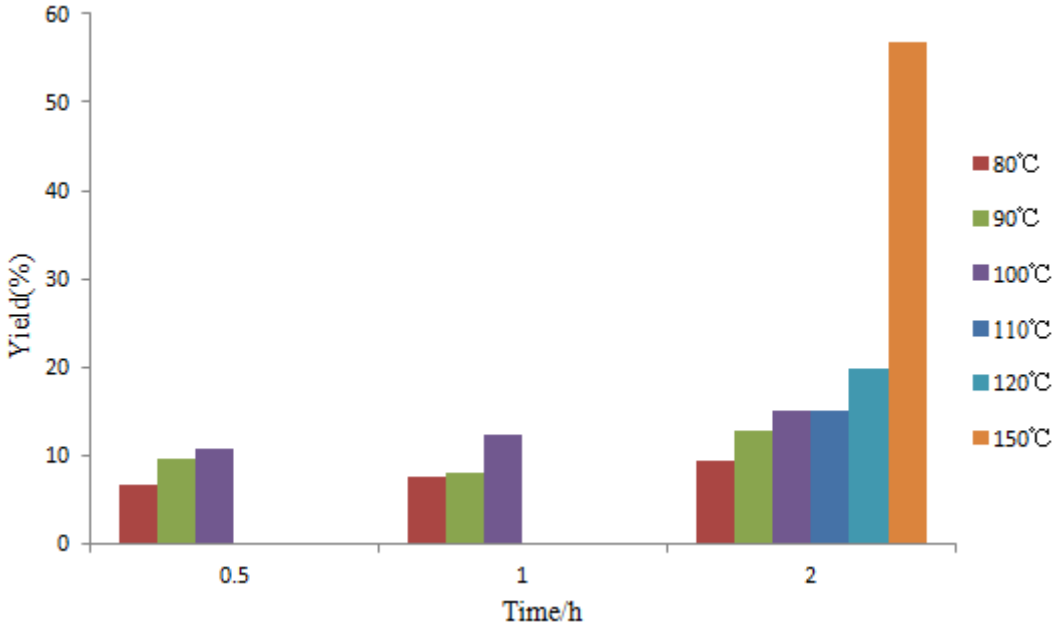

Figure 1-4 Acetophenone yield *vs.* reaction time at different temperatures with catalyst Au@AC (DIM).

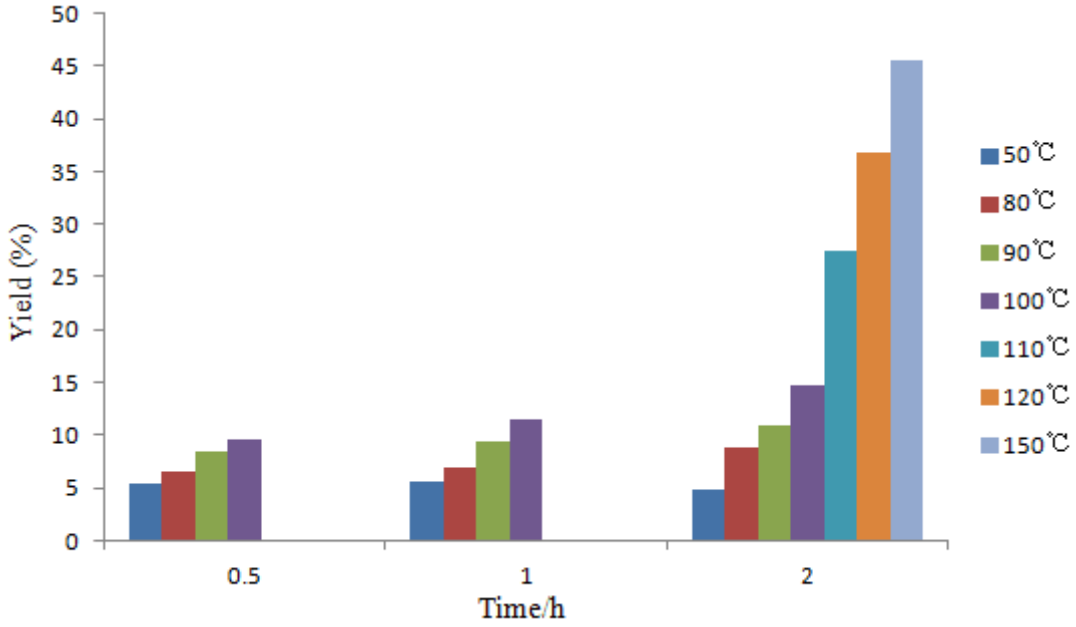

Figure 1-5 Acetophenone yield *vs.* reaction time at different temperatures with catalyst Au@AC (COL).

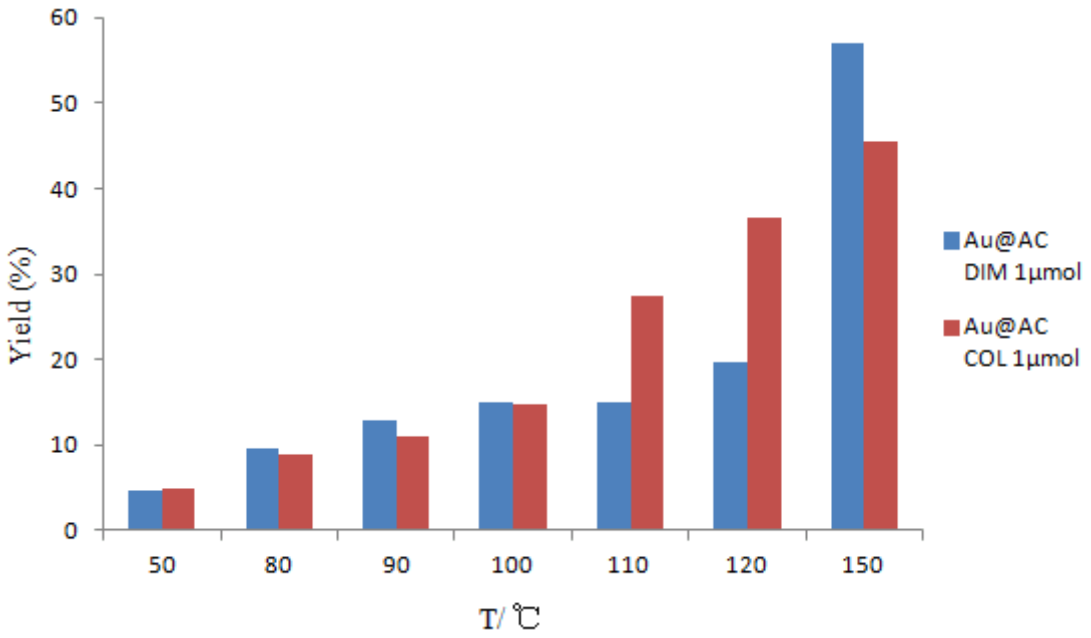

Figure 1-6 Comparison of the acetophenone yield *vs.* temperature for 2 h reaction time with catalyst Au@AC obtained by different heterogenization methods.

From the graphs above it can be seen that the reaction temperature has a great influence on the 1-phenylethanol oxidation with assisted microwave method. In the case of 1% Au supported at AC prepared with DIM or COL method, the yields increased from 50 to 150 ℃, so the most suitable temperature for the oxidation of 1-phenylethanol catalyzed by Au@AC is 150 ℃.

3.1.2 Influence of reaction time

Several experiments, at different reaction times, have been performed and it was found that the reaction time influenced the acetophenone yield. The results are shown in **Figures 1-7 and 1-8.**

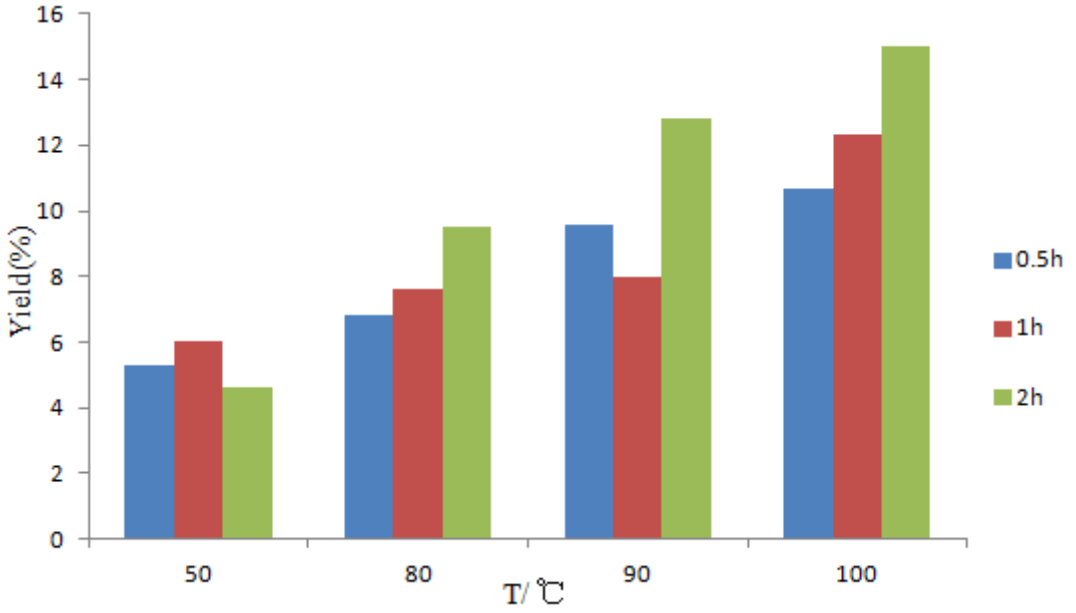

Figure 1-7 Acetophenone yield *vs.* temperature at different reaction time with catalyst Au@AC (DIM).

From **Figure 1-7**, it can be observed that with catalyst Au@AC, a longer reaction time (2 h) leads to higher yields. The exception is at 50 ℃, where the yield decreased after 1 h reaction. The abnormal behavior could be attributed to possible mistakes occurred in the experimental procedure, the most probable reason is the inaccurate measuring of the catalyst.

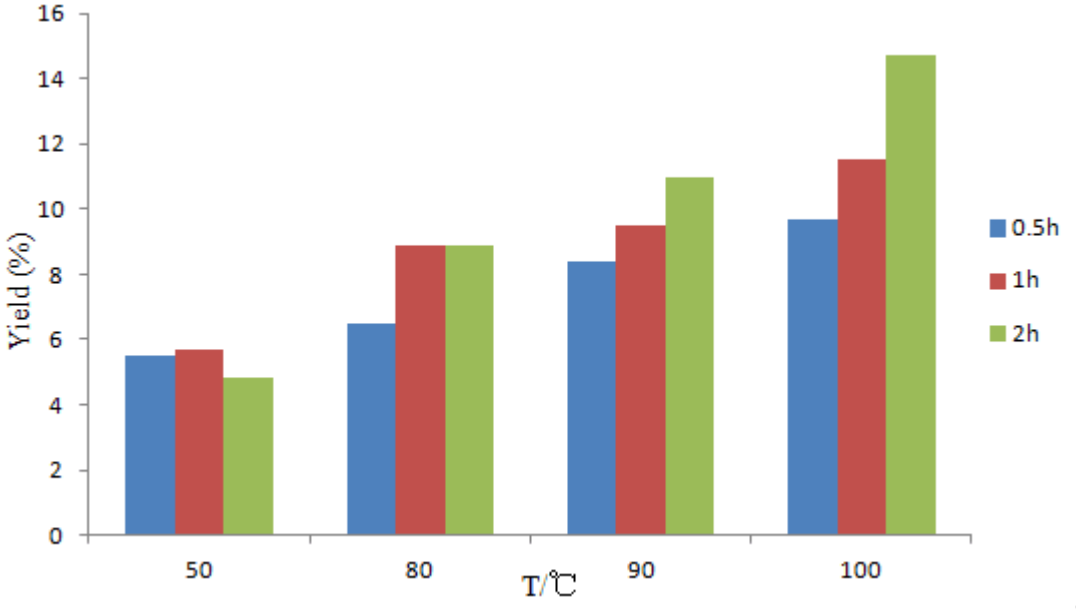

Figure 1-8 Acetophenone yield *vs.* temperature at different reaction time with catalyst Au@AC (COL)

From **Figure 1-8**, it can be observed that the yields increased steadily with time at 90 and 100 ℃, while the best reaction time for 50 and 80 ℃ is 1 hour. The catalytic activity of DIM and COL at 100 ℃ after 2 hours reaction do not show significant differences.

3.1.3 Influence of catalyst quantity

To know the influence of the quantity of catalyst on product yield, the reactions have been performed during 2 hours at 80 and 110 ℃. The results are shown in **Figure 1-9**.

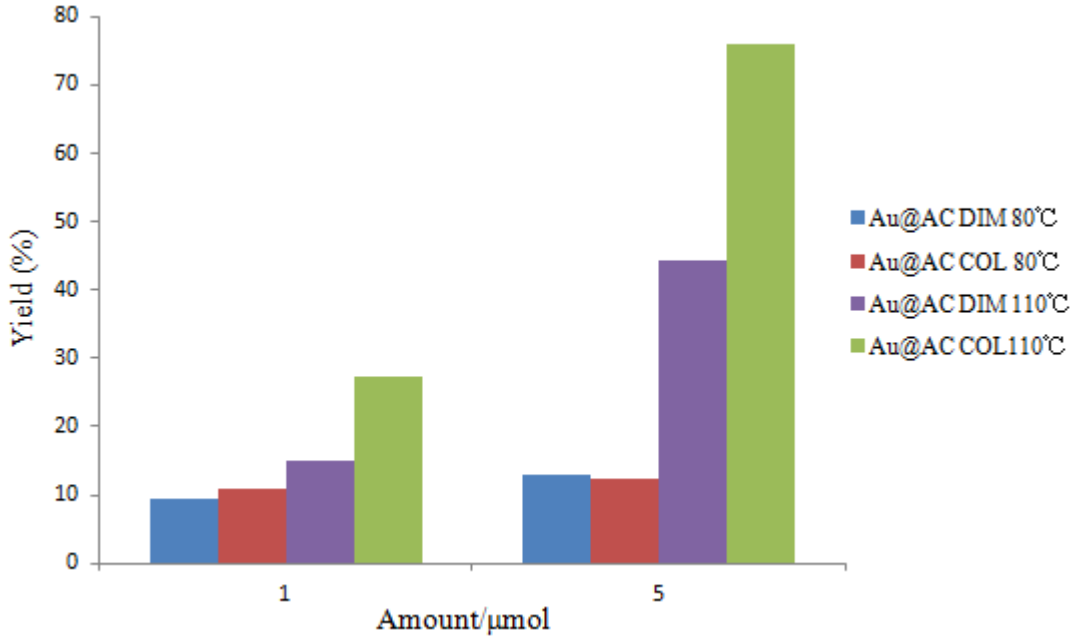

Figure 1-9 Acetophenone yield *vs.* amount of catalyst at different temperatures for 2 h reaction of catalyst Au@AC.

Regarding **Figure 1-9**, it can be found that the quantity of catalyst affects the catalytic activity at 110 ℃. In the case of 1% Au supported at AC (COL) the yield increased almost 50 %, and in the case of 1% Au supported at AC (DIM) the yield increased 30%. At 80 ℃, the yield declined even with the quintuple amount of catalysts, so it can be observed that the higher quantity of catalysts with higher temperature was the desirable conditions for the oxidation of 1-phenylethanol.

Tamao[100] *et al* have found that, in the case of catalyst Au (2 wt%) supported at

AC at 80 ℃ for 3 h reaction, by solid grinding method (catalyst was 5.025 mol% *vs.* substrate), the yield of oxidation of 1-phenylethanol to acetophenone is 8%. While in our case, either by DIM method or COL preparation, the yield is below 8% when the reaction time is 2 h. Especially needed to mention is that the catalyst was 0.04 mol% *vs.* substrate, so in the presence of much less catalyst and less reaction time, we obtained similar yield when compared to the literature[100], which means for gold loaded on carbon supports, colloidal method, and double impregnation preparation are more efficient than solid grinding method.

3.1.4 Influence of additive TEMPO

After performing experiments regarding parameters such as different temperatures, reaction times and catalyst quantities, the best condition found is 5 μmol of catalyst Au@AC (COL) at 110 ℃ for 2 hours. Then we have changed the amount of ^{t}BuOOH and added additive TEMPO. The results are presented in **Figure 1-10**.

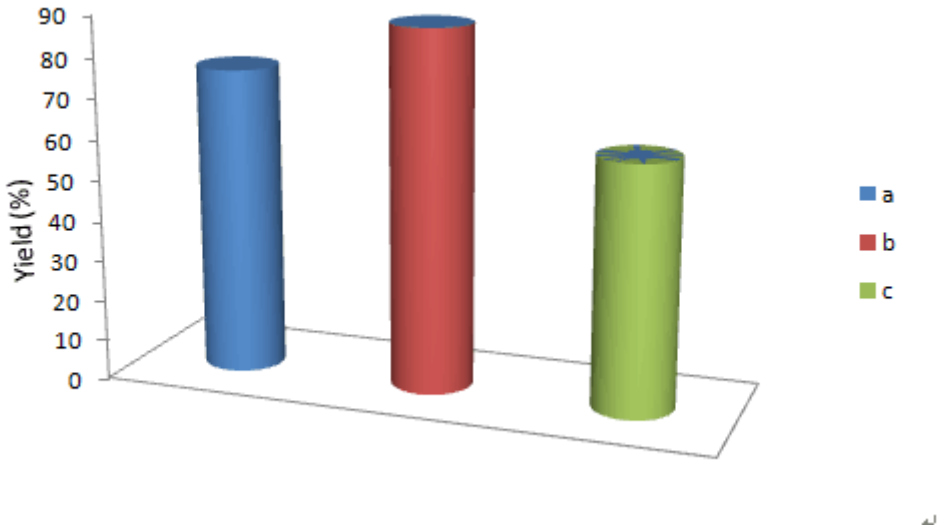

Figure 1-10 Acetophenone yield *vs.* additive with catalyst Au@AC (COL). Reaction conditions: catalyst (5 μmol), 110 ℃, 2 h, **a**: TBHP (5 mmol); **b**: TBHP (10 mmol); **c**: TBHP (10 mmol), in the presence of TEMPO (2.5 mol %).

It can be observed that when twice the amount of TBHP was added at 110 ℃ with catalyst Au@AC (COL), the yield increased 12.9%, while when 2.5mol%

TEMPO was added, the yield decreased 27.9%, so it can be concluded that 10 mmol of TBHP is better than 5 mmol TBHP for the oxidation of 1-phenylethanol with catalyst Au@AC (COL), and the TEMPO additive has an inhibitor effect on the catalytic activity.

3.2 Oxidation of 1-phenylethanol catalyzed by Au@SC

1% Au NPs supported at silicon carbide (SC) was tested as a heterogeneous catalyst for the microwave-assisted solvent-free alcohol oxidation of 1-phenylethanol by ^{t}BuOOH. The catalytic performances were studied as a function of the temperature, reaction time and other experimental conditions. The results are presented as follows.

3.2.1 Influence of temperature

A set of experiments have been done to demonstrate that different temperatures influence the acetophenone yields. The results are presented in **Figures 1-11** to **1-13**.

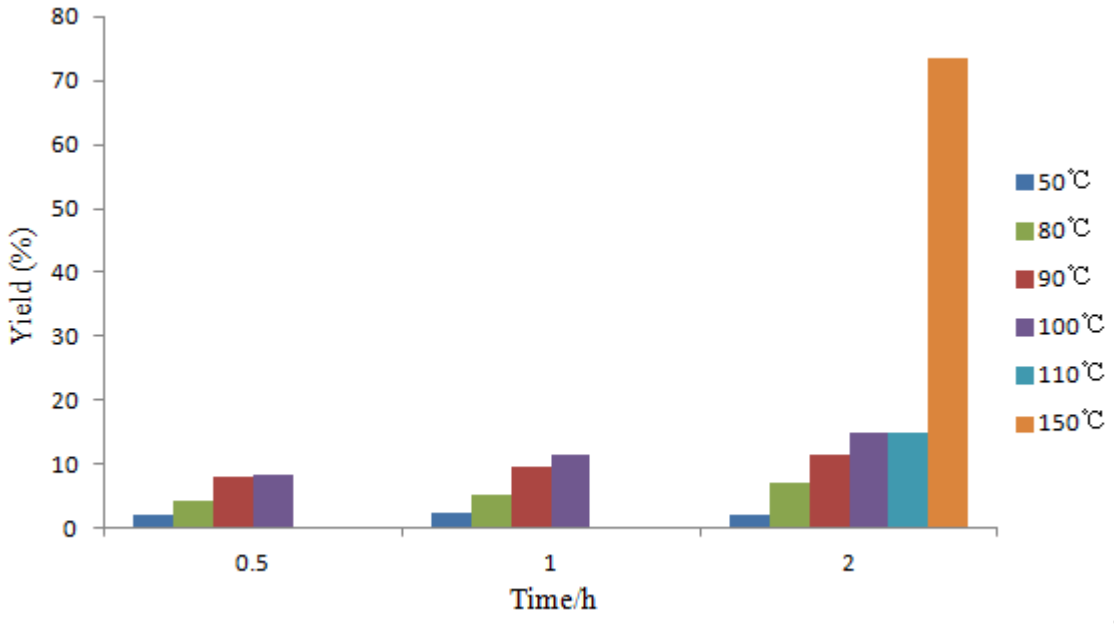

Figure 1-11 Acetophenone yield *vs.* reaction time at different temperatures with catalyst Au@SC (DIM).

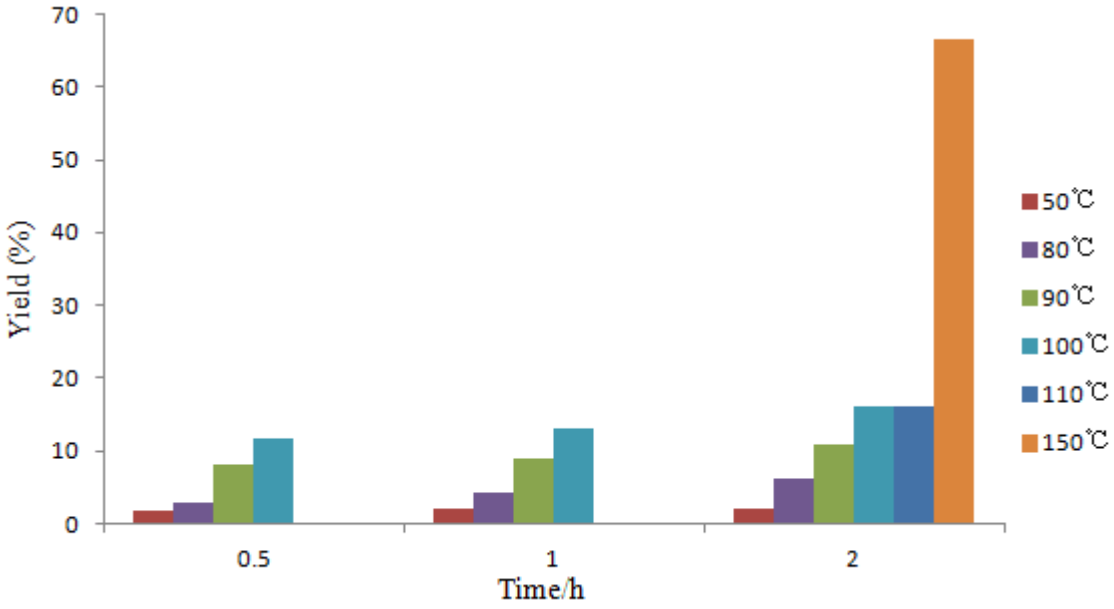

Figure 1-12 Acetophenone yield *vs.* reaction time at different temperatures with catalyst Au@SC (COL).

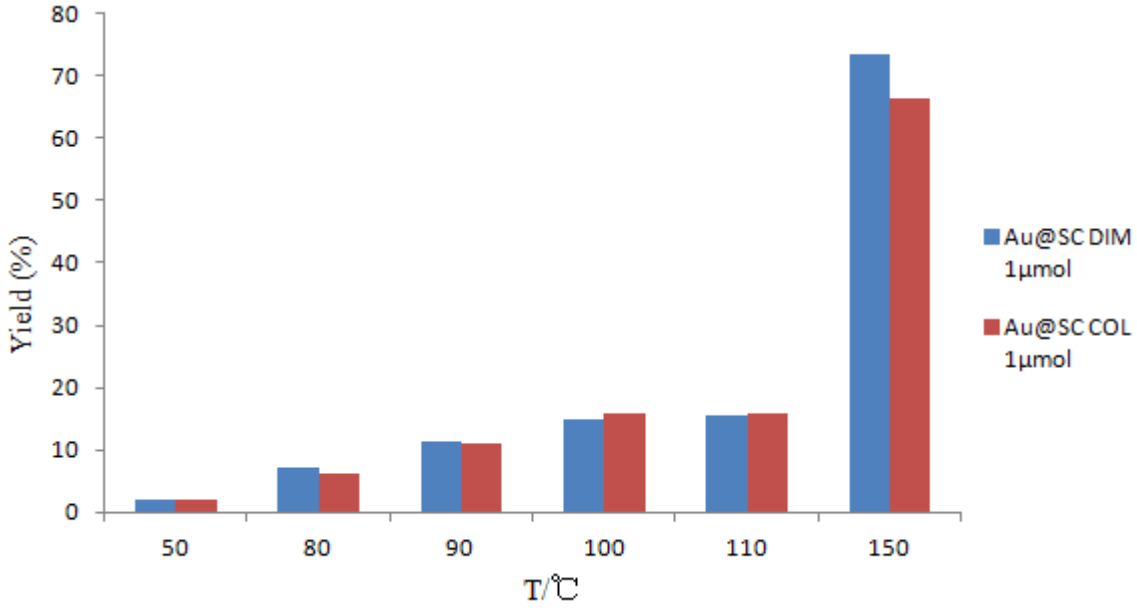

Figure 1-13 Comparison of the acetophenone yield *vs.* temperature for 2 h reaction time with catalyst Au@SC obtained by different heterogenization methods.

From the graphs showed above, it can be observed that a comparatively higher yield is obtained at 150 ℃ both in DIM and COL methods, and the yield increased 58.5% with catalyst Au@SC (DIM); when the temperature increased from 110 to 150 ℃. The yield showed an increase of 50.5% with catalyst Au@SC (COL) from 110 to 150 ℃, which means that the suitable temperature for catalyst Au@SC

regarding the oxidation of 1-phenylethanol is 150 ℃.

3.2.2 Influence of reaction time

A series of experiments have been done to understand how catalytic performance is affected by the duration of the microwave irradiation. The yields of acetophenone in these conditions were presented in **Figures 1-14** and **1-15**, as a function of temperature, programmed in the microwave reactor.

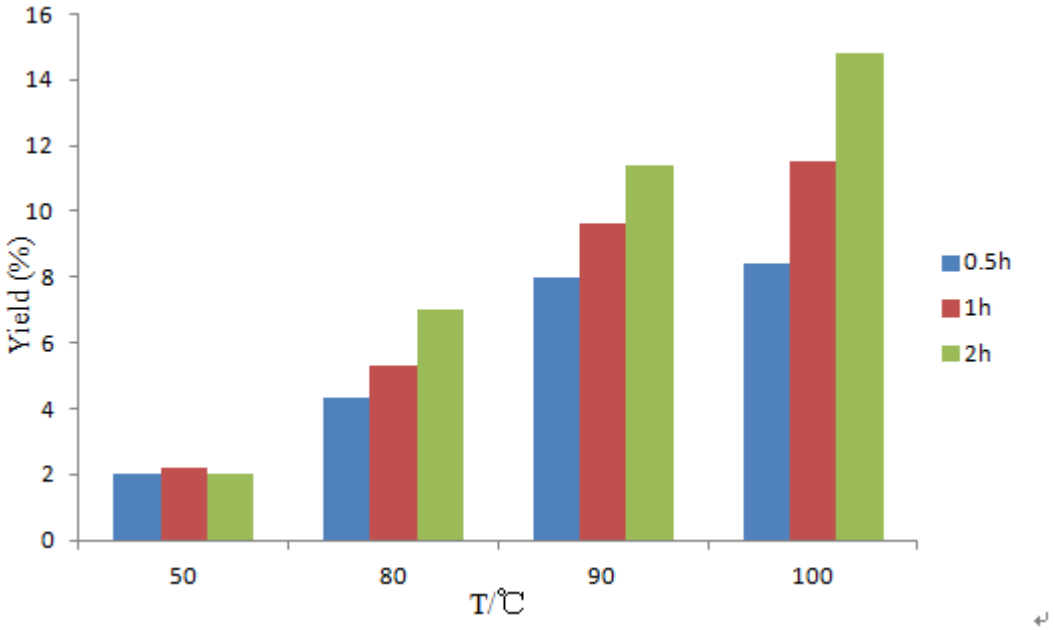

Figure 1-14 Acetophenone yield *vs.* temperature at different reaction time with catalyst Au@SC (DIM).

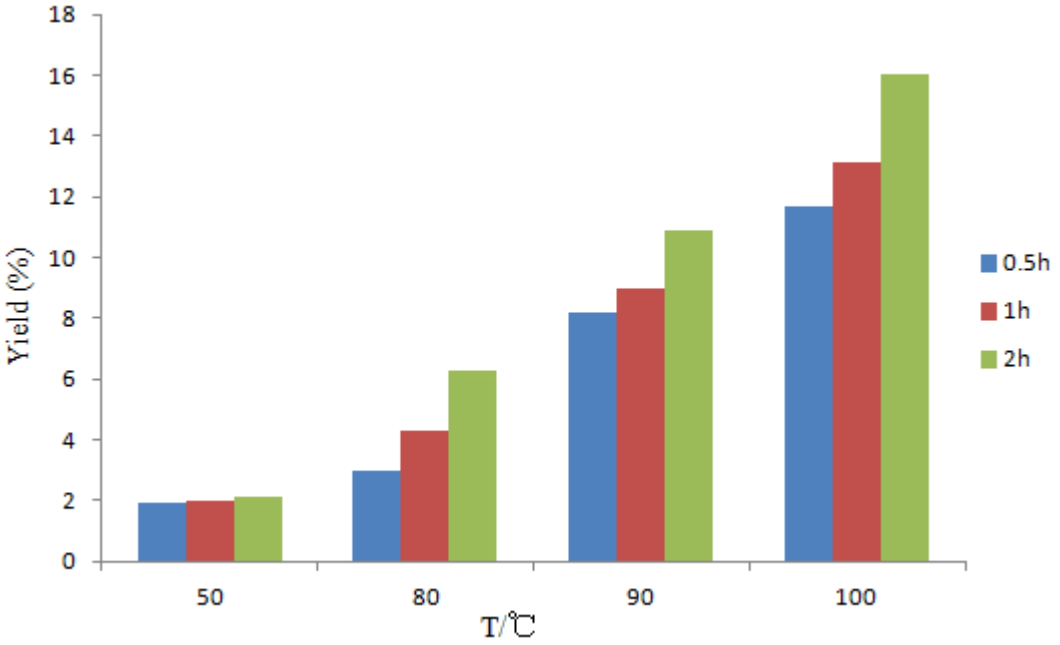

Figure 1-15 Acetophenone yield *vs.* temperature at different reaction time with catalyst Au@SC (COL).

Regarding **Figures 1-14** and **1-15**, in the case of 1% Au supported at SC (DIM and COL), it can be observed that the yields are increased by increasing the reaction time at different temperatures, so 2 hours is the appropriate time for the oxidation of 1-phenylethanol of catalyst Au@SC.

3.2.3 Influence of catalyst quantity

A series of experiments have been done to know the influence of catalyst quantity on the acetophenone yield. The results are shown in **Figure 1-16**.

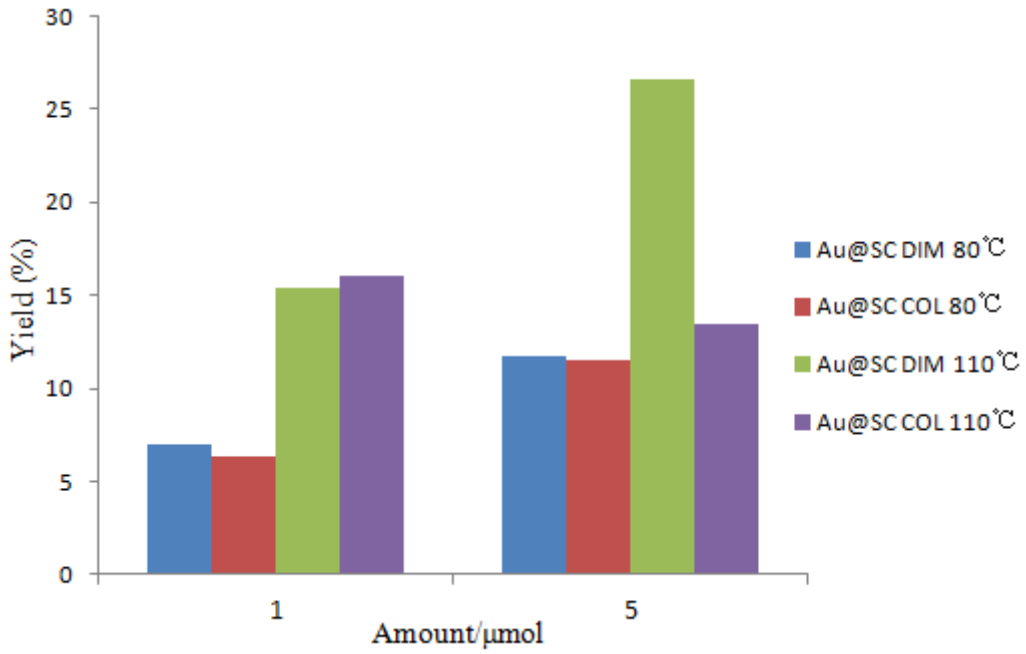

Figure 1-16 Acetophenone yield *vs.* amount of catalyst at different temperatures for 2 h reaction with catalyst Au@SC.

From **Figure 1-16**, it can be observed that with the quintuple amount of the catalysts, the yield increased 4.7% and 5.2%, respectively, for catalyst Au@SC (DIM) and Au@SC (COL) at 80 ℃. In the case of 1% Au supported at SC (DIM), the yield increased 29.3% at 110 ℃, so it can be concluded that a higher quantity of catalysts produced a higher amount of acetophenone.

3.2.4 Influence of additive TEMPO

After carrying out experiments involving parameters such as different temperatures, reaction times and catalyst quantities, the best condition found is 5 μmol of catalyst Au@SC (DIM) at 110 ℃ for 2 hours. Thus we have changed the amount of ^{t}BuOOH and added additive TEMPO. The results are presented in **Figure 1-17**.

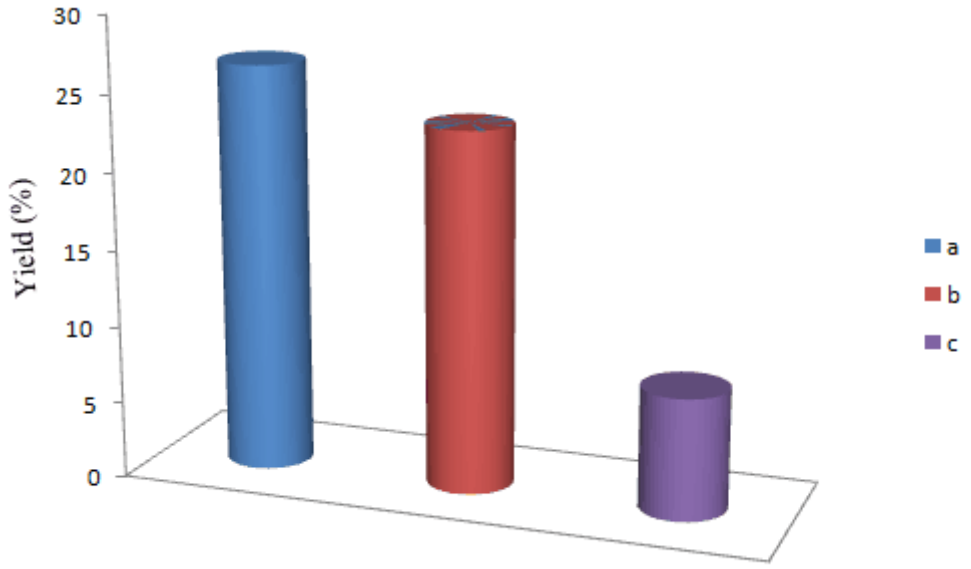

Figure 1-17 Acetophenone yield *vs.* additive with catalyst Au@SC (DIM). Reaction conditions: catalyst (5 μmol), 110 ℃, 2 h, **a**: TBHP (5 mmol); **b**: TBHP (10 mmol); **c**: TBHP (5 mmol), in the presence of TEMPO (2.5 mol %).

From **Figure 1-17** it showed that when twice the amount TBHP at 110 ℃ with catalyst Au@SC (DIM), the yield decreased 3.2%, as well as when adding 2.5 mol% TEMPO (in the presence of 5 mmol TBHP), the yield decreased 18.7%. So it can be concluded that twice the amount of TBHP and the TEMPO additive did not improve the catalytic activity of Au@SC (DIM).

3.3 Oxidation of 1-phenylethanol catalyzed by Au@GR

1% Au NPs supported at graphite (GR) was tested as a heterogeneous catalyst for the microwave-assisted solvent-free oxidation of 1-phenylethanol by ^{t}BuOOH. The catalytic parameters were related to the temperature, reaction time, additive and other conditions. The results are presented as follows.

3.3.1 Influence of temperature

Several experiments have been performed and it was found that the temperature influenced the acetophenone yield. All the results are shown in **Figures 1-18** to **1-20**.

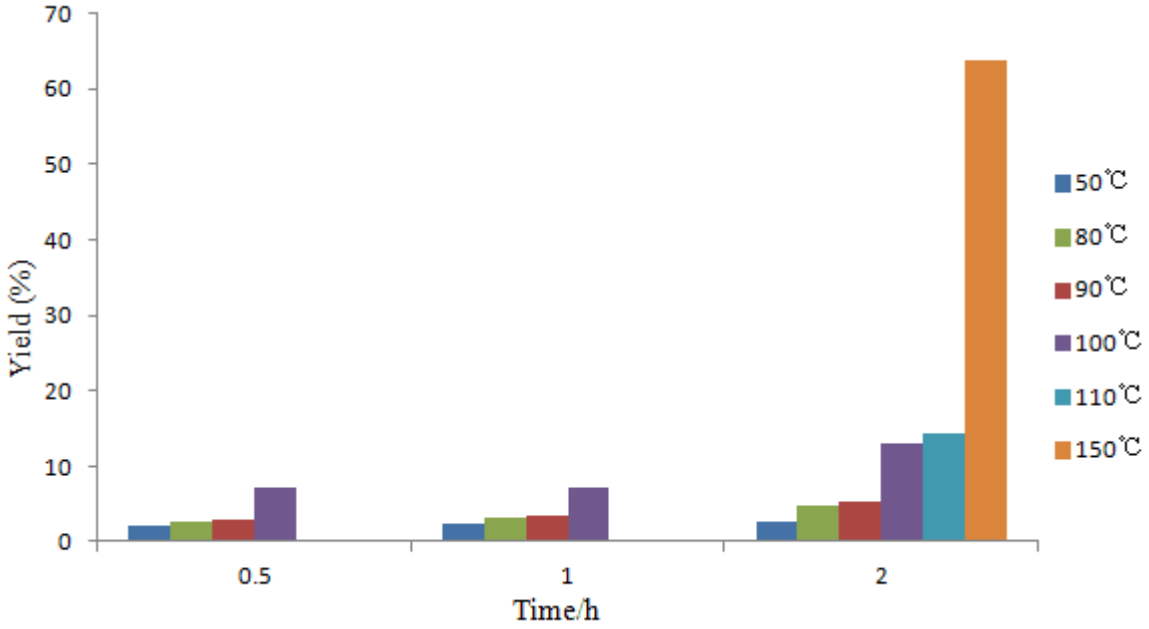

Figure 1-18 Acetophenone yield *vs.* reaction time at different temperatures with catalyst Au@GR (DIM).

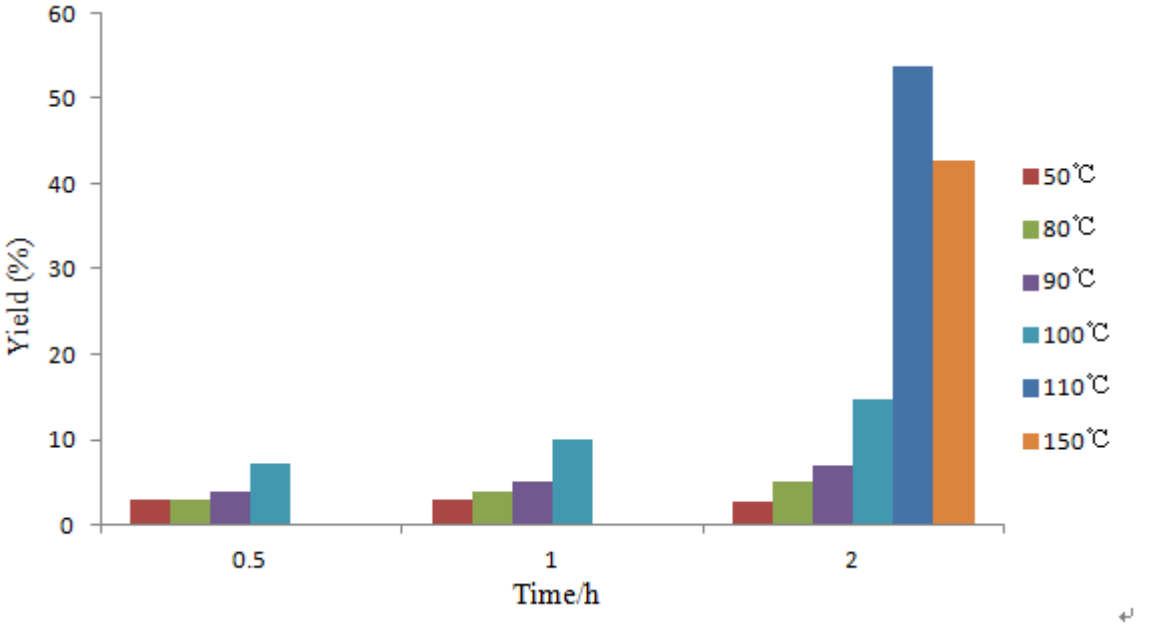

Figure 1-19 Acetophenone yield *vs.* reaction time at different temperatures with catalyst Au@GR (COL).

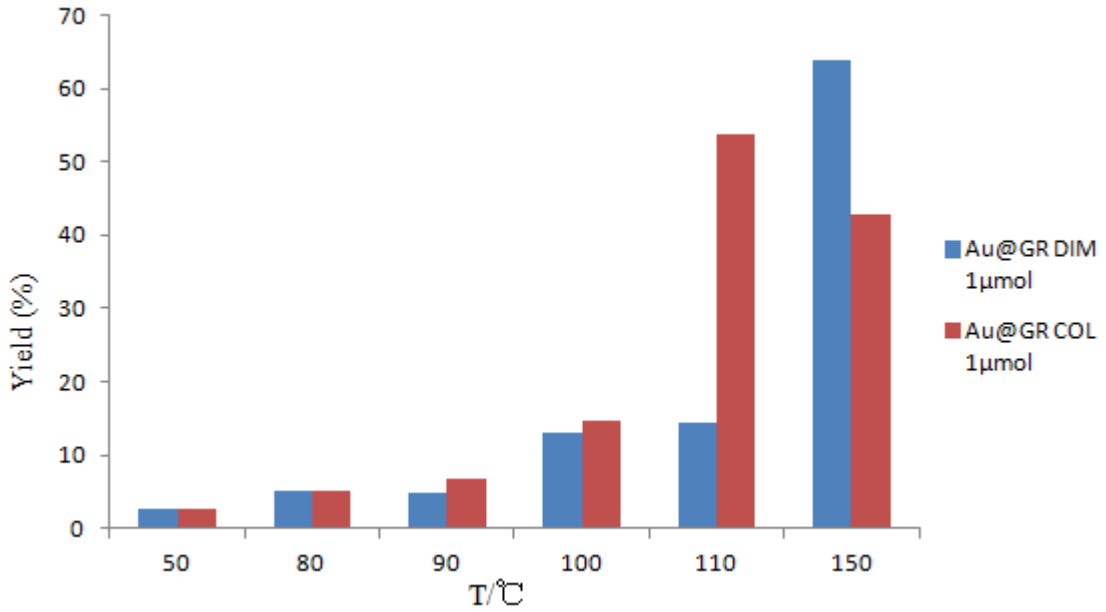

Figure 1-20 Comparison of the acetophenone *vs.* temperature for 2 h reaction time with catalyst Au@GR obtained by different heterogenization methods.

From **Figure 1-20**, it can be observed that the yield of acetophenone is increased with raising the reaction temperature, except for catalyst 1% Au supported at GR (COL), the yield decreased 11% from 110 to 150 ℃. While for catalyst Au@GR (DIM), the yield increased 49.5% from 110 to 150 ℃. So it can be figured out that the suitable reaction temperature for Au@GR (DIM) is 110 ℃, and the suitable temperature for Au@GR (COL) is 150 ℃.

3.3.2 Influence of reaction time

A series of experiments was performed to investigate how the reaction time influenced the product yield. The results are shown in **Figures 1-21** and **1-22**.

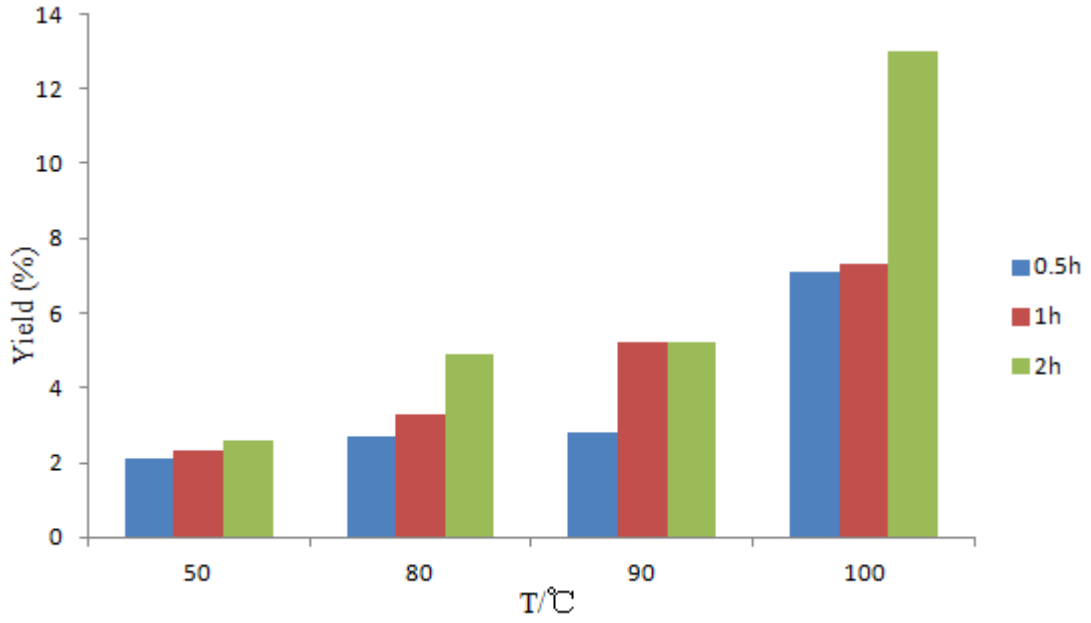

Figure 1-21 Acetophenone yield *vs.* temperature at different reaction time with catalyst Au@GR (DIM).

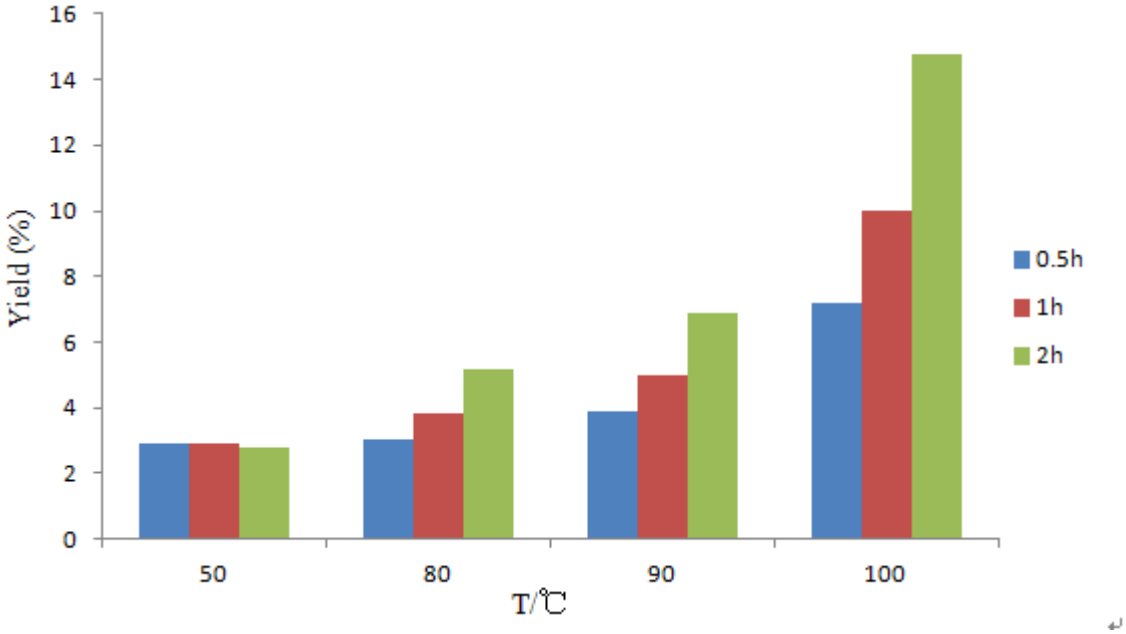

Figure 1-22 Acetophenone yield *vs.* temperatures at different reaction time with catalyst Au@GR (COL).

It can be observed from the graphs above that the yield increased for a longer reaction time for both catalysts Au@GR (DIM) and Au@GR (COL). 2 h reaction time produced a higher quantity of acetophenone when compared with 0.5 and 1 h reaction time.

3.3.3 Influence of catalyst quantity

In this section, different quantities (1 and 5 μmol) of catalysts were used to evaluate the catalytic activity of the gold supported catalysts with oxidation of 1-phenylethanol. The results are shown in **Figure 1-23**.

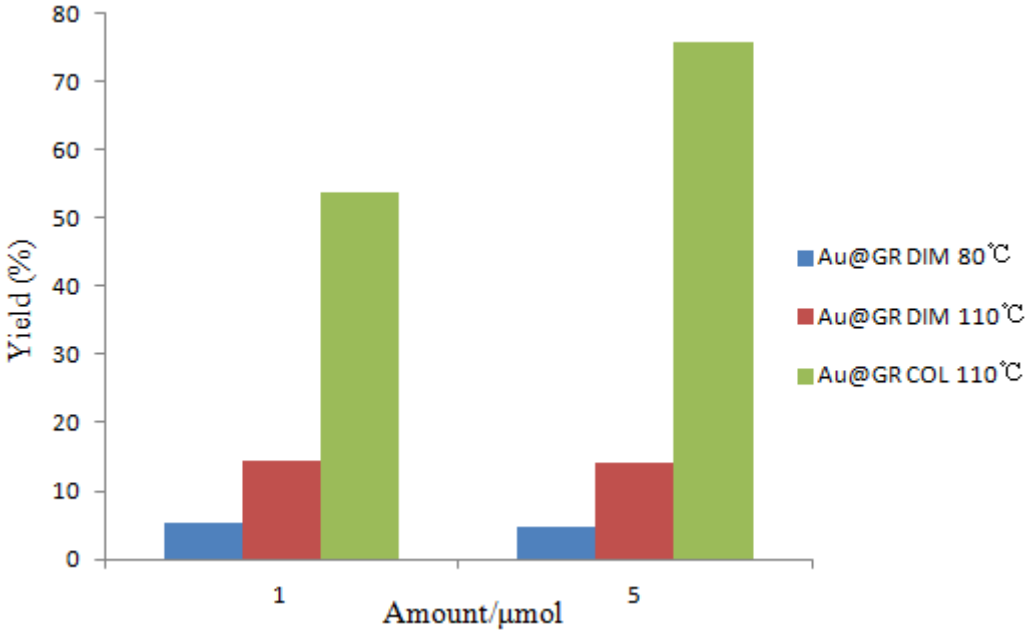

Figure 1-23 Acetophenone yield *vs.* amount of catalyst at different temperatures for 2 h-reaction with catalyst Au@GR.

From **Figure 1-23**, in the case of 1% supported at GR (DIM) at 80 ℃, the yield decreased 0.5% with quintuple the amount of catalyst, as well as at 110 ℃, the yield decreased 0.2%. However, the yield increased 22% with the quintuple quantity of catalyst Au@GR (COL) at 110 ℃. So it can be concluded that higher quantity of catalyst was considered as a better condition for the oxidation of 1-phenylethanol of catalyst Au@GR (COL) with high temperature.

3.3.4 Influence of additive TEMPO

After performing experiments involving parameters such as different temperatures, reaction time and catalyst quantities, the desirable condition found is 5 μmol of catalyst Au@GR (DIM) at 110 ℃ for 2 hours. Thus we have changed the amount of ^{t}BuOOH and added the TEMPO additive. The results are shown in **Figure**

1-24.

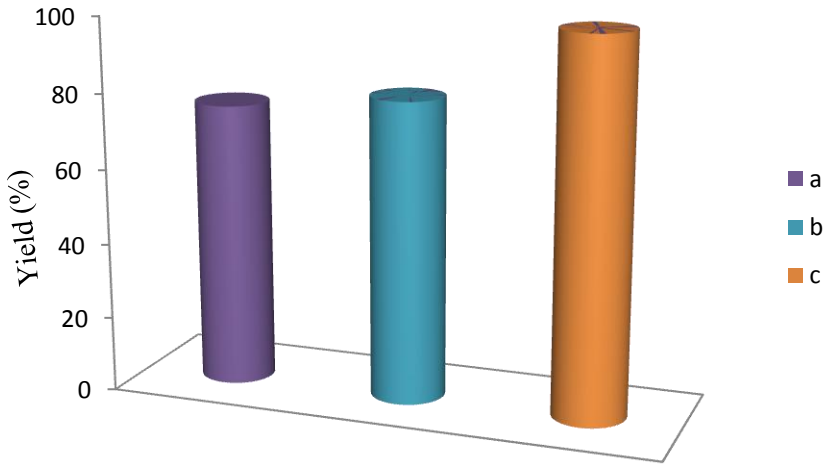

Figure 1-24 Acetophenone yield *vs.* additive with catalyst Au@GR (DIM). Reaction conditions: catalyst (5 μmol), 110 ℃, 2 h, **a**: TBHP (5 mmol); **b**: TBHP (10 mmol); **c**: TBHP (10 mmol), in the presence of TEMPO (2.5 mol %).

From **Figure 1-24**, it can be observed that when twice the amount of TBHP was added, in the case of catalyst Au@AC at 110 ℃, the yield increased 4.5%, while when 2.5mol % TEMPO additive was added, the yield increased 19.8%. Thus it can be concluded that in the presence of 10 mmol TBHP and 2.5mol % TEMPO, the catalytic activity was higher when compared with 5mmol TBHP and without TEMPO.

3.4 Oxidation of 1-phenylethanol catalyzed by Au@CX

1% Au NPs supported at carbon xerogel (CX) was tested as a heterogeneous catalyst for the microwave-assisted solvent-free oxidation of 1-phenylethanol by ^{t}BuOOH. The catalytic activity was related to temperature, reaction time and other conditions.

3.4.1 Influence of temperature

A series of experiments have been done indicated that the reaction temperature influences the product yield. The results are shown in **Figures 1-25** to **1-27**.

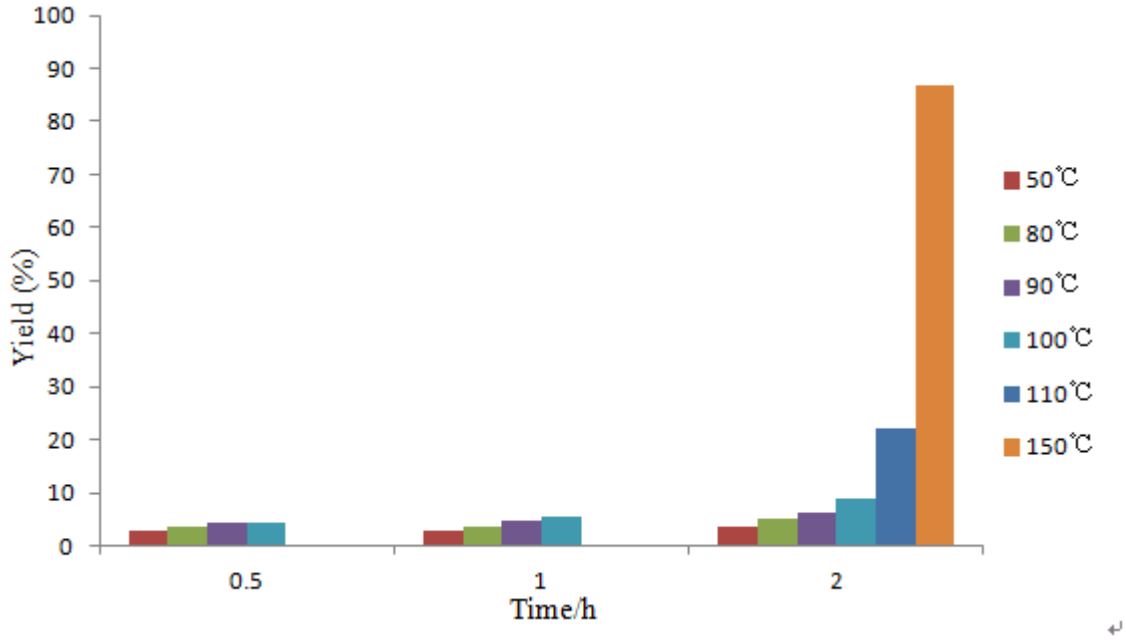

Figure 1-25 Acetophenone yield *vs.* reaction time at different temperatures with catalyst Au@CX (DIM).

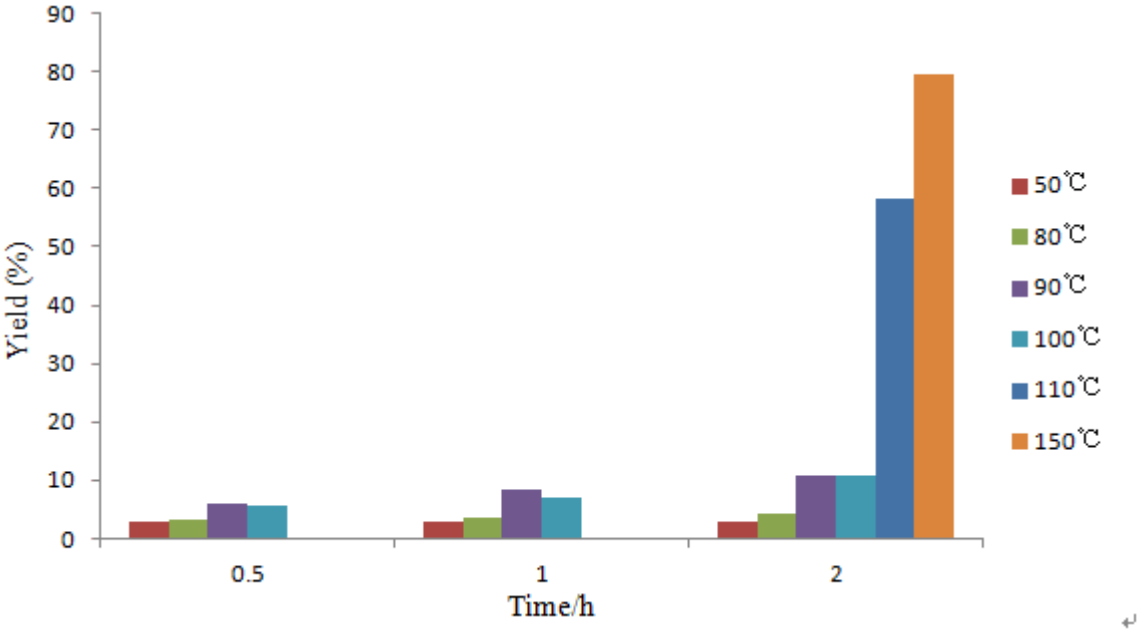

Figure 1-26 Acetophenone yield *vs.* reaction time at different temperatures with catalyst Au@CX (COL).

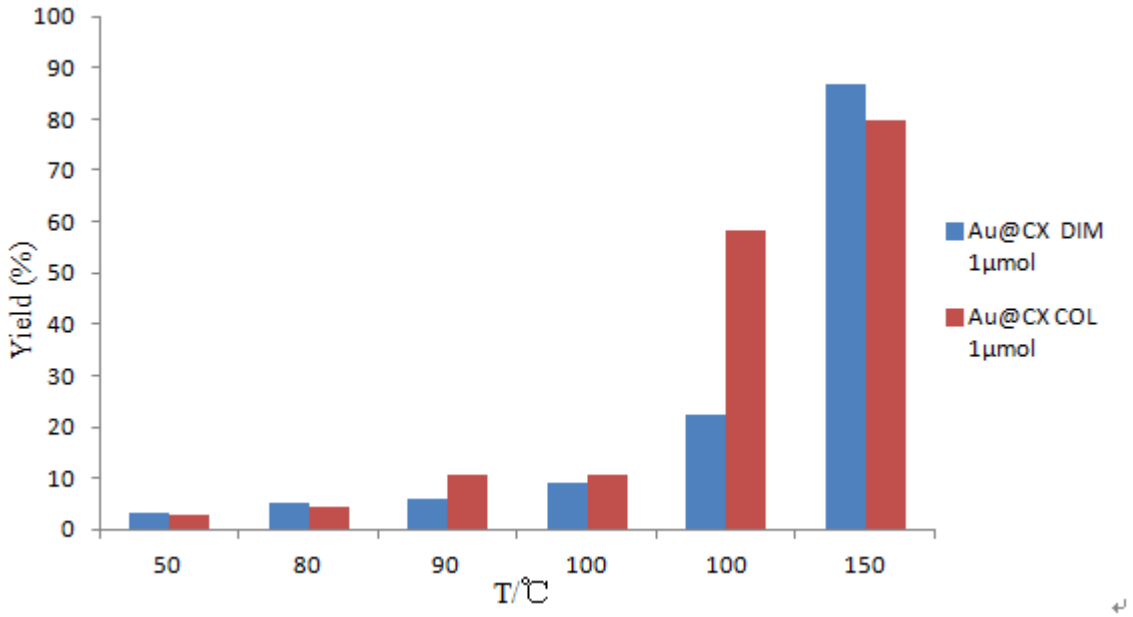

Figure 1-27 Comparison of the acetophenone yield *vs.* temperature for 2 h reaction time with catalyst Au@CX obtained by different heterogenization methods.

From **Figure 1-27**, it can be observed that the acetophenone yield increased when raised the temperature, and in the case of 1% Au supported at CX (DIM), the yield increased 64.5% from 110 to 150 ℃. Therefore, it can be concluded that the best reaction temperature for catalyst Au@CX either by DIM method or COL preparation is 150 ℃.

3.4.2 Influence of reaction time

In this section, different reaction times were performed to discuss the relationship between reaction time and catalyst catalytic activity of catalyst Au@CX. The detailed results are present in **Figures 1-28** and **1-29.**

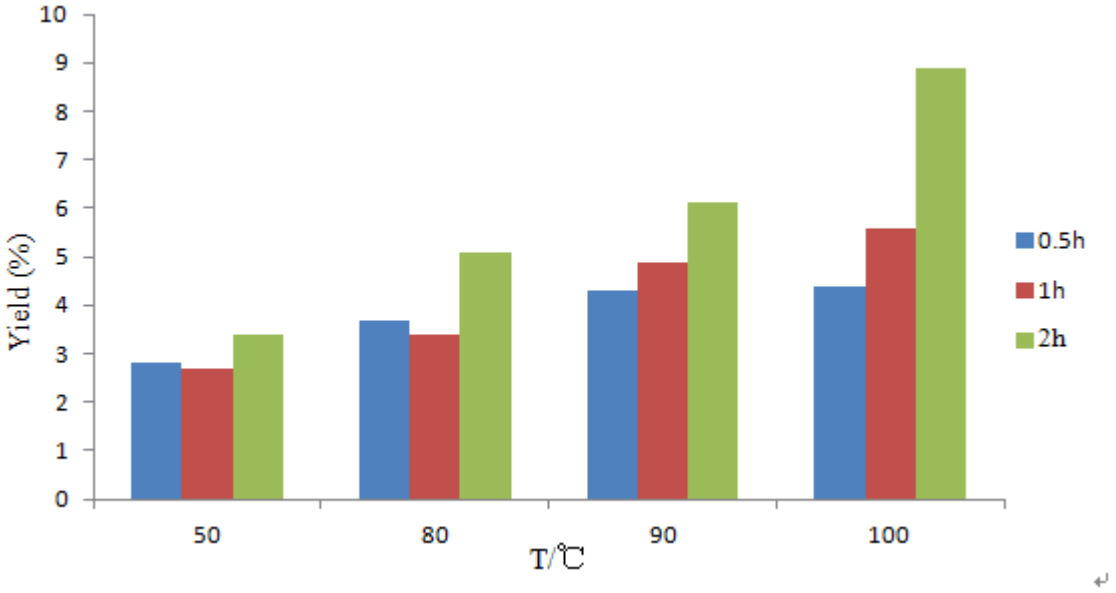

Figure 1-28 Acetophenone yield *vs.* temperature at different reaction time with catalyst Au@CX (DIM).

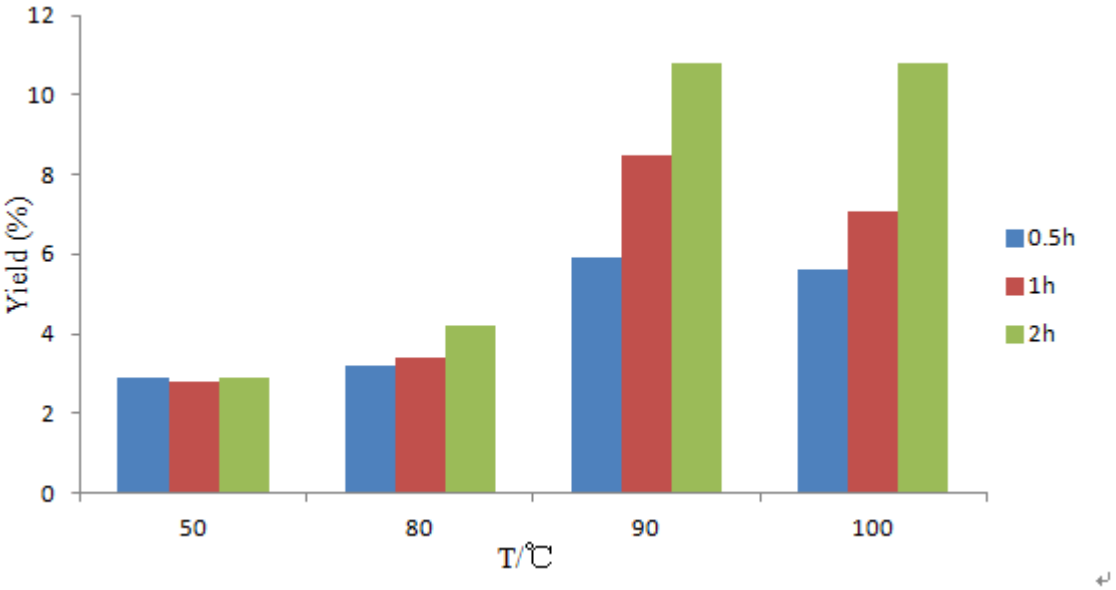

Figure 1-29 Acetophenone yield *vs.* temperatures at different reaction times with catalyst Au@CX (DIM).

From **Figures 1-28** and **1-29**, it can be figured out that a longer reaction time (2 h) led to higher yields. Therefore, in the case of 1% Au supported on CX, the suitable reaction time is 2 hours.

3.4.3 Influence of catalyst quantity

A series of experiments have been performed to know the influence of the

quantity of catalyst on acetophenone yield. The results are shown in **Figure 1-30**.

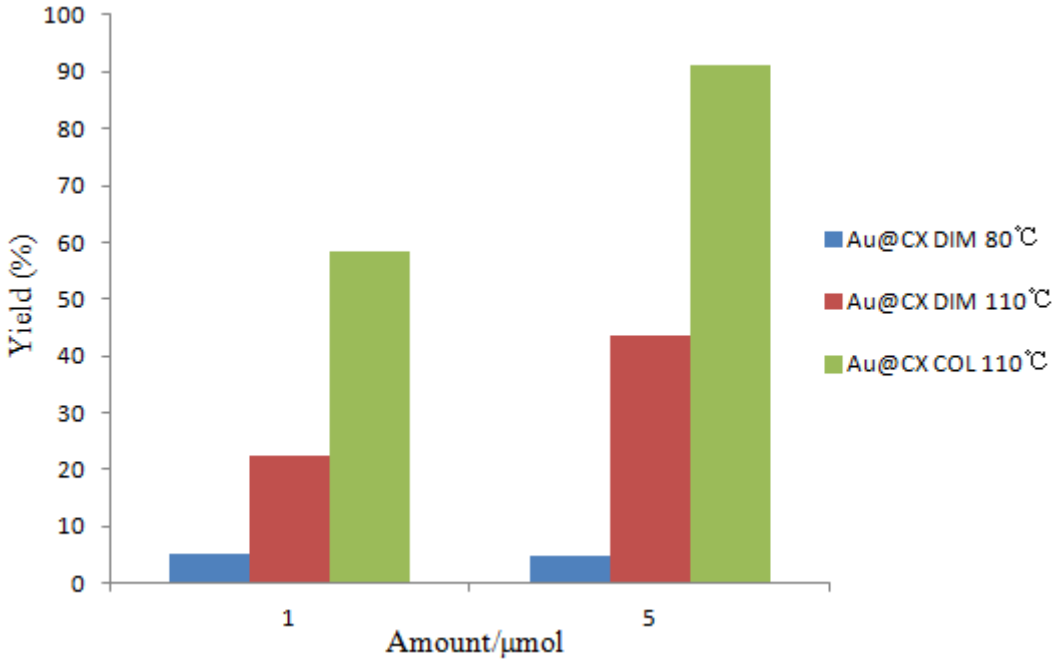

Figure 1-30 Acetophenone yield *vs.* amount of catalyst at different temperatures for 2 h reaction with catalyst Au@CX.

From **Figure 1-30**, it can be observed that with the quintuple quantity of the catalysts, the yield decreased 0.5% at 80 ℃ regarding catalyst Au@CX (DIM). However in the case of 1% Au supported at CX at 110 ℃, both in DIM and COL method, the yields increased. So the higher quantities of catalysts are regarded as better conditions for the oxidation of 1-phenylethanol with catalyst Au@CX.

3.4.4 Influence of additive TEMPO

After carrying out experiments regarding parameters such as different temperatures, reaction times and catalyst quantities, the best condition found is catalyst Au@CX (COL) with 5 μmol quantity under 110 ℃ for 2 hours. Then we have changed the amount of ^{t}BuOOH and added TEMPO additive. The results are shown in **Figure 1-31**.

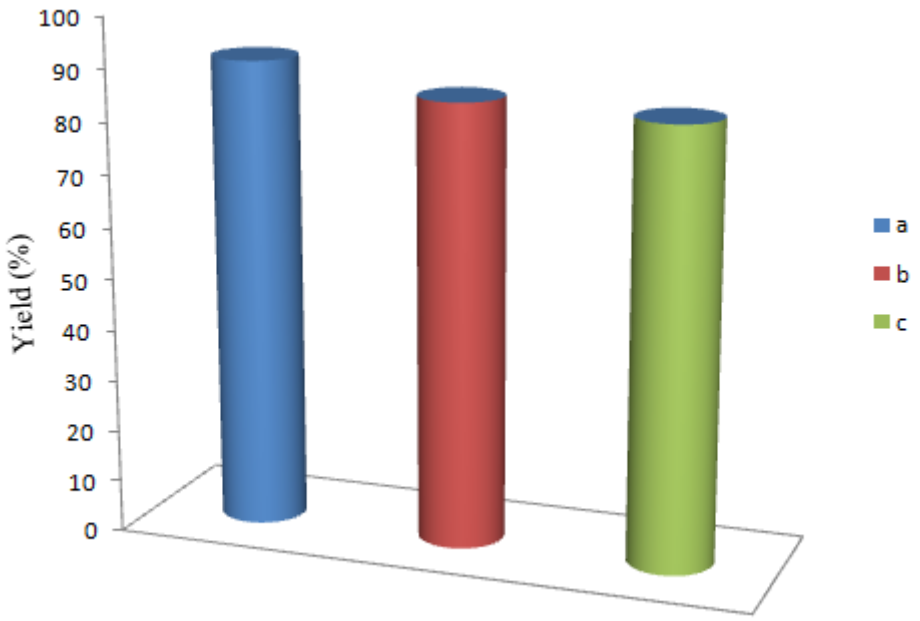

Figure 1-31 Acetophenone yield *vs.* additive with catalyst Au@CX (COL). Reaction conditions: catalyst (5 μmol), 110 ℃, 2 h, **a**: TBHP (5 mmol); **b**: TBHP (10 mmol); **c**: TBHP (5 mmol), in the presence of TEMPO (2.5 mol %).

From **Figure 1-31**, it can be observed that when adding twice the amount of TBHP at 110 ℃ of catalyst Au@CX (COL), the yield decreased 5.3%, as well as when adding 2.5 mol% TEMPO, the yield decreased 1.3%. Thus it can be concluded that 10 mmol TBHP and 2.5 mol% TEMPO did not help the increasing of the activity of the catalyst Au@CX (COL).

3.5 Oxidation of 1-phenylethanol catalyzed by Au@CXL

1% Au NPs supported on carbon xerogel (CXL) was tested as a heterogeneous catalyst for the microwave-assisted solvent-free oxidation of 1-phenylethanol by ^{t}BuOOH. The catalytic activity was related to the temperature, reaction time and other conditions. The results are presented as follows.

3.5.1 Influence of temperature

Several experiments have been done at different reaction times, more specifically, the catalytic activity can be performed at different reaction temperatures (60, 100, 110 and 150 ℃). The results are presented in **Figure 1-32**.

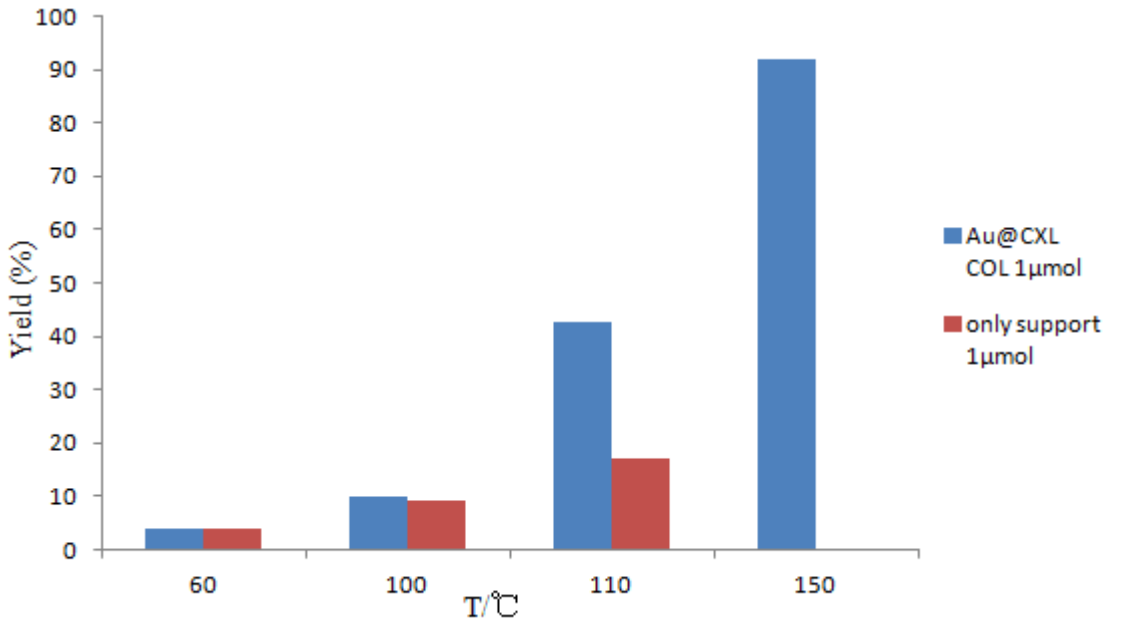

Figure 1-32 Comparison of the acetophenone yield *vs.* temperature for 2 h reaction time with catalyst Au@CXL obtained by different heterogenization methods.

It can be found that regarding the catalyst 1% Au supported at CXL that the yield of acetophenone increased by raising the temperature from 60 to 150 ℃, so it can be concluded that the best reaction temperature for catalyst Au@CXL was 150 ℃.

3.5.2 Influence of the support

From **Figure 1-32**, in the presence of carbon material, the yield of the product was much lower than Au supported at CXL prepared with COL method, at 110 ℃.

3.5.3 Influence of catalyst quantity

Catalyst Au@CXL (COL) was selected to discuss how the quantity of catalyst influences the catalytic activity. The results are shown in **Figure 1-33**.

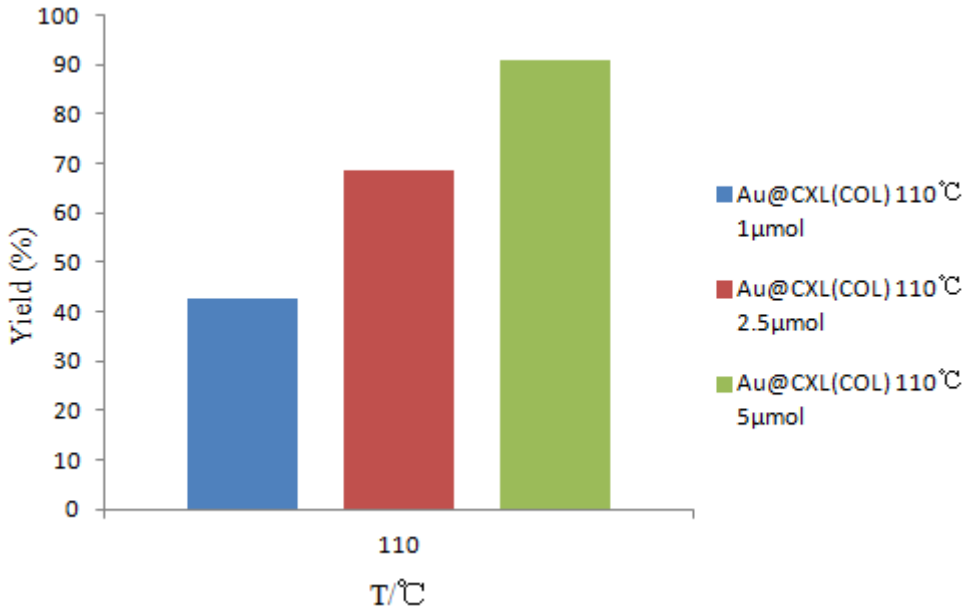

Figure 1-33 Acetophenone yield *vs.* amount of catalyst for 2 h reaction at 110 ℃ with catalyst Au@CXL (COL).

From **Figure 1-33**, it can be observed that with 2 hours reaction at 110 ℃, the yield increased by raising the quantity of Au@CXL catalyst. Thus in this case, the higher quantity of catalyst was considered as a better condition for the oxidation of 1-phenylethanol with catalyst Au@CXL (COL).

3.5.4 Influence of additive TEMPO

After performing experiments regarding parameters such as different temperatures, reaction times and catalyst quantities, the best condition found is catalyst Au@CX (COL) with 5 μmol quantity at 110 ℃ for 2 hours. Then we have changed the amount of ^{t}BuOOH and added TEMPO additive. The results are as follows.

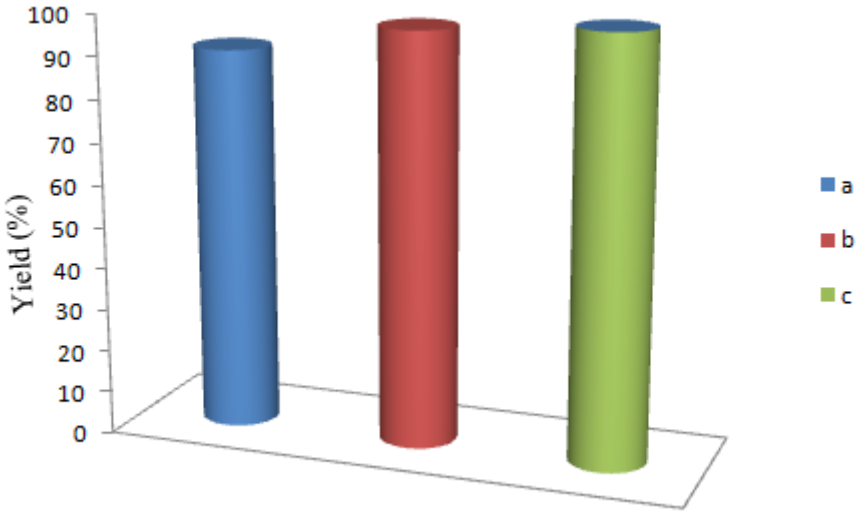

Figure 1-34 Acetophenone yield *vs.* additive with catalyst Au@CXL (COL). Reaction conditions: catalyst (5 μmol), 110 ℃, 2 h, **a**: TBHP (5 mmol); **b**: TBHP (10 mmol); **c**: TBHP (10 mmol), in the presence of TEMPO (2.5 mol %).

From **Figure 1-34**, in the case of 1% Au@CXL (COL), the yield increased 7% when adding twice the amount of TBHP, as well as when adding 2.5mol% TEMPO additive, the yield was almost 99%, thus it can be concluded that 10 mmol TBHP and 2.5mol % TEMPO additive promote the catalytic activity of Au@CXL (COL).

When compared with Au@CX (COL), the catalytic activity of catalyst Au@CXL (COL) was different when adding twice the amount of TBHP. As mentioned before, Elodie and his colleagues have found that for glycerol oxidation, Au/5CX (d_{BJH} =5 nm) catalyst leads to GLYCEA as the main product (selectivity of 48% at X_{GLY} =90%), while Au/20CX (d_{BJH} =20 nm) favors the constitution of DIHA (selectivity of 42% at X_{GLY} =90%), the reason is that narrow pores in the support can result in an easier over-oxidation of the primary products. As in our case, there is no secondary products, but when twice the amount of TBHP was added, the yield was decreased with catalyst Au@CX (COL), and yield increased with catalyst Au@CXL (COL), it might because that the over-oxidation was occurred more for narrow pores than large pores, and become an obstructive factor for the oxidation for 1-phenylethanol.

3.6 Oxidation of 1-phenylethanol catalyzed by Au@ND

1% Au NPs supported at nanodiamonds (ND) was used as a heterogeneous

catalyst for the microwave-assisted solvent-free oxidation of 1-phenylethanol by ^{t}BuOOH. The catalytic activity was influenced by temperature, reaction time and other conditions. The results are shown below.

3.6.1 Influence of temperature

A series of experiments with different temperatures have been performed, and it was observed that the temperature affects the catalytic activity. The results are shown below.

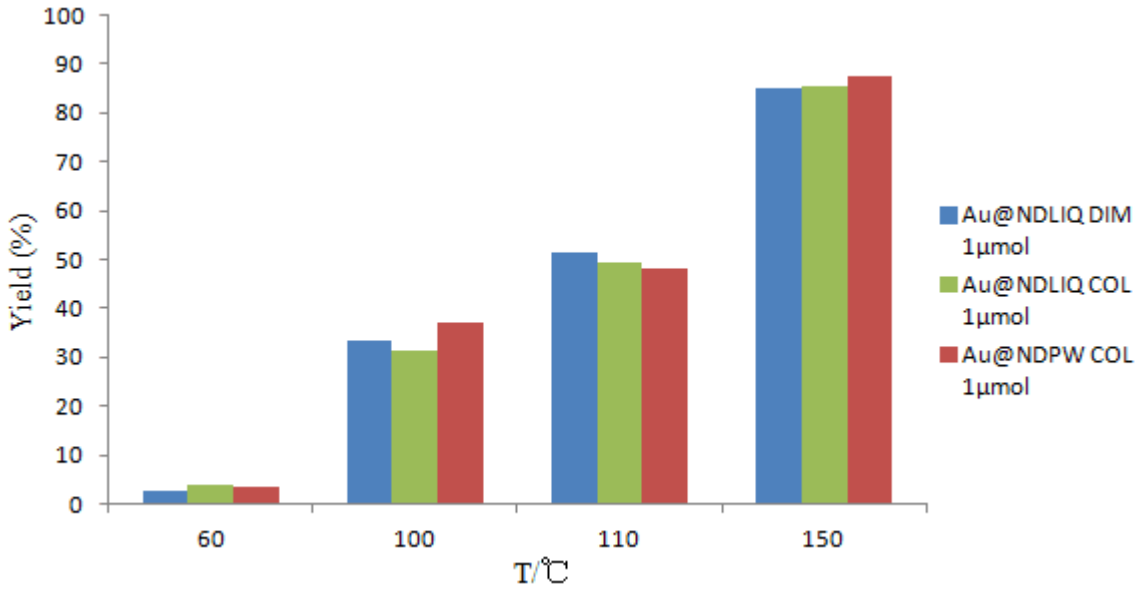

Figure 1-35 Acetophenone yield *vs.* temperature for 2 h reaction with catalyst Au@ND.

Figure 1-35 shows that the acetophenone yield increases for higher temperatures, and the yield was much higher at 150 ℃ than 60 ℃, for example, the acetophenone yield of 1% Au supported at NDLIQ (DIM) at 60 ℃ is 2.7%, while the yield at 150 ℃ is 84.9%, so it can be concluded that temperature above 100 ℃ is better for the oxidation of 1-phenylethanol.

3.6.2 Influence of catalyst quantity

Several experiments with different catalyst quantities have been performed, and it was found that the catalyst quantity influenced the acetophenone yield. The results are shown in **Figure 1-36**.

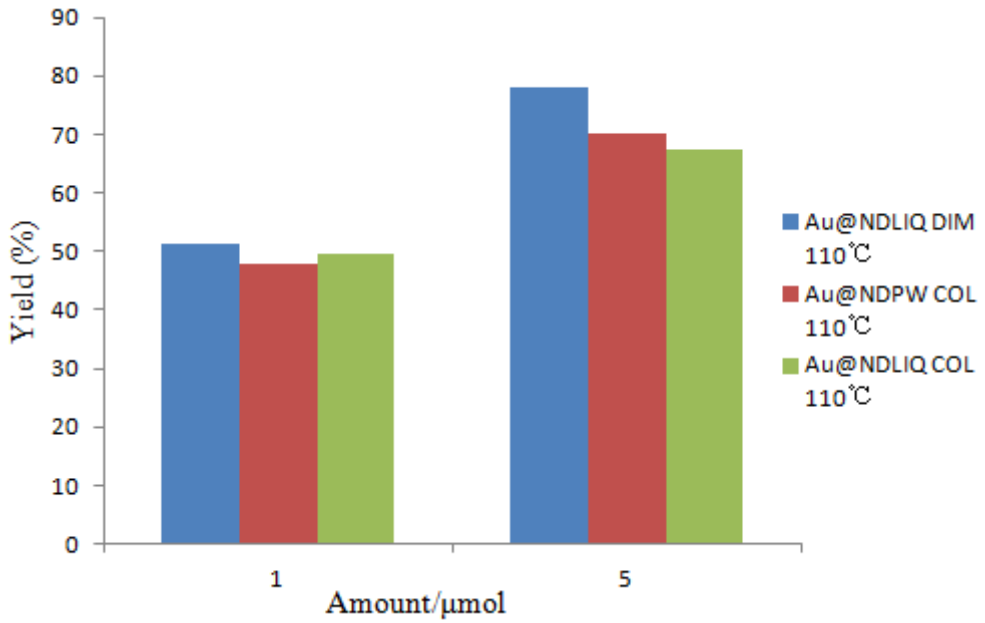

Figure 1-36 Acetophenone yield *vs.* amount of catalyst for 2 h reaction with catalyst Au@ND.

From **Figure 1-36**, it can be observed when the quintuple amount of catalysts, the yield of catalyst 1% Au supported at ND increased at 110 ℃, and for instance, the yield of Au@NDLIQ (DIM) increased 26.8% when adding quintuple quantity catalyst. It can be concluded that a higher quantity of catalyst was regarded as a better condition for the oxidation of 1-phenylethanol with catalyst Au@ND.

3.6.3 Influence of additive TEMPO

After carrying out experiments regarding parameters change, such as different temperatures, reaction time and catalyst quantities, it can be concluded that the best conditions are: 5 μmol of catalyst Au@NDLIQ (DIM) at 110 ℃ for 2 hours. Thus we have changed the amount of ^{t}BuOOH and added additive TEMPO. The results of the catalytic activity are shown as follows.

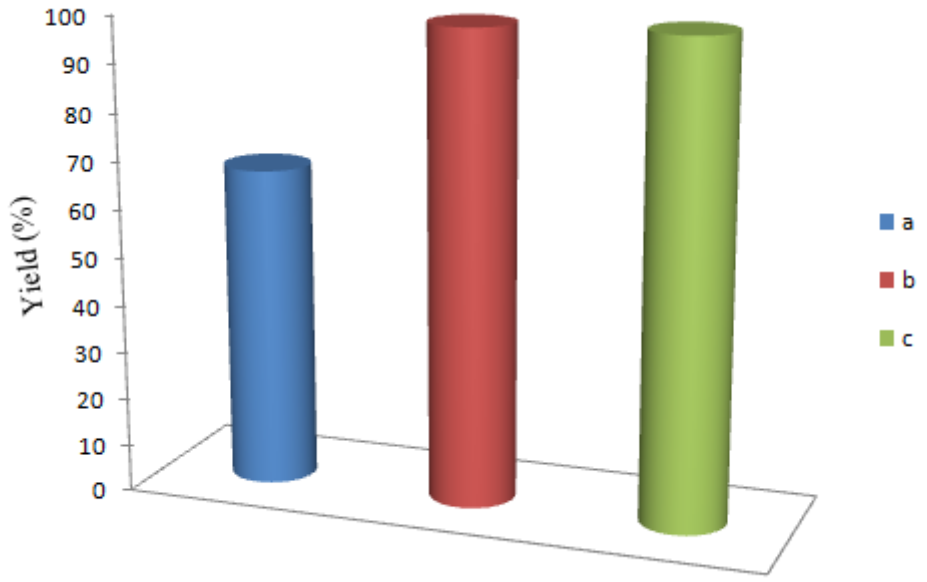

Figure 1-37 Acetophenone yield *vs.* additive with catalyst Au@NDLIQ (DIM). Reaction conditions: catalyst (5 μmol), 110 ℃, 2 h, **a**: TBHP (5 mmol); **b**: TBHP (10 mmol); **c**: TBHP (10 mmol), in the presence of TEMPO (2.5 mol %).

Figure 1-37 showed that when twice the amount of TBHP was added in the reaction, the yield increased 31.9% with catalyst Au@NDLIQ (DIM), since the yield is already 99.2% after the TBHP was added, so the catalytic activity did not have a significant difference after 2.5 mol % TEMPO additive was added.

3.7 Oxidation of 1-phenylethanol catalyzed by Au@MD

1% Au NPs supported at micro-diamonds (MD) was used as a heterogeneous catalyst for the microwave-assisted solvent-free oxidation of 1-phenylethanol by ^{t}BuOOH. The catalytic activity was influenced by temperature, reaction time and other conditions. The results are presented below.

3.7.1 Influence of temperature

Several experiments with different temperatures have been performed with catalyst Au@MD (COL), and it was found that temperature has influenced the catalytic activity. The results are shown below.

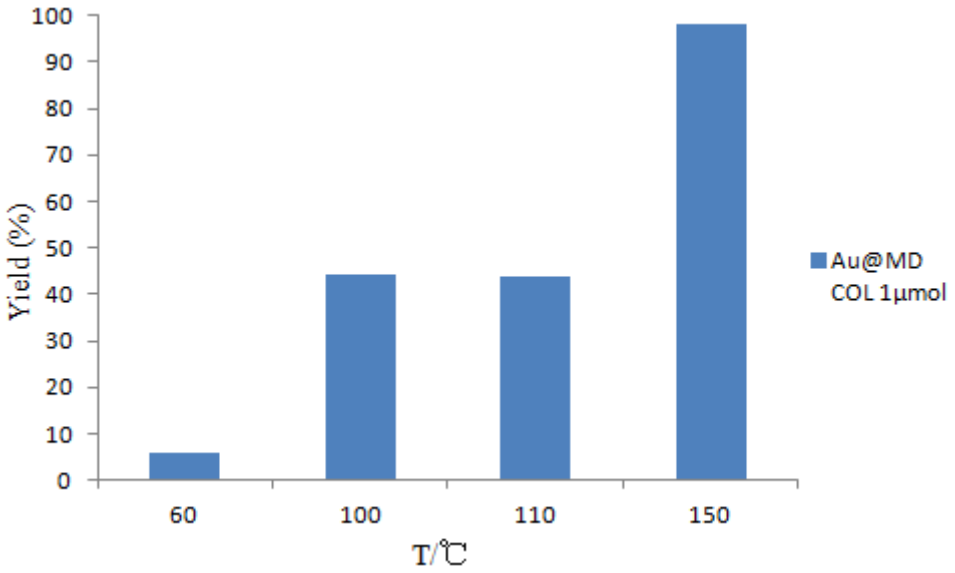

Figure 1-38 Acetophenone yield *vs.* temperature for 2 h reaction with catalyst Au@MD (COL).

From **Figure 1-38**, in the case of 1% Au supported at MD (COL), the yield increased 38.4% from 60 to 100 ℃, and the yield in 110 ℃ is lower than in 100 ℃, while the yield increased 54.5% from 110 to 150 ℃, so the best temperature for the oxidation of 1-phenylethanol with catalyst Au@MD (COL) is 150 ℃.

3.7.2 Influence of catalyst quantity

In this section, a series of experiments with different catalyst quantities have been performed, and it was observed that the catalyst quantity influenced acetophenone yield. The results are presented below.

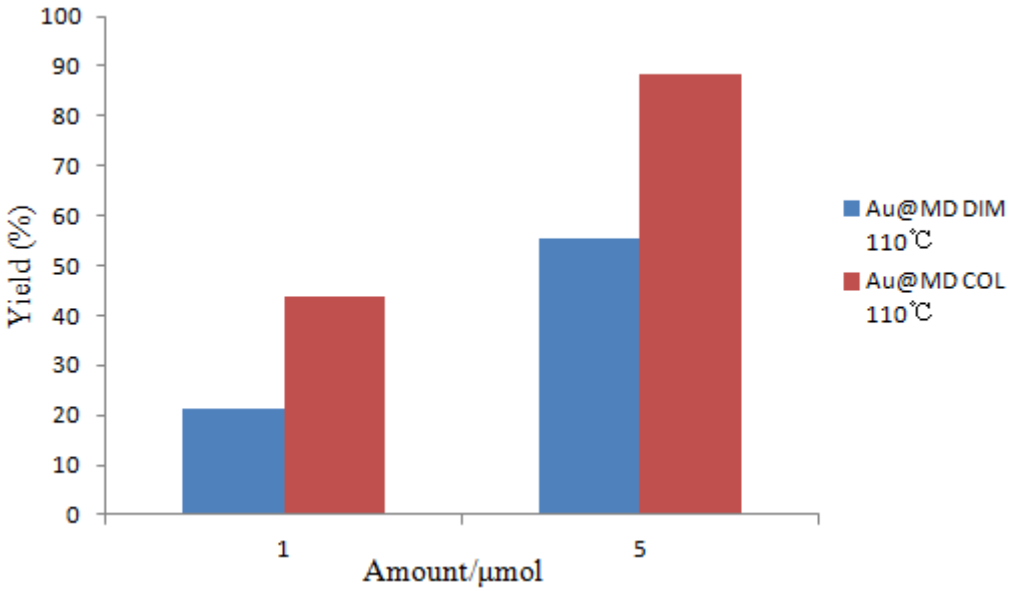

Figure 1-39 Acetophenone yield *vs.* amount of catalyst for 2 h reaction of catalyst Au@MD.

It can be seen from **Figure 1-39** that higher quantity of catalyst obtained higher product yield, for example, in the case of 1% Au supported MD (DIM), the yield increased 34.1% by adding a quintuple quantity of catalyst. So it can be concluded that higher quantity of catalyst promotes a significant increase in catalytic activity of Au@MD.

3.7.3 Influence of heterogenization method

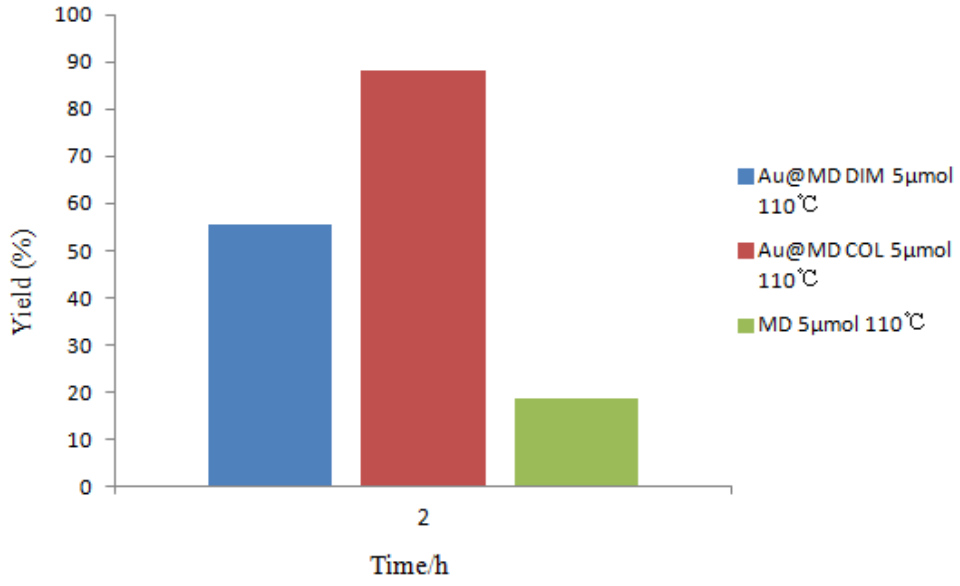

Figure 1-40 Acetophenone yield *vs.* heterogenization method at 110 ℃ for 2 h

reaction time with Au@MD.

From **Figure 1-40**, in the case of the reaction only with support, the yield of product decreased 69.5%, when compared with 1% Au supported at catalyst MD (COL). So it can be concluded that Au is the main active part for the increasing of the catalytic activity of Au@MD catalyst. Moreover, COL heterogenization method leads to better acetophenone yields than DIM procedure.

3.7.4 Influence of oxidant amount

After performing experiments regarding parameters such as different temperatures, reaction times and catalyst quantities, the best conditions found is catalyst Au@MD (COL) with 5 μmol quantity under 110 ℃ for 2 hours. Then we have changed the amount of ^{t}BuOOH. The results are shown as follows.

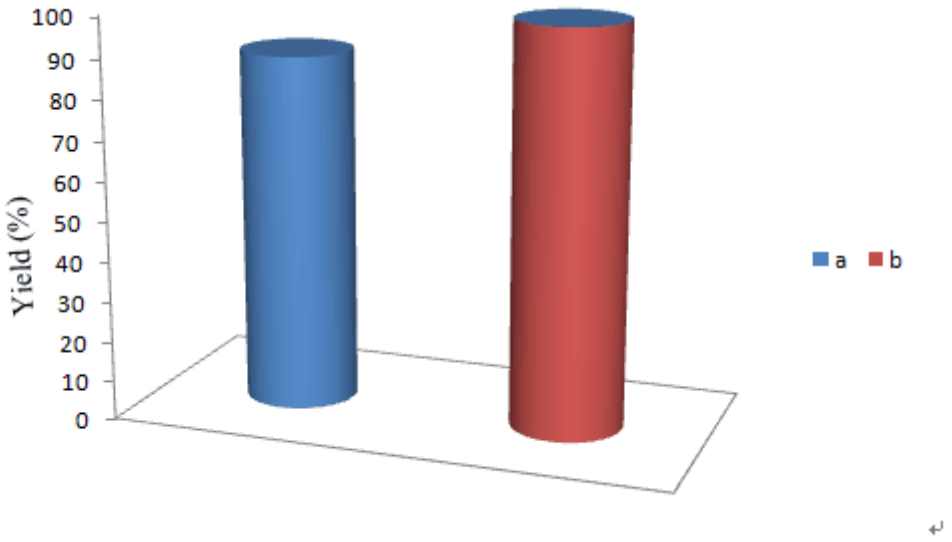

Figure 1-41 Acetophenone yield *vs.* amount of oxidant for catalyst Au@MD (COL). Reaction conditions: catalyst (5 μmol), 110 ℃, 2 h, **a**: TBHP (5 mmol); **b**: TBHP (10 mmol).

From **Figure 1-41**, it can be observed that in the presence of Au@MD (COL), when twice the amount of TBHP was added in the reaction, the yield increased 10%. So 10 mmol TBHP can promote Au@MD (COL) to have better catalytic activity.

3.8 Recycling experiments

The conditions selected for recycling experiments were those leading to the highest yield for each carbon supported material, and they were all tested up to 6 consecutive cycles. In each cycle, the product was tested by gas chromatography and then the catalyst was collected from the reaction vessel and centrifuged (repeated at least 2 times), thoroughly washed and dried under compressed air. Afterward, it was reused for the next 1-phenylethanol oxidation cycle experiment. The molar ratio of substrate to catalyst and oxidant to catalyst was constant. The results are as follows.

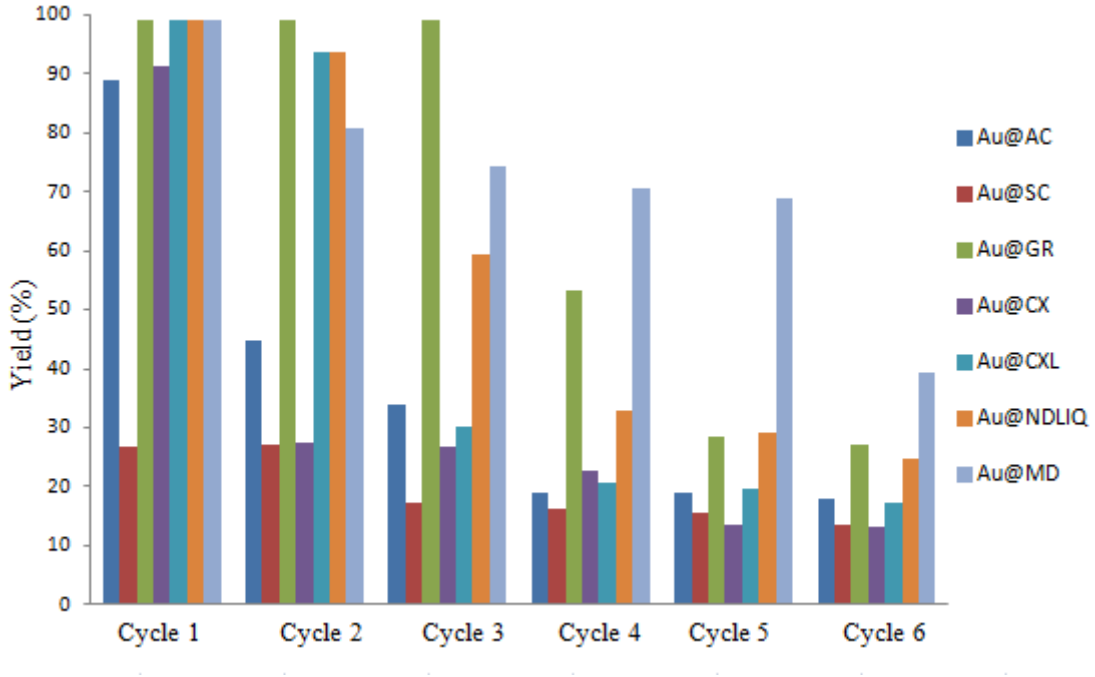

Figure 1-42 Effect of the catalyst recycling on the yield of acetophenone with catalysts. Reaction conditions： 110 ℃ , 2 h. Au@AC (COL) (catalyst (1:5 μmol; 2-4: 3.25 μmol); TBHP (10 mmol)); Au@SC (DIM) (catalyst (1:5 μmol; 2-4: 4.5 μmol); TBHP (5 mmol)); Au@GR (COL) (catalyst (1:5 μmol; 2-4: 3 μmol); TBHP (10 mmol); TEMPO (2.5 mol %)); Au@CX (COL)(catalyst (1:5 μmol; 2-4:4 μmol); TBHP (5 mmol)); Au@CXL (COL) (catalyst (1:5 μmol; 2-4:1.5 μmol); TBHP (10 mmol); TEMPO (2.5 mol %)); Au@NDLIQ (DIM) (catalyst (1:5 μmol; 2-4:2 μmol); TBHP (10 mmol); TEMPO (2.5 mol %)); Au@MD (COL) (catalyst (1:5 μmol; 2-4:2 μmol); TBHP (10 mmol)).

There was no obvious activity loss with catalyst Au@GR (COL) after 3 cycles, but the yield decreased 45.9% in the 4th cycle when compared with the 3rd cycle.

Moreover, for the last two cycles the yield stays around 27%.

In the presence of catalyst Au@MD (COL), the catalytic activity was above 90% in the first two cycles, but it decreased 34.2% in the 3rd cycle. The yield is 24.7% after the 6th cycle.

For the catalyst Au@NDLIQ (DIM), in the second, third, fourth and fifth cycle, the obtained catalytic activity was 81%, 74%, 71% and 69%, respectively, so the activity remains in a high level in the first 5 cycles, but decreased in the 6th cycle, the yield decreased 29.3% when compared with 5th cycle.

For catalyst Au@CXL (COL), the catalytic activity remained at a high level in the first two cycles; the yield is 93.5% in the second cycle, and the yield began to fall sharply after the 3rd cycle, while the yield stays around 20% in the last three cycles.

The catalytic activity of Au@CX (COL) and Au@AC (COL) dropped sharply after the first cycle, the yield decreased 63.1% and 44.1%, respectively.

3.9 Catalytic performance comparison of the different supported gold nanoparticles for the oxidation of 1-phenylethanol

The initial yields for mostly catalysts under the best conditions are close to 100%. While for Au@AC (COL), Au@SC (DIM) and Au@CX (COL), the yields are still low in initial yield. Longer reaction time was then tested, in the case to know how reaction time can influence the acetophenone yield. The results are as follows.

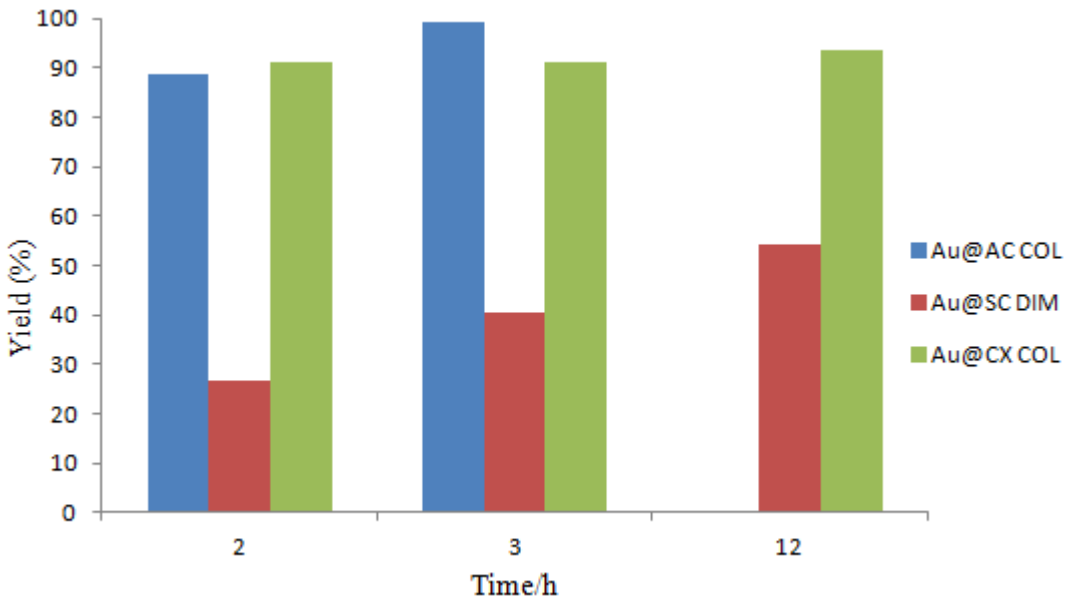

Figure 1-43 Acetophenone yield *vs.* reaction time with different catalysts. Reaction conditions: catalyst (5 μmol), TBHP (10 mmol), 110 ℃, 2 h.

It can be observed from **Figure 1-43**, that the reaction time has different effects on the acetophenone yield regarding different catalysts. In the case of catalyst Au@AC (COL), the yield increased 10.4% when increased reaction time from 2 to 3 hours and the yield is almost 100% after 3 hours reaction. Regarding catalyst Au@SC (DIM), the yield of acetophenone increased with more reaction time, while the yield is 54.3% after 12 hours reaction. The yield is low when compared with other catalysts, since the SC is usually covered by a silicon dioxide layer at its surface, even after longer reaction time, the passivation layer is still a disadvantage for the oxidation reaction. In the presence of catalyst Au@CX (COL), the yield of acetophenone only increased 2.7% when increased reaction time from 2 to 12 hours, the reason could be that CX material shows mesoporous properties with large pore size, and the adequate reaction can be done in a limited time. So shorter time is the appropriate reaction condition for industrial purposes.

Thus after performing the experiments for all catalysts, varying parameters such as different temperatures, reaction times, catalyst quantities and others, it is important to compare the properties of the various supports under the same conditions. The results are as follows.

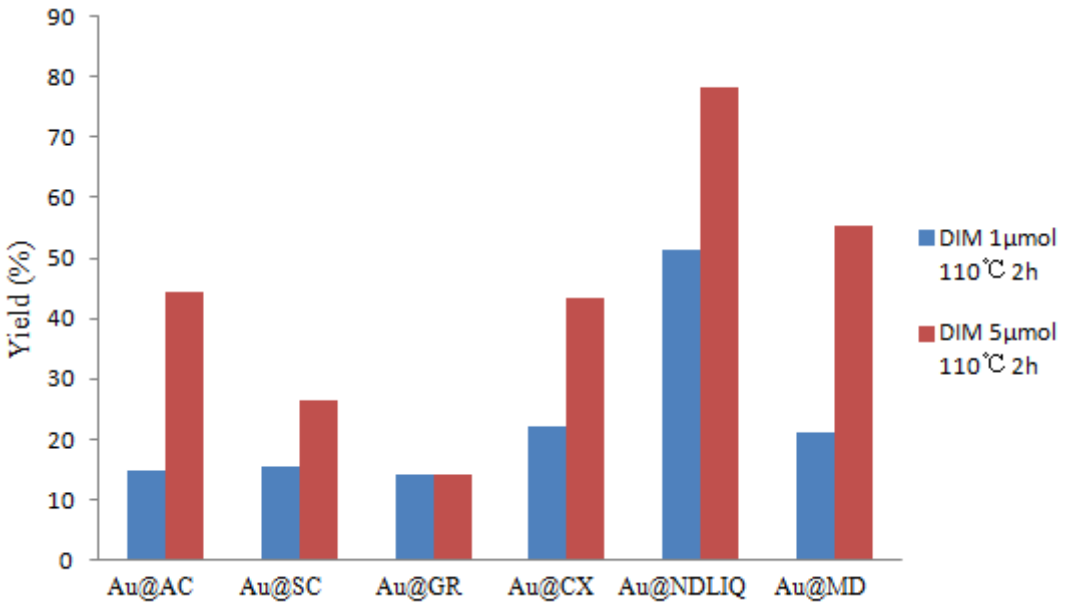

Figure 1-44 Effect of catalyst quantity on the yield of acetophenone for the MW-assisted oxidation (2 h) of 1-phenylethanol with TBHP (5 mmol), at 110 ℃ with catalysts obtained by DIM method.

From **Figure 1-44**, it can be observed that catalyst quantity has a significant influence on the MW-assisted oxidation of 1-phenylethanol. With 5 times increasing in catalyst quantity regarding double impregnation (DIM) method, the yield increased in most of the catalysts, especially the yields of Au@NDLIQ and Au@MD increased 26.8% and 34.1%, respectively, while with 5µmol of catalyst, catalyst Au@AC, and Au@GR obtained lower yields when to compared with 1 µmol of catalyst. Additionally, Au@NDLIQ formed by DIM preparation obtained better yield than another catalyst; this could owe to the existence of variety surface groups and mesoporosity of nanodiamonds which increasing the catalytic activity.

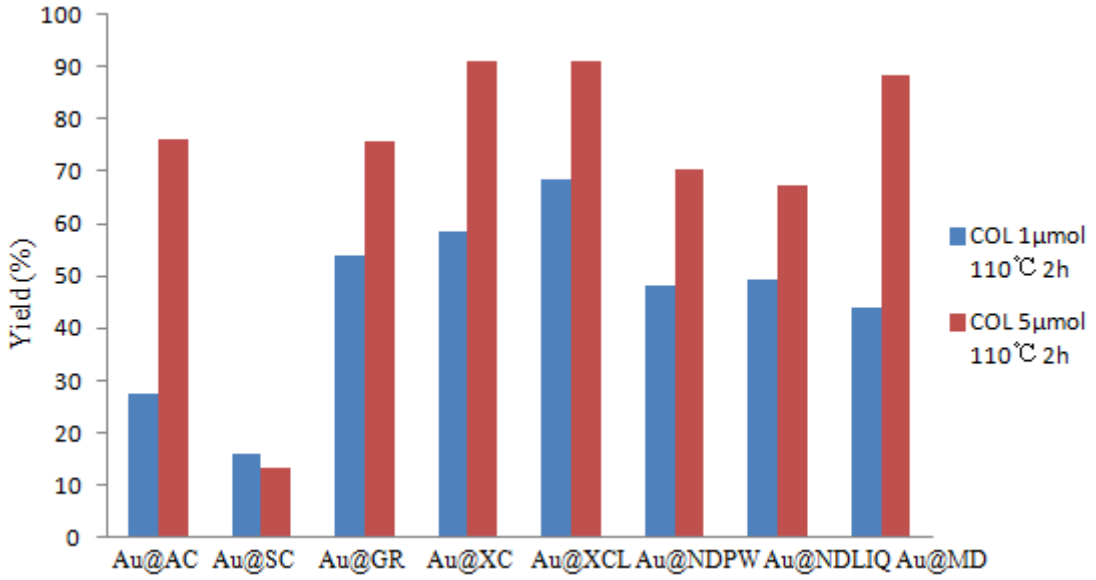

Figure 1-45 Effect of catalyst quantity on the yield of acetophenone for the MW-assisted oxidation (2 h) of 1-phenylethanol with TBHP (5 mmol), at 110 ℃ with catalysts formed by COL preparation.

It can be seen from **Figure 1-45** that catalyst quantity has an important effect on the MW-assisted oxidation of 1-phenylethanol. When the catalyst quantity is changed from 1 to 5μmol, it showed improvement in the yield for most of the catalysts (expect for Au@SC) with COL method, more specifically, the yield increased 48.6% with catalyst Au@AC, as well as increased 44.7% with catalyst Au@MD. Moreover, Au supported on CX and CXL formed by COL method obtained a higher yield than other catalyst. It was found in the literature recently that well-developed mesoporosity of carbon supports was useful for the catalytic activity of Au supported on carbon materials in hydroamination of alkynes[101].

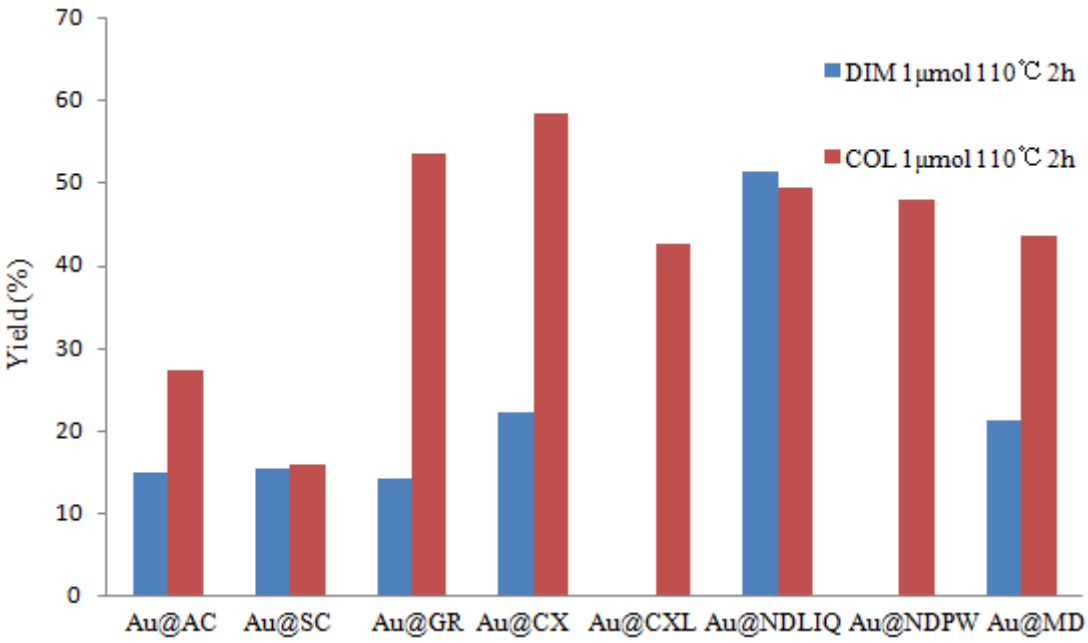

Figure 1-46 Effect of the heterogenization method for catalysts (1 µmol) on the yield of acetophenone for the MW-assisted oxidation (2 h) of 1-phenylethanol with TBHP (5 mmol) at 110 ℃.

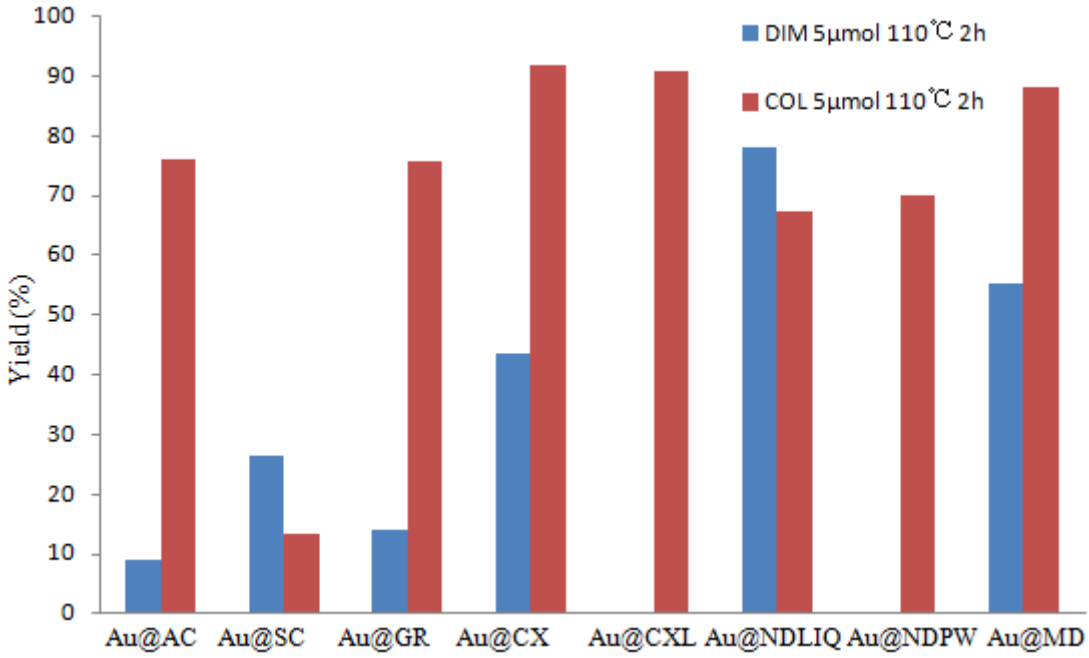

Figure 1-47 Effect of the heterogenization method for catalysts (5 µmol) on the yield of acetophenone for the MW-assisted oxidation (2 h) of 1-phenylethanol with TBHP (5 mmol) at 110 ℃.

As it can be seen from **Figures 1-46** and **47** that catalysts prepared by COL method led to higher yields of acetophenone than those prepared by DIM method, as reported previously[71], which means that catalysts obtained by COL preparation are

more active than those formed by DIM method, except for catalyst Au@SC.

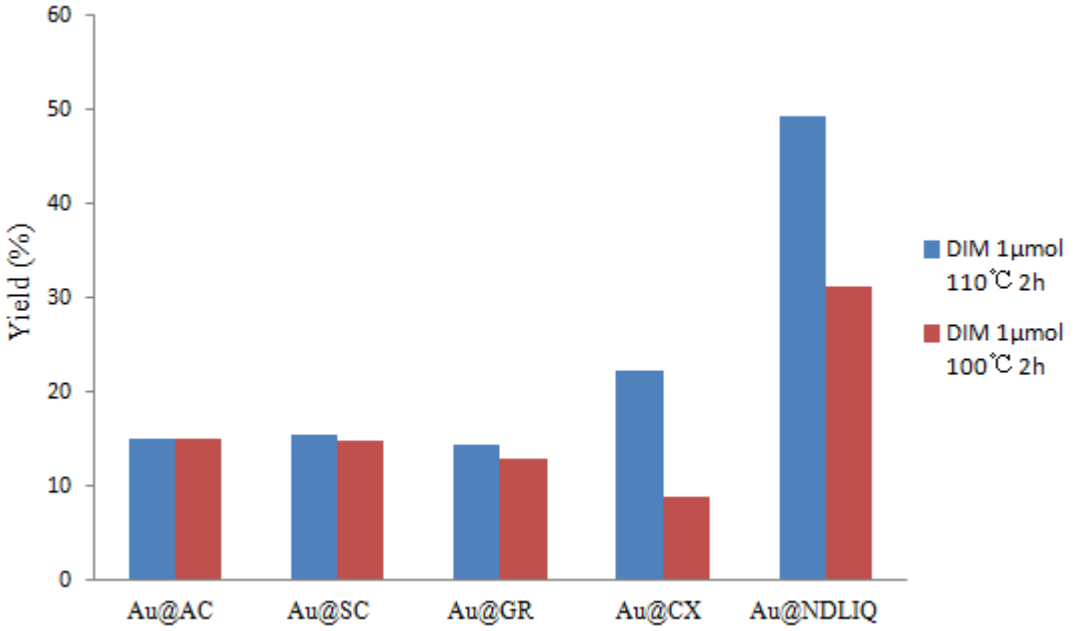

Figure 1-48 Yield of acetophenone carried by MW-assisted oxidation of 1-phenylethanol (2 h) with catalysts formed by DIM method with different temperatures.

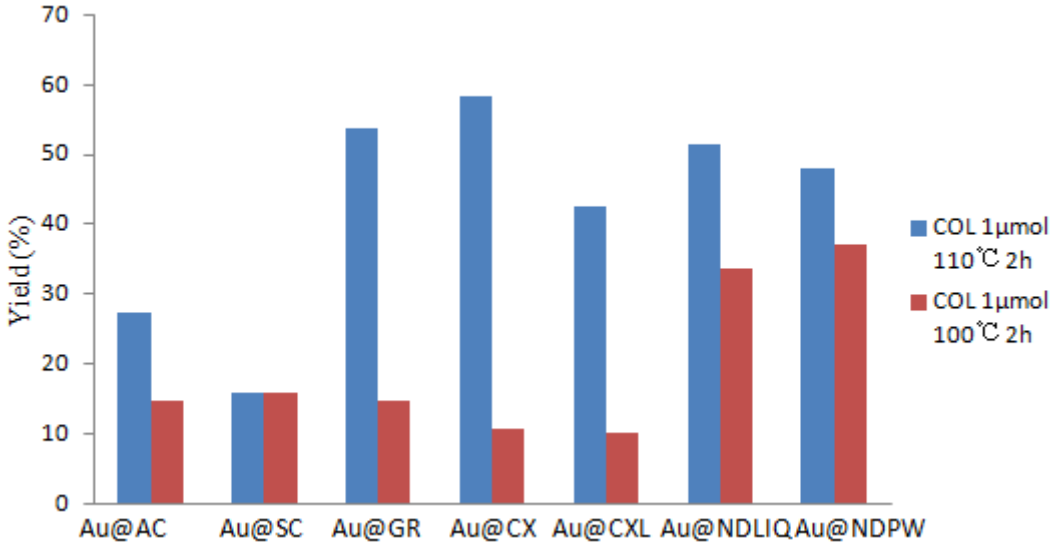

Figure 1-49 Yield of acetophenone produced by MW-assisted oxidation of 1-phenylethanol (2 h) with catalysts obtained by COL preparation with different temperatures.

A 10 ℃ increasing in temperature leads to a significant increase in the yield of acetophenone, for both catalysts obtained by DIM method and COL preparation, except for SC (the yield did not change sharply by increasing the temperature from

100 to 110 ℃). Normally SiC is covered by a protective layer of silicon dioxide formed on its surface, and high temperature is needed to increase the catalytic activity. It also can be observed that catalysts Au@AC and Au@GR formed by COL method are more active than those obtained by DIM preparation at 110 ℃, which means that higher temperature (110 ℃) is needed with catalysts obtained by COL method.

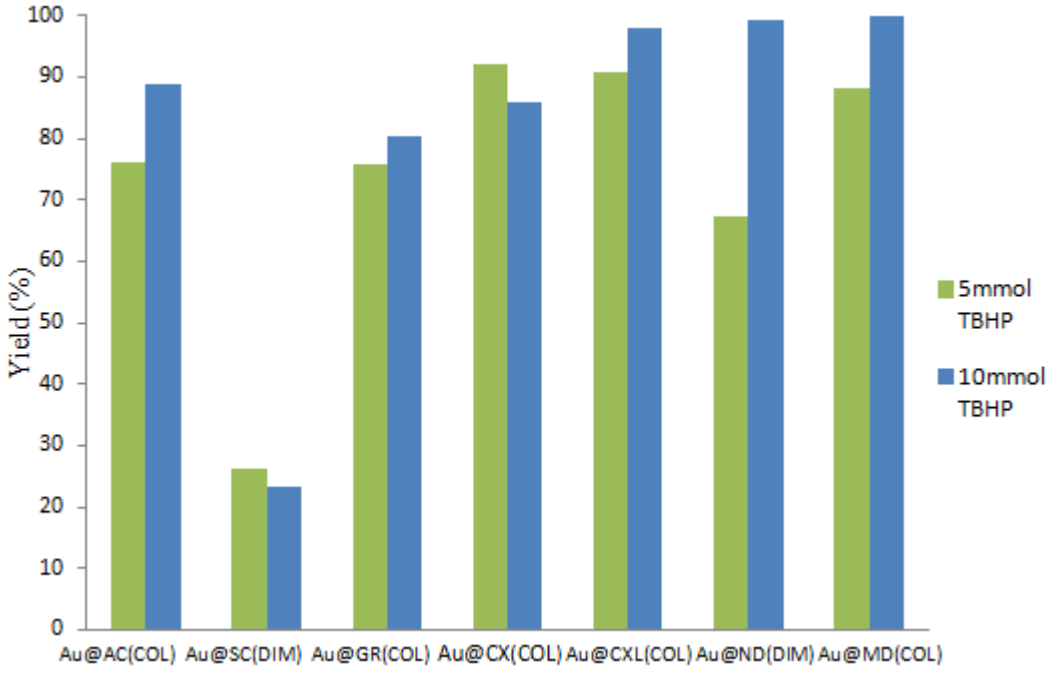

Figure 1-50 Catalytic activities of different catalysts. Reaction conditions: catalyst (5 μmol), TBHP (5mmol; 10mmol), 2 h, 110 ℃.

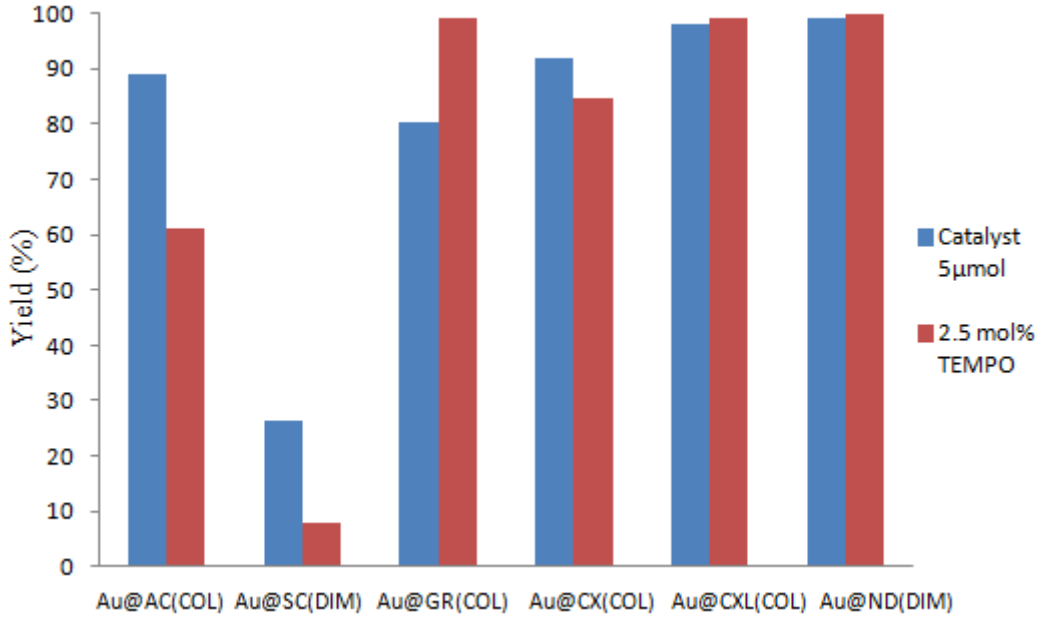

Figure 1-51 Catalytic activities of different catalysts. Reaction conditions: catalyst (5 μmol), TEMPO (2.5 mol %), 2 h, 110 ℃, in the presence of TBHP: Au@AC (COL): 10 mmol; Au@SC (DIM): 5 mmol; Au@GR (COL): 10 mmol; Au@CX (COL): 5 mmol; Au@CXL (COL): 10 mmol; Au@ND (DIM): 10 mmol.

From **Figure 1-50**, it can be found that the amount of TBHP has a significant influence on the MW-assisted oxidation of 1-phenylethanol. Using 10 mmol of TBHP, a higher yield was obtained when compared with using 5 mmol of TBHP among most of the catalysts, except for catalysts Au@SC (DIM) and Au@CX (COL). For the Au@ND, the yield increased 31.9% by adding the double amount of TBHP, which is the highest increasing of the product among all the catalysts. The main reason is that ND has the largest amount of surface group.

It can be found from **Figure 1-51** that TEMPO additive does not play a major role in the oxidation of 1-phenylethanol under the tested conditions. Especially for the catalysts Au@AC (COL), the yield decreased 27.9% when adding 2.5 mol% of TEMPO, while the existence of TEMPO additive increases 18.8% the yield of acetophenone with catalyst Au@GR (COL).

As reported in the literature[102], copper(II) complex $[Cu(H_2R)(HL)]\cdot H_2O$, used for the solvent free microwave (MW) assisted oxidation of 1-phenylethanol with TBHP, the yield is 65.9% in 15 minutes under 25W MW irradiation, while in the presence of TEMPO, the yield increases up to 80% in the same conditions, showing high efficiency of using TEMPO additive. In the present study, the yield did not increase significantly when 2.5 mol% TEMPO was added. Moreover, for some catalysts such as Au@SC (DIM), addition TEMPO hampers the reaction. This can be considered an advantage of the present system, as it can convert 1-phenylethanol to acetophenone in high yields without the need of additive promoters.

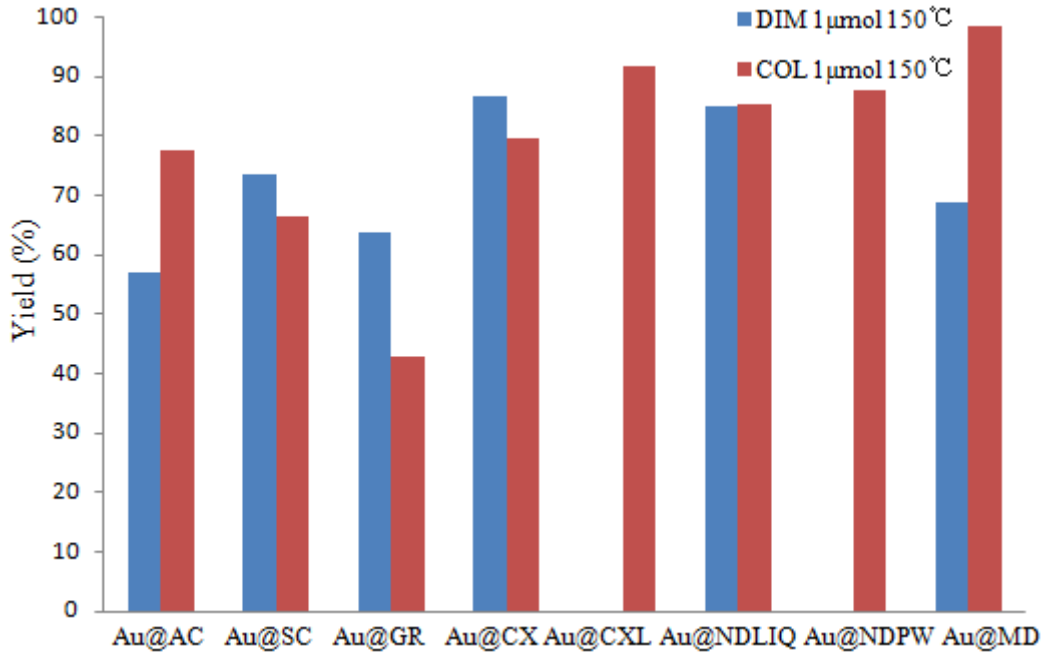

Figure 1-52 Effect of the heterogenization method for catalysts (1 µmol) on the yield of acetophenone for the MW-assisted oxidation (2 h) of 1-phenylethanol with TBHP (5 mmol) at 150 ℃.

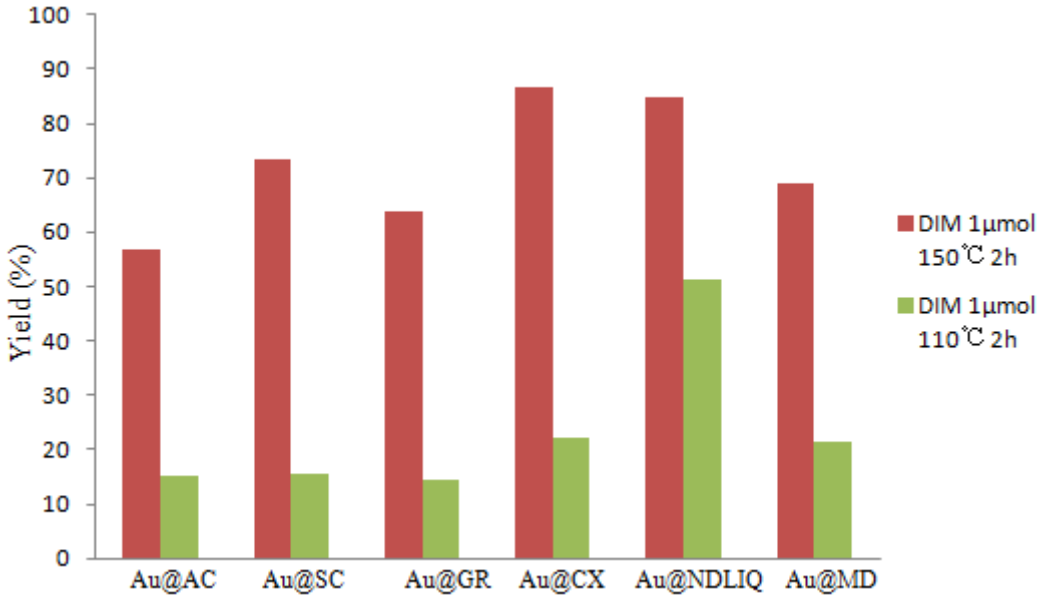

Figure 1-53 Effect of catalyst quantity on the yield of acetophenone for the MW-assisted oxidation (2 h) of 1-phenylethanol with TBHP (5 mmol), at 150 ℃ with catalysts obtained by DIM method.

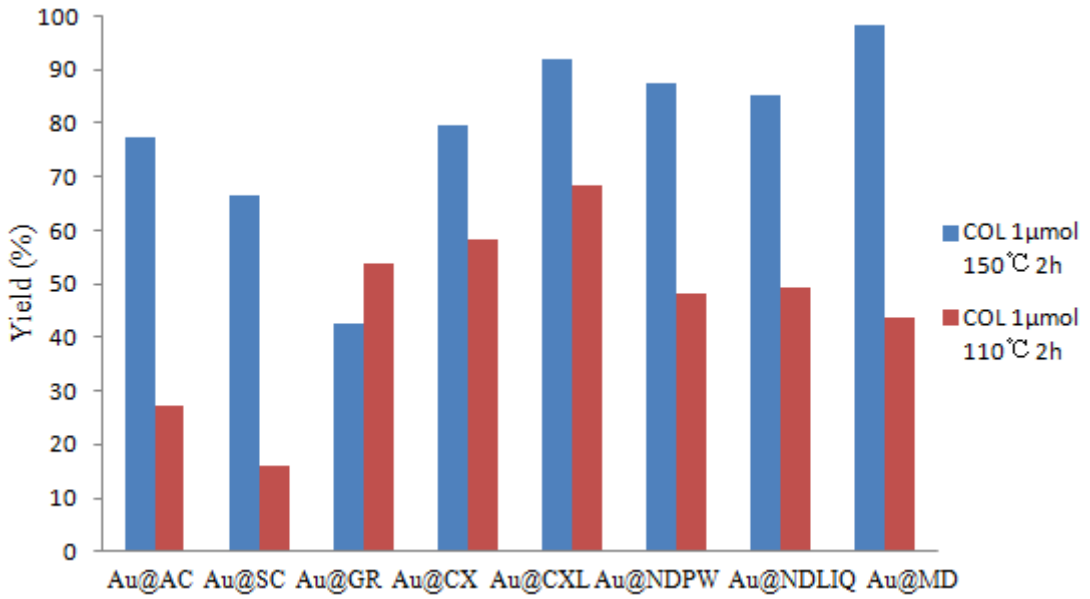

Figure 1-54 Effect of reaction temperature on the yield of acetophenone for the MW-assisted oxidation (2 h) of 1-phenylethanol with TBHP (5 mmol), at 150 ℃ with catalysts obtained by COL method.

From **Figure 1-52** it can be seen that for catalysts Au@AC and Au@MD, COL method obtained higher a yield than DIM preparation, while for catalyst Au@SC, Au@GR, and Au@CX, COL method was more efficient than DIM. Moreover, from **Figures 1-53** and **1-54**, higher temperature (150 ℃) obtained better catalytic activity than lower temperature (110 ℃), both in DIM preparation and COL method. Especially for catalyst Au@SC, the yield increased 58.1% in DIM method, also 50.5% increment with COL preparation, but for catalyst Au@GR, the yield decreased from 110 to 150 ℃.

4. Conclusion

This study was focused on the catalytic activity of different Au NPs@carbon materials, prepared by two different methods (double impregnation and colloidal method), which were used as catalysts for the microwave-assisted solvent-free oxidation of 1-phenylethanol under different conditions. The presence of higher catalyst quantity (5 µmol) led to a higher yield of acetophenone when compared with lower quantity (1 µmol) for most catalysts. For example, for catalyst Au@MD (COL) the yield increased 49% when the catalyst quantity is changed from 1 to 5 µmol.

Moreover, with longer reaction time, a higher yield of acetophenone was obtained; for instance, regarding catalyst Au@SC (DIM), with TON of *ca.*135 and a yield of 54.3% after 12 h reaction, while with TON of *ca.*17.6 and a yield of 7.9% after 2 h reaction. In addition, the temperature was also very important for the product yield; the yield increased 58% with catalyst Au@SC (DIM) when the temperature increased from 110 to 150 ℃. Besides, the catalytic activity of adding twice the amount of TBHP depends on the different carbon supports, and 2.5 mol% TEMPO did not promote or even hamper the oxidation reaction, the yield decreased 28% when adding TEMPO regarding catalyst Au@AC (COL). It was also found that the catalysts synthesized by COL method led to higher acetophenone at 110 ℃ when compared with DIM preparation because normally COL method resulting in a larger dispersion and lower average particle size.

Catalyst recycling was tested up to six consecutive cycles for each carbon supporting materials at the best operation conditions. It was found that for catalyst Au@NDLIQ (DIM), the activity dropped to 69% after the fifth cycle, while the catalytic activity was 55% higher when compared with catalyst Au@CX (COL) in the 5^{th} cycle.

The catalytic performance is different among all the Au@carbon catalysts that we have been studied; the different behavior can be explained by the gold nanoparticle size, mesoporosity properties of the support and dispersibility characteristics in the heterogeneous reaction medium.

References

[1] Enache, D. I.; Knight, D. W.; Hutchings, G. J. Solvent-free oxidation of primary alcohols to aldehydes using supported gold catalysts. *Catal. Lett.* **2005**, *103*, 43-52.

[2] Shestakov, A. F. Application of quantum-chemical methods for investigation of gold nanoclusters properties. *Rev. Adv. Mater. Sci*. **2009**, *20*, 48-54.

[3] Haruta, M. Catalysis of gold nanoparticles deposited on metal oxides. *Cattech*. **2002**, *6*, 102-115.

[4] Liu, Z. P.; Gong, X. Q.; Kohanoff, J.; et al. Catalytic Role of Metal Oxides in Gold-Based Catalysts: A First Principles Study of CO oxidation on TiO_2 Supported Au. *Phys. Rev. Lett*. **2003**, *91*, 266102.

[5] Xu, X.; Zhu, J.; Faria, J. L.; et al. Tuning the textural and surface properties of carbon xerogels to be used as supports for gold catalysts. *Cent. Eur. J. Chem*. **2012**, *10*, 1867-1874.

[6] Dimitratos, N.; Porta, F.; Prati, L. Au, Pd (mono and bimetallic) catalysts supported on graphite using the immobilization method: Synthesis and catalytic testing for liquid phase oxidation of glycerol. *Appl. Catal., A.* **2005**, *291*, 210-214.

[7] Bianchi, C.; Porta, F.; Prati, L.; et al. Selective liquid phase oxidation using gold catalysts. *Top. Catal*. **2000**, *13*, 231-236.

[8] Carrettin, S.; McMorn, P.; Johnston, P.; et al. Selective oxidation of glycerol to glyceric acid using a gold catalyst in aqueous sodium hydroxide. *Chem. Commun*. **2002**, *7*, 696-697.

[9] Enache, D. I.; Edwards, J. K.; Landon, P.; et al. Solvent-free oxidation of primary alcohols to aldehydes using Au-Pd/TiO_2 catalysts. *Science*. **2006**, *311*, 362-365.

[10] Liu, Y.; Tsunoyama, H.; Akita, T.; et al. Aerobic oxidation of cyclohexane catalyzed by size-controlled Au clusters on hydroxyapatite: size effect in the sub-2 nm regime. *Acs Catal.* **2011**, *1*, 2-6.

[11] Auffan, M.; Rose, J.; Bottero, J. Y.; et al. Towards a definition of inorganic nanoparticles from an environmental, health and safety perspective. *Nature Nanotech*. **2009**, *4*, 634-641.

[12] Daniel, M. C.; Astruc, D. Gold nanoparticles: assembly, supramolecular chemistry, quantum-size-related properties, and applications toward biology, catalysis, and nanotechnology. *Chem.Rev*. **2004**, *104*, 293-346.

[13] Sperling, R. A.; Gil, P. R.; Zhang, F.; et al. Biological applications of gold nanoparticles. *Chem. Soc. Rev*. **2008**, *37*, 1896-1908.

[14] Souza, C. R.; Oliveira, H. R.; Pinheiro, W. M. Gold Nanoparticle and Berberine Entrapped into Hydrogel Matrix as Drug Delivery System. *J. Biomater. Nanobiotechnol*. **2015**, *6*, 53-63.

[15] Hainfeld, J. F.; Powell, R. D. New frontiers in gold labeling. *J. Histochem Cytochem*. **2000**, *48*, 471-480.

[16] Jain, P. K.; Lee, K. S.; El-Sayed, I. H.; et al. Calculated absorption and scattering properties of gold nanoparticles of different size, shape, and composition: applications in biological imaging and biomedicine. *J. Phys. Chem. B.* **2006**, *110*, 7238-7248.

[17] Mieszawska, A. J.; Mulder, W. J. M.; Fayad, Z. A.; et al. Multifunctional gold nanoparticles for diagnosis and therapy of disease. *Mol. Pharmacol*. **2013**, *10*, 831-847.

[18] Liang, S.; Hammond, G. B.; Xu, B. Supported gold nanoparticles catalyzed cis-selective semihydrogenation of alkynes using ammonium formate as the reductant. *Chem. Commun*. **2016**, *52*, 6013-6016.

[19] Lopez, N.; Janssens, T. V. W.; Clausen, B. S.; et al. On the origin of the catalytic activity of gold nanoparticles for low-temperature CO oxidation. *J. Catal*. **2004**, *223*, 232-235.

[20] Chen, M. S.; Goodman, D. W. Structure–activity relationships in supported Au catalysts. *Catal. Today*. **2006**, *111*, 22-33.

[21] Benaglia, M.; Puglisi, A.; Cozzi, F. Polymer-supported organic catalysts. *Chem. Rev*. **2003**, *103*, 3401-3430.

[22] Ketchie, W. C.; Fang, Y. L.; Wong, M. S.; et al. Influence of gold particle size on the aqueous-phase oxidation of carbon monoxide and glycerol. *J. Catal*. **2007**, *250*, 94-101.

[23] Abad, A.; Corma, A.; Garc á, H. Catalyst parameters determining activity and selectivity of supported gold nanoparticles for the aerobic oxidation of alcohols. The molecular reaction mechanism.*Chem. Eur. J*. **2008**, *14*, 212-222.

[24] Cole-Hamilton, D. J. Homogeneous catalysis--new approaches to catalyst separation, recovery, and recycling. *Science*. **2003**, *299*, 1702-1706.

[25] Campanati, M.; Fornasari, G.; Vaccari, A. Fundamentals in the preparation of heterogeneous catalysts. *Catal. Today*. **2003**, *77*, 299-314.

[26] Centeno, M. Á.; Carrizosa, I.; Odriozola J A. Deposition–precipitation method to obtain supported gold catalysts: dependence of the acid–base properties of the support exemplified in the system TiO_2–TiO_xN_y–TiN. *Appl Catal., A*. **2003**, *246*, 365-372.

[27] Kozlova, A. P.; Sugiyama, S.; Kozlov, A. I.; et al. Iron-oxide supported gold catalysts derived from gold-phosphine complex $Au(PPh_3)(NO_3)$: state and structure of the support. *J. Catal.* **1998**, *176*, 426-438.

[28] Cauqui, M. A.; Rodriguez-Izquierdo, J. M. Application of the sol-gel methods to catalyst preparation. *J. Non-Cryst. Solids.* **1992**, *147*, 724-738.

[29] Wang, W.; Serp, P.; Kalck, P.; et al. Photocatalytic degradation of phenol on MWNT and Titania composite catalysts prepared by a modified sol–gel method.*Appl. Catal., B*. **2005**, *56*, 305-312.

[30] Heveling, J. Heterogeneous catalytic chemistry by example of industrial applications. *J. Chem. Educ*. **2012**, *89*, 1530-1536.

[31] He, J.; Ichinose, I.; Kunitake, T.; et al. Facile fabrication of Ag-Pd bimetallic nanoparticles in ultrathin TiO_2-gel films: nanoparticle morphology and catalytic activity. *J. Chem. Soc*. **2003**, *125*, 11034-11040.

[32] Astruc, D.; Lu, F.; Aranzaes, J. R. Nanoparticles as recyclable catalysts: the frontier between homogeneous and heterogeneous catalysis. *Angew. Chem. Int. Ed*. **2005**, *44*, 7852-7872.

[33] Serp, P.; Castillejos, E. Catalysis in carbon nanotubes. *Chem. Cat. Chem*. **2010**, *2*, 41-47.

[34] Shamsudin, M. S.; Mahmud, M. R; Husairi, F. S; et al. Micro-Raman, optical and

impedance characteristics of CNT-substituted acrylate/CNT nanocomposite thin film. *Adv. Mater. Res*. **2013**, *832*, 286-291.

[35] Steel, K. M.; Koros, W. J. Investigation of porosity of carbon materials and related effects on gas separation properties. *Carbon*. **2003**, *41*, 253-266.

[36] Barbieri, O.; Hahn, M.; Herzog, A.; et al. Capacitance limits of high surface area activated carbons for double layer capacitors. *Carbon*. **2005**, *43*, 1303-1310.

[37] Rodriguez-Reinoso, F. The role of carbon materials in heterogeneous catalysis. *Carbon*. **1998**, *36*, 159-175.

[38] Gogotsi, Y.; Nikitin, A.; Ye, H.; et al. Nanoporous carbide-derived carbon with tunable pore size. *Nat. Mater*. **2003**, *2*, 591-594.

[39] Bleda-Martínez, M. J.; Maciá-Agulló, J. A.; Lozano-Castelló, D.; et al. Role of surface chemistry on electric double layer capacitance of carbon materials. *Carbon*. **2005**, *43*, 2677-2684.

[40] Kim, Y. T.; Mitani, T. Competitive effect of carbon nanotubes oxidation on aqueous EDLC performance: Balancing hydrophilicity and conductivity. *J. Power Sources*. **2006**, *158*, 1517-1522.

[41] Silva, A. R.; Figueiredo, J. L.; Freire, C.; et al. Manganese (III) salen complexes anchored onto activated carbon as heterogeneous catalysts for the epoxidation of olefins. *Microporous and Mesoporous Mater*. **2004**, *68*, 83-89.

[42] Moreno-Castilla, C.; Maldonado-Hódar, F. J. Carbon aerogels for catalysis applications: An overview. *Carbon*. **2005**, *43*, 455-465.

[43] So, M. H.; Liu, Y.; Ho, C. M.; et al. Graphite‐Supported Gold Nanoparticles as Efficient Catalyst for Aerobic Oxidation of Benzylic Amines to Imines and N‐Substituted 1, 2, 3, 4‐Tetrahydroisoquinolines to Amides: Synthetic Applications and Mechanistic Study. *Chem Asian J*. **2009**, *4*, 1551-1561.

[44] Serp, P.; Corrias, M.; Kalck, P. Carbon nanotubes and nanofibers in catalysis. *Appl. Catal., A*. **2003**, *253*, 337-358.

[45] Auer, E.; Freund, A.; Pietsch, J.; et al. Carbons as supports for industrial precious metal catalysts. *Appl. Catal., A*. **1998**, *173*, 259-271.

[46] Hameed, B. H.; Din, A. T. M.; Ahmad, A. L. Adsorption of methylene blue onto

bamboo-based activated carbon: kinetics and equilibrium studies. *J. Hazard. Mater*. **2007**, *141*, 819-825.

[47] Job, N.; Pirard, R.; Marien, J.; et al. Porous carbon xerogels with texture tailored by pH control during sol–gel process. *Carbon*. **2004**, *42*, 619-628.

[48] Samant, P. V.; Gonçalves, F.; Freitas, M. M. A.; et al. Surface activation of a polymer based carbon. *Carbon*. **2004**, *42*, 1321-1325.

[49] Rodrigues, E. G.; Pereira, M. F. R, Órfão, J. J. M. Glycerol oxidation with gold supported on carbon xerogels: Tuning selectivities by varying mesopore sizes. *Appl.Catal. B*. **2012**, *115*, 1-6.

[50] Rodrigues, E G.; Pereira, M. F. R.; Órfão, J. J. M. Corrigendum to "Glycerol oxidation with gold supported on carbon xerogels: Tuning selectivities by varying mesopore sizes" [*Appl. Catal. B: Environ.* **2012**, *115–116*, 1–6]. *Appl.Catal. B. Environ.* **2012**, *125*, 567-568.

[51] Li, H. Q.; Wang, Y. G.; Wang, C. X.; et al. A competitive candidate material for aqueous supercapacitors: High surface-area graphite. *J. Power Sources*. **2008**, *185*, 1557-1562.

[52] Marquez-Alvarez, C.; Rodriguez-Ramos, I.; Guerrero-Ruiz, A. Removal of no over carbon-supported copper catalysts. I. Reactivity of no with graphite and activated carbon. *Carbon*. **1996**, *34*, 339-346.

[53] Bachiller-Baeza, B.; Guerrero-Ruiz, A.; Wang, P.; et al. Hydrogenation of citral on activated carbon and high-surface-area graphite-supported ruthenium catalysts modified with iron. *J. Catal*. **2001**, *204*, 450-459.

[54] Eom J H.; Kim Y W.; Raju S. Processing and properties of macroporous silicon carbide ceramics: A review. *J. Am. Ceram. Soc*. **2013**, *1*, 220-242.

[55] Zhou, Y.; Hirao, K.; Watari, K.; et al. Thermal conductivity of silicon carbide densified with rare-earth oxide additives. *J. Eur. Ceram. Soc*. **2004**, *24*, 265-270.

[56] Katoh, Y.; Snead, L. L.; Cheng, T.; et al. Radiation-tolerant joining technologies for silicon carbide ceramics and composites. *J. Nucl. Mater*. **2014**, *448*, 497-511.

[57] Srivastava, P.; Das, J.; Visalli, D.; et al. Silicon substrate removal of GaN DHFETs for enhanced (< 1100 V) breakdown voltage. *IEEE Electron Device Lett*.

2010, *31*, 851-853.

[58] Makarova, M.; Vuckovic, J.; Sanda, H.; et al. Silicon-based photonic crystal nanocavity light emitters. *Appl. Phys. Lett*. **2006**, *89*, 221101.

[59] Kappe, C. O. Unraveling the mysteries of microwave chemistry using silicon carbide reactor technology. *Acc. Chem. Res*. **2013**, *46*, 1579-1587.

[60] Ashrafi, B.; Hubert, P.; Vengallatore, S. Carbon nanotube-reinforced composites as structural materials for microactuators in microelectromechanical systems. *Nanotechnology*. **2006**, *17*, 4895.

[61] Serp, P.; Castillejos, E. Catalysis in carbon nanotubes. *Chem. Cat. Chem*. **2010**, *2*, 41-47.

[62] Han, J.; Jiang, L.; Li, F.; et al. Ultrasensitive non-enzymatic immunosensor for carcino-embryonic antigen based on palladium hybrid vanadium pentoxide/multiwalled carbon nanotubes. *Biosens. Bioelectron*. **2016**, *77*, 1104-1111.

[63] He, B.; Sun, W.; Wang, M.; et al. New magnetic phenomena of rare earth ions-modified carbon nanotubes. *Mater. Chem. Phys*. **2006**, *95*, 202-205.

[64] Cao, Q.; Rogers, J. A. Ultrathin films of single‐walled carbon nanotubes for electronics and sensors: a review of fundamental and applied aspects. *Adv. Mater*. **2009**, *21*, 29-53.

[65] Hernadi, K.; Ljubović, E.; Seo, J. W.; et al. Synthesis of MWNT-based composite materials with inorganic coating. *Acta Mater*. **2003**, *51*, 1447-1452.

[66] Kuskova, N I.; Baklar, V. Y.; Ivashchuk, L. I. Physical aspects of the formation of various allotropic modifications of nanocarbon during electric explosion. *Tech Phys*. **2010**, *55*, 1288-1293.

[67] Ozawa, M.; Inaguma, M.; Takahashi, M.; et al. Preparation and behavior of brownish, clear nanodiamond colloids. *Adv. Mater*. **2007**, *19*, 1201-1206.

[68] Schrand, A. M; Hens, S. A. C.; Shenderova, O. A. Nanodiamond particles: properties and perspectives for bioapplications. *Crit. Rev. Solid State Mater. Sci*. **2009**, *34*, 18-74.

[69] Xing, Z.; Pedersen, T. O.; Wu, X.; et al. Biological effects of functionalizing

copolymer scaffolds with nanodiamond particles. *Tissue Eng Part A*. **2013**, *19*, 1783-1791.

[70] Salaam, A. D.; Dean, D. Electrospun Polycaprolactone-Nanodiamond Composite Scaffolds for Bone Tissue Engineering. *ASME 2010 First Global Congress on NanoEngineering for Medicine and Biology*. *American Society of Mechanical Engineers*. **2010**, 367-370.

[71] Carabineiro, S. A. C.; Martins, L.; Avalos-Borja, M.; et al. Gold nanoparticles supported on carbon materials for cyclohexane oxidation with hydrogen peroxide. *Appl. Catal., A*. **2013**, *467*,279-290.

[72] Manzke, A.; Vogel, N.; Weiss, C. K.; et al. Arrays of size and distance controlled platinum nanoparticles fabricated by a colloidal method. *Nanoscale*. **2011**, *3*, 2523-2528.

[73] Lopez-Sanchez, J. A.; Dimitratos, N.; Hammond, C.; et al. Facile removal of stabilizer-ligands from supported gold nanoparticles. *Nat. Chem*. **2011**, *3*, 551-556.

[74] Kawaguchi, T.; Sugimoto, W.; Murakami, Y.; et al. Particle growth behavior of carbon-supported Pt, Ru, PtRu catalysts prepared by an impregnation reductive-pyrolysis method for direct methanol fuel cell anodes. *J. Catal*. **2005**, *229*, 176-184.

[75] Bowker, M.; Nuhu, A.; Soares, J. High activity supported gold catalysts by incipient wetness impregnation. *Catal. Today*. **2007**, *122*, 245-247.

[76] Ishida, T.; Kinoshita, N.; Okatsu, H.; et al. Influence of the support and the size of gold clusters on catalytic activity for glucose oxidation. *Angew. Chem*. **2008**, *120*, 9405-9408.

[77] Hvolbæk, B.; Janssens, T. V. W.; Clausen, B. S.; et al. Catalytic activity of Au nanoparticles. *Nano Today*. **2007**, *2*, 14-18.

[78] Daniel, M. C.; Astruc, D. Gold nanoparticles: assembly, supramolecular chemistry, quantum-size-related properties, and applications toward biology, catalysis, and nanotechnology. *Chem. Rev*. **2004**, *104*, 293-346.

[79] Hong, S. G.; Kang, K. B.; Park, C. G. Strain-induced precipitation of NbC in Nb

and Nb–Ti micro alloyed HSLA steels. *Scripta Mater*. **2002**, *46*, 163-168.

[80] Lopez, N.; Nørskov, J. K. Catalytic CO oxidation by a gold nanoparticle: A density functional study. *J. Amer. Chem. Soc*. **2002**, *124*, 11262-11263.

[81] Zhou, X.; Xu, W.; Liu, G.; et al. Size-dependent catalytic activity and dynamics of gold nanoparticles at the single-molecule level. *J. Am. Chem. Soc*. **2009**, *132*, 138-146.

[82] Valden, M.; Pak, S.; Lai, X.; et al. Structure sensitivity of CO oxidation over model Au/TiO_2 catalysts. *Catal. Lett.* **1998**, *56*, 7-10.

[83] Claus, P.; Brückner, A.; Mohr, C.; et al. Supported gold nanoparticles from quantum dot to mesoscopic size scale: effect of electronic and structural properties on catalytic hydrogenation of conjugated functional groups. *J. Am. Chem. Soc*. **2000**, *122*, 11430-11439.

[84] Haruta, M. Gold as a novel catalyst in the 21st century: Preparation, working mechanism and applications. *Gold Bull.* **2004**, *37*, 27-36.

[85] Grisel, R.; Weststrate, K. J.; Gluhoi, A.; et al. *Catalysis by gold nanoparticles. Gold Bull.* **2002**, *35*, 39-45.

[86] Ishida, T.; Haruta, M. Gold catalysts: towards sustainable chemistry. *Angew. Chem. Int. Ed*. **2007**, *46*, 7154-7156.

[87] Miyamura, H.; Matsubara. R.; Miyazaki, Y.; et al. Aerobic oxidation of alcohols at room temperature and atmospheric conditions catalyzed by reusable gold nanoclusters stabilized by the benzene rings of polystyrene derivatives. *Angew. Chem. Int. Ed*. **2007**, *119*, 4229-4232.

[88] Della, Pina, C.; Falletta, E.; Prati, L.; et al. Selective oxidation using gold. *Chem. Soc. Rev*. **2008**, *37*, 2077-2095.

[89] Corma, A.; Domine, M. E. Gold supported on a mesoporous CeO_2 matrix as an efficient catalyst in the selective aerobic oxidation of aldehydes in the liquid phase. *Chem. Commun*. **2005**, *32*, 4042-4044.

[90] Corma, A.; Concepción, P.; Domínguez, I.; et al. Gold supported on a biopolymer (chitosan) catalyzes the regioselective hydroamination of alkynes. *J. Catal*. **2007**, *251*, 39-47.

[91] Abad, A.; Concepción, P.; Corma, A.; et al. A collaborative effect between gold and a support induces the selective oxidation of alcohols. *Angew. Chem. Int. Ed.* **2005**, *44*, 4066-4069.

[92] Della, Pina, C.; Falletta, E.; Rossi, M. Update on selective oxidation using gold. *Chem. Soc. Rev*. **2012**, *41*, 350-369.

[93] Su, F. Z.; Liu, Y. M.; Wang, L. C.; et al. Gold Nanoparticles Supported on Mesostructured Ga-Al Mixed Oxide with Enhanced Activity for Aerobic Alcohol Oxidation. **2007**, *47*, 334-337.

[94] Miedziak, P. J.; Tang, Z.; Davies, T. E.; et al. Ceria prepared using supercritical antisolvent precipitation: a green support for gold–palladium nanoparticles for the selective catalytic oxidation of alcohols. *J. Mater. Chem*. **2009**, *19*, 8619-8627.

[95] Mertens, P. G. N.; Corthals, S. L. F.; Ye, X.; et al. Selective alcohol oxidation to aldehydes and ketones over base-promoted gold–palladium clusters as recyclable quasihomogeneous and heterogeneous metal catalysts. *J. Mol. Catal. A., Chem.* **2009**, *313*, 14-21.

[96] Mitsudome, T.; Noujima, A.; Mizugaki, T.; et al. Efficient Aerobic Oxidation of Alcohols using a Hydrotalcite Supported Gold Nanoparticle Catalyst. *Adv. Synth. Catal.* **2009**, *351*, 1890-1896.

[97] Ni, J.; Yu, W. J.; He, L.; et al. A green and efficient oxidation of alcohols by supported gold catalysts using aqueous H_2O_2 under organic solvent-free conditions. *Green Chem.* **2009**, *11*, 756-759.

[98] Allen, S. E.; Walvoord, R. R.; Padilla-Salinas, R.; et al. Aerobic copper-catalyzed organic reactions. *Chem. Rev*. **2013**, *113*, 6234-6458.

[99] Figiel, P. J.; Kopylovich, M. N.; Lasri, J.; et al. Solvent-free microwave-assisted peroxidative oxidation of secondary alcohols to the corresponding ketones catalyzed by copper (II) 2,4-alkoxy-1,3,5-triazapentadienato complexes. *Chem. Commun*. **2010**, *46*, 2766-2768.

[100] Ishida, T.; Nagaoka, M.; Akita, T.; et al. Deposition of gold clusters on porous coordination polymers by solid grinding and their catalytic activity in aerobic oxidation of alcohols. *Chem. Eur. J*. **2008**, *14*, 8456-8460.

[101] Seral-Ascaso, A.; Luquin, A.; Lázaro, M. J.; et al. Synthesis and application of gold-carbon hybrids as catalysts for the hydroamination of alkynes. *Appl. Catal., A.* **2013**, *456*, 88-95.

[102] Sabbatini, A.; Martins, L. M.; Mahmudov, K. T.; et al. Microwave-assisted and solvent-free peroxidative oxidation of 1-phenylethanol to acetophenone with a Cu II–TEMPO catalytic system. *Catal. Commun*. **2014**, *48*, 69-72.

Appendix I -Experimental results for the oxidation of 1-phenylethanol with gold nanoparticles supported on carbon materials as catalysts

Table AI-1 Experimental results for the oxidation of 1-phenylethanol with Au@AC (DIM) as catalyst.

Entry	Catalyst (μmol)	Time (h)	T (°C)	TON_CAT[c]	TOF[d]	Yield (%)
1	1	0.5	50	134.6	269	5.3
2	1	1	50	195.7	196	6.0
3	1	2	50	101.4	101	4.6
4	1	0.5	80	188.0	376	6.7
5	1	1	80	184.5	185	7.6
6	1	2	80	316.2	158	9.5
7	5	0.5	80	41.9	84	10.9
8	5	1	80	45.1	45	10.5
9	5	2	80	51.7	26	12.8
10	1	0.5	90	187.3	187	9.6
11	1	1	90	163.4	163	8.0
12	1	2	90	292.4	292	12.8
13	1	0.5	100	198.4	397	10.7
14	1	1	100	257.2	257	12.3
15	1	2	100	345.5	173	15.0
16	1	2	110	175.5	88	15.0
17	5	2	110	95.7	48	44.3
18	1	2	120	238.3	119	19.8
19	1	2	150	658.4	329	56.9
20[a]	1	2	100	155.5	78	7.7
21[b]	1	2	100	103.8	52	11.8

[a] in the presence of 10 mmol TBHP

[b] in the presence of 2.5 mol% of TEMPO.

[c] turnover number (mole of product per mol of Au catalyst)

[d] turnover frequency (turnover number per unit of time)

Table AI-2 Experimental results for the oxidation of 1-phenylethanol with Au@AC (COL) as catalyst.

Entry	Catalyst (μmol)	Time (h)	T (°C)	TON_CAT[c]	TOF[d]	Yield (%)
1	1	0.5	50	171.6	343	5.5
2	1	1	50	152.4	152	5.7
3	1	2	50	110.4	55	4.8
4	1	0.5	80	156.1	312	6.5
5	1	1	80	254.0	254	8.9
6	1	2	80	213.1	107	8.9
7	5	0.5	80	34.4	69	8.5
8	5	1	80	39.3	39	9.8
9	5	2	80	52.2	26	12.4
10	1	0.5	90	234.1	468	8.4
11	1	1	90	201.2	201	9.5
12	1	2	90	239.0	120	11.0
13	1	0.5	100	198.4	397	9.7
14	1	1	100	227.4	227	11.5
15	1	2	100	321.7	161	14.7
16	1	2	110	303.7	152	27.4
17	5	2	110	158.8	80	76.0
18	1	2	120	433.4	217	36.7
19	1	2	150	854.9	428	45.5
20[a]	5	2	110	196.1	98	88.9
21[b]	5	2	110	129.0	65	61.0
22[a]	5	3	110	233.7	80	99.3

[a] in the presence of 10 mmol TBHP

[b] in the presence of 2.5 mol% of TEMPO.

[c] turnover number (mole of product per mol of Au catalyst)

[d] turnover frequency (turnover number per unit of time)

Table AI-3 Experimental results for the oxidation of 1-phenylethanol with Au@SC (DIM) as catalyst.

Entry	Catalyst (μmol)	Time (h)	T (°C)	TON_CAT[c]	TOF[d]	Yield (%)
1	1	0.5	50	42.7	86	2.0
2	1	1	50	45.7	46	2.2
3	1	2	50	42.8	21	2.0
4	1	0.5	80	86.9	174	4.3
5	1	1	80	123.4	123	5.3
6	1	2	80	164.0	82	7.0
7	5	0.5	80	50.4	101	9.0
8	5	1	80	57.3	57	9.7
9	5	2	80	76.2	38	11.7
10	1	0.5	90	221.2	443	8.0
11	1	1	90	266.5	267	9.6
12	1	2	90	332.6	166	11.4
13	1	0.5	100	212.6	425	8.4
14	1	1	100	302.0	302	11.5
15	1	2	100	397.4	199	14.8
16	1	2	110	189.8	95	15.4
17	5	2	110	56.6	28	26.6
18	1	2	150	830.7	415	73.5
19[a]	1	2	100	362.4	181	14.6
20[b]	1	2	100	267.7	134	8.4
21[a]	1	2	110	52.1	26	23.4
22[b]	1	2	110	17.6	9	7.9
23[a]	5	3	110	98.8	33	40.6
24[a]	5	12	110	134.9	11	54.3

[a] in the presence of 10 mmol TBHP
[b] in the presence of 2.5 mol% of TEMPO.
[c] turnover number (mole of product per mol of Au catalyst)
[d] turnover frequency (turnover number per unit of time)

Table AI-4 Experimental results for the oxidation of 1-phenylethanol with Au@SC (COL) as catalyst.

Entry	Catalyst (μmol)	Time (h)	T (℃)	TON_CAT[a]	TOF[b]	Yield (%)
1	1	0.5	50	40.6	81	1.9
2	1	1	50	45.3	45	2.0
3	1	2	50	45.8	23	2.1
4	1	0.5	80	79.0	158	3.0
5	1	1	80	107.4	107	4.3
6	1	2	80	187.5	94	6.3
7	5	0.5	80	45.9	92	8.5
8	5	1	80	58.8	59	10.1
9	5	2	80	75.9	38	11.5
10	1	0.5	90	222.4	445	8.2
11	1	1	90	255.5	256	9.0
12	1	2	90	348.1	174	10.9
13	1	0.5	100	241.0	482	11.7
14	1	1	100	423.6	424	13.1
15	1	2	100	676.3	338	16.0
16	1	2	110	167.8	84	16.0
17	5	2	110	28.9	15	13.4
18	1	2	150	813.0	407	66.5

[a] turnover number (mole of product per mol of Au catalyst)
[b] turnover frequency (turnover number per unit of time)

Table AI-5 Experimental results for the oxidation of 1-phenylethanol with Au@GR (DIM) as catalyst.

Entry	Catalyst (μmol)	Time (h)	T (°C)	TON_CAT[c]	TOF[d]	Yield (%)
1	1	0.5	50	46.1	23	2.1
2	1	1	50	63.4	32	2.3
3	1	2	50	76.6	38	2.6
4	1	0.5	80	66.7	134	2.7
5	1	1	80	84.3	84	3.3
6	1	2	80	157.7	79	4.9
7	5	0.5	80	14.6	29	3.0
8	5	1	80	18.0	18	3.5
9	5	2	80	25.7	13	4.7
10	1	0.5	90	79.8	160	2.8
11	1	1	90	92.1	92	5.2
12	1	2	90	158.6	80	5.2
13	1	0.5	100	226.1	452	7.1
14	1	1	100	203.2	203	7.3
15	1	2	100	378.2	189	13.0
16	1	2	110	29.6	15	14.1
17	5	2	110	159.2	80	14.3
18	1	2	150	709.8	355	63.8
19[a]	1	2	110	542.3	226	14.8
20[b]	1	2	110	152.2	76	6.2

[a] in the presence of 10 mmol TBHP
[b] in the presence of 2.5 mol% of TEMPO.
[c] turnover number (mole of product per mol of Au catalyst)
[d] turnover frequency (turnover number per unit of time)

Table AI-6 Experimental results for the oxidation of 1-phenylethanol with Au@GR (COL) as catalyst.

Entry	Catalyst (μmol)	Time (h)	T (°C)	TON_CAT[c]	TOF[d]	Yield (%)
1	1	0.5	50	69.0	138	2.9
2	1	1	50	67.8	68	2.9
3	1	2	50	71.6	36	2.8
4	1	0.5	80	72.9	146	3.0
5	1	1	80	98.2	98	3.8
6	1	2	80	138.8	69	5.2
7	1	0.5	90	91.6	183	3.9
8	1	1	90	120.4	120	5.0
9	1	2	90	193.9	97	6.9
10	1	0.5	100	167.2	335	7.2
11	1	1	100	288.4	288	10.0
12	1	2	100	458.8	229	14.8
13	1	2	110	574.3	287	53.7
14	5	2	110	157.5	78.8	75.7
15	1	2	150	494.6	247	42.7
16[a]	5	2	110	165.8	83	80.2
17[b]	5	2	110	211.2	106	99.9

[a] in the presence of 10 mmol TBHP
[b] in the presence of 2.5 mol% of TEMPO.
[c] turnover number (mole of product per mol of Au catalyst)
[d] turnover frequency (turnover number per unit of time)

Table AI-7 Experimental results for the oxidation of 1-phenylethanol with Au@CX (DIM) as catalyst.

Entry	Catalyst (μmol)	Time (h)	T (°C)	TON_CAT[a]	TOF[b]	Yield (%)
1	1	0.5	50	64.1	128	2.8
2	1	1	50	59.4	59	2.7
3	1	2	50	70.8	35	3.4
4	1	0.5	80	87.9	176	3.7
5	1	1	80	79.4	79	3.4
6	1	2	80	143.3	71	5.1
7	5	0.5	80	14.5	29	2.8
8	5	1	80	18.7	19	3,5
9	5	2	80	29.3	15	4.6
10	1	0.5	90	101.9	204	4.3
11	1	1	90	132.0	132	4.9
12	1	2	90	154.8	77	6.1
13	1	0.5	100	110.5	221	4.4
14	1	1	100	153.9	154	5.6
15	1	2	100	275.5	138	8.9
16	1	2	110	207.0	104	22.3
17	5	2	110	90.4	45	43.4
18	1	2	150	1018.6	509	86.8

[a] turnover number (mole of product per mol of Au catalyst)
[b] turnover frequency (turnover number per unit of time)

Table AI-8 Experimental results for the oxidation of 1-phenylethanol with Au@CX (COL) as catalyst

Entry	Catalyst (μmol)	Time (h)	T (°C)	TON_CAT[c]	TOF[d]	Yield (%)
1	1	0.5	50	67.5	135	2.9
2	1	1	50	70.8	71	2.8
3	1	2	50	68.3	34	2.9
4	1	0.5	80	75.7	151	3.2
5	1	1	80	79.4	79	3.4
6	1	2	80	111.0	56	4.2
7	1	0.5	90	149.8	300	5.9
8	1	1	90	236.9	237	8.5
9	1	2	90	311.1	156	10.8
10	1	0.5	100	159.7	320	5.6
11	1	1	100	215.6	216	7.1
12	1	2	100	338.7	170	10.8
13	1	2	110	593.1	297	58.4
14	5	2	110	208.2	104	91.1
15[a]	1	2	100	155.8	78	6.3
16[b]	1	2	100	108.9	55	3.9
17[a]	5	2	110	189.3	95	85.8
18[b]	5	2	110	178.6	89	84.5
19	5	3	110	209.7	70	91.2
20	5	12	110	204.5	17	93.8

[a] in the presence of 10 mmol TBHP
[b] in the presence of 2.5 mol% of TEMPO.
[c] turnover number (mole of product per mol of Au catalyst)
[d] turnover frequency (turnover number per unit of time)

Table AI-9 Experimental results for the oxidation of 1-phenylethanol with Au@CXL (COL) as catalyst

Entry	Catalyst (μmol)	Time (h)	T (°C)	TON_CAT[c]	TOF[d]	Yield (%)
1	1	2	60	53.5	27	4.0
2	1	2	100	226.0	113	10.0
3	1	2	110	787.1	394	42.6
4	2.5	2	110	335.1	168	74.5
5	5	2	110	188.0	94	90.9
6[a]	5	2	110	214.2	107	97.9
7[b]	5	2	110	230.0	116	99.9
8	1	2	150	970.2	485	91.8

[a] in the presence of 10 mmol TBHP
[b] in the presence of 2.5 mol% of TEMPO.
[c] turnover number (mole of product per mol of Au catalyst)
[d] turnover frequency (turnover number per unit of time)

Table AI-10 Experimental results for the oxidation of 1-phenylethanol with Au@MD (DIM) as catalyst.

Entry	Catalyst (μmol)	Time (h)	T (°C)	TON_CAT[a]	TOF[b]	Yield (%)
1	1	2	110	237.7	119	21.3
2	5	2	110	126.2	63	55.4
3	1	2	150	815.0	408	68.9

[a] turnover number (mole of product per mol of Au catalyst)
[b] turnover frequency (turnover number per unit of time)

Table AI-11 Experimental results for the oxidation of 1-phenylethanol with Au@MD (COL) as catalyst.

Entry	Catalyst (μmol)	Time (h)	T (℃)	TON_CAT[b]	TOF[c]	Yield (%)
1	1	2	100	500.9	250	44.1
2	1	2	110	454.8	227	43.8
3	5	2	110	177.6	89	88.2
4[a]	5	2	110	202.6	101	99.9
5	1	2	150	1365.1	683	98.3

[a] in the presence of 10 mmol TBHP
[b] turnover number (mole of product per mol of Au catalyst)
[c] turnover frequency (turnover number per unit of time)

Table AI-12 Experimental results for the oxidation of 1-phenylethanol with Au@NDLIQ (DIM) as catalyst.

Entry	Catalyst (μmol)	Time (h)	T (℃)	TON_CAT	TOF	Yield (%)
1	1	2	60	28.1	14	2.7
2	1	2	100	393.6	197	33.2
3	1	2	110	553.2	277	51.4
4	5	2	110	173.2	87	78.2
5	1	2	150	960.8	480	84.9
6[a]	5	2	110	224.3	112	99.2
7[b]	5	2	110	249.3	125	99.9

[a] in the presence of 10 mmol TBHP
[b] in the presence of 2.5 mol% of TEMPO.
[c] turnover number (mole of product per mol of Au catalyst)
[d] turnover frequency (turnover number per unit of time)

Table AI-13 Experimental results for the oxidation of 1-phenylethanol with Au@NDLIQ (COL) as catalyst.

Entry	Catalyst (μmol)	Time (h)	T (℃)	TON_CAT[a]	TOF[b]	Yield (%)
1	1	2	60	23.8	12	3.9
2	1	2	100	272.2	136	31.3
3	1	2	110	542.2	271	49.5
4	5	2	110	135.3	68	67.3
5	1	2	150	1055.5	528	85.3

[a] turnover number (mole of product per mol of Au catalyst)
[b] turnover frequency (turnover number per unit of time)

Table AI-14 Experimental results for the oxidation of 1-phenylethanol with Au@NDPW (COL) as catalyst.

Entry	Catalyst (μmol)	Time (h)	T (℃)	TON_CAT[a]	TOF[b]	Yield (%)
1	1	2	60	33.5	17	3.5
2	1	2	100	400.3	200	37.0
3	1	2	110	484.1	242	48.0
4	1	2	150	1008.8	504	87.5

[a] turnover number (mole of product per mol of Au catalyst)l
[b] turnover frequency (turnover number per unit of time)

Appendix II – Copper nanoparticles supported at CNT used for degradation of dyes

1. Introduction

Carbon nanotubes (CNT) are allotropes of carbon with the cylindrical nanostructure, and the ratio of length to diameter can up to 132,000,000:1[1], which is much larger than other materials. They exhibit predominant thermal conductivity[2], mechanical properties[3] and electrical properties[4], so they can be used as additives to different kinds of material. CNT can be produced as single (SWCNT) or multi-walled (MWCNT), where multi-walled carbon nanotubes contain several tubes in concentric cylinders, and normally the numbers of the concentric walls can up to 25 layers or more. Thus the diameter of MWCNT can be 30 nm when in comparison with 0.7-20 nm for typical SCWNTs [5].

Many researchers have been preparing Cu@CNT using different methods, for example, chemical reduction preparation[6], thermal reduction[7], microemulsion method[8], polyol process[9] and dc and arc discharge[10]. A small amount of CuO/Cu_2O is formed along with the preparation of CuNPs. Thus the difficulty in the synthesis of Cu@CNT is to avoid the oxidation of Cu nanoparticles[11]. **Figure 2-1** presents the SEM images of Cu@CNT nanocomposite used in this study[12], obtained by using ethylene glycol as the oxidant since it is a mild oxidizing agent that can prevent contamination or unexpected materials. From SEM images it can be seen that Cu is well dispersed through the CNT matrix.

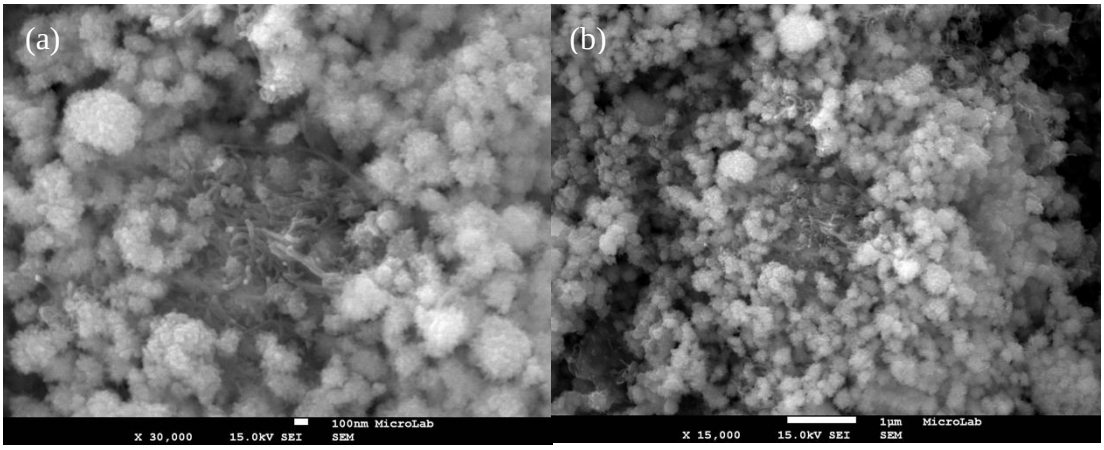

Figure 2-1 SEM images of Cu-CNT nanocomposite powder. (a) x30000; (b) x15000.

Pigments have many industrial applications; for instance, they can be used for coloring fabric, cosmetics, food and other materials[13]. Colored wastewater from textile, dyeing, and food, raised several important environmental risks. Given an example from textile industry, ca. 15% of the dye not used during the dyeing process is released as effluent. Besides, a lot of organic compounds are formed during the period of the dyeing process, and some of them are carcinogenic[14]. So it is very urgent to solve the wastewater issues, it is a big threat since the hydrolysis reaction of the contamination in the wastewater can form a lot of toxic compounds[15].

The methods for dye decoloration can be classified into physical, chemical and biological techniques[16]. Environmental catalysis plays an important role in decreasing the form of the toxic chemicals by using energy efficient, residue-free methods[17]. Sunil and colleagues[18] have been found that a Cu@CNT composite has immense potential used as antimicrobial agents, since Cu nanoparticles have good compatibility with the bacterial cell walls (because of the surface groups), and the function of the carbon nanotubes is to increase the interface area between the Cu@CNT nanocomplex and bacterial cell walls. Thus, they have a big advantage for antimicrobial applications. Kuo[19] have been observed that TiO_2 conjunct with CNT composite have a high efficiency for photodegradation. In this case, CNT not only blocks the electron--hole pair generation; but also can increase the surface area. Thus the number of hydroxyl groups also increased on the surface of the composite, so it can be assumed that appropriate quantity of CNT can rise the photocatalytic activity of TiO_2 greatly.

2. Experimental

2.1. Materials and instruments

Hydrogen peroxide (H_2O_2, 30% aq. solution), NaOH (≥ 97.0%, pellets), copper (Cu)-CNT were from Sigma-Aldrich. The hydrochloric acid (HCl; purity of 37%) from Panreac. Acetone (p.a.) and acetonitrile (MeCN, 99.99%) were from Fisher Scientific, deionised water from Merck KGaA (AFS® D water purification systems).

The pigments were brilliant blue, methyl violet, amaranth, and tartrazine, which were purchased from Merck. The TLC plates (Silica Gel 60) were from WVR.

The catalytic activity of Cu@CNT was measured by UV-Visible spectrophotometry at a Perkin-Elmer Lambda 750 spectrophotometer.

2.2. Experimental Procedure

2.2.1 Catalytic decoloration of organic pigments

Brilliant blue, methyl violet, amaranth, and tartrazine (**Table 2-1**) were selected as pigments to investigate the catalytic activity of Cu@CNT. The pigment solution was prepared at different pH values (pH=2, pH=7, and pH=12) since the pH value is very important regarding the catalytic degradation reactions; it does not only influence the surface charge[20] of the catalysts but also determine the absorption behavior of pigments[21]. So in order to understand the effect of pH, the pigment solution under acid (pH=2), neutral (pH=7) and base (pH=12) were needed in the experimental section First of all, the pigment solution was prepared with suitable concentration according to the calibration curve of each pigment, which presents in **Table 2-2**. Then, 15 mg of catalyst Cu-CNT was added, and the reaction suspension was magnetically stirred for 30min. Then 3 ml of 30% H_2O_2 aq. solution was added. Afterward, the sample was put into a 10 mm quartz cell, and the UV test started immediately. Each sample was carried out every five minutes. Also, all the reactions should be occurred under the dark circumstance, to avoid the sunlight irradiation.

Table 2-1 Structure and molecular mass of the pigments used in the present work.

Name	Structure	Molecular mass (g/mol)
Brilliant blue	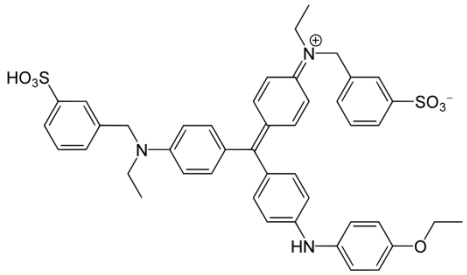	825.97
Tartrazine	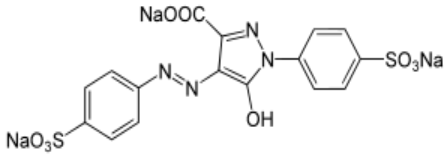	534.36
Amaranth	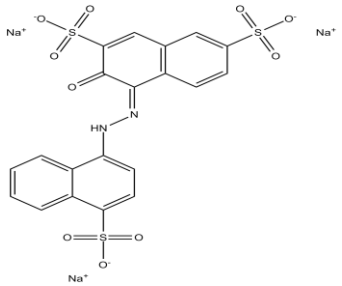	604.473
Methyl violet	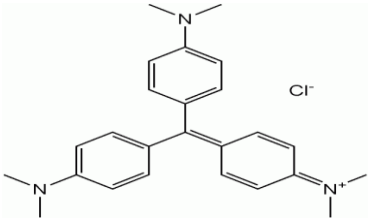	407.98

IUPAC name of each pigment:

[a]ethyl-[4-{[4-[ethyl-[(3-sulfophenyl)methyl]amino]phenyl]-(2-sulfophenyl)methylidene]-1-cyclohexa-2, 5-dienylidene]-[(3-sulfophenyl)methyl]azanium;

[b]Trisodium(4E)-5-oxo-1-(4-sulfonatophenyl)-4-[(4-sulfonatophenyl)hydrazono]-3-pyrazolecarboxylate;

[c]Trisodium(4E)-3-oxo-4-[(4-sulfonato-1-naphthyl)hydrazono]naphthalene-2,7-disulfonate;

[d]4-{Bis[4-(dimethylamino)phenyl]methylen}-N,N-dimethyl-2,5-cyclohexadien-1-iminiumchlorid.

Table 2-2 Concentration of the pigments used for the study of their decoloration at different pH values.

Pigment	**concentration (pH=7) /(mg/L)**	**concentration (pH=2) /(mg/L)**	**concentration (pH=12) /(mg/L)**
Brilliant blue	5.6	4.2	–
tartrazine	66.7	50.0	51.2
Amaranth	35.6	18.5	30.8
Methyl violet	16.2	15.9	–

Different concentrations were chosen under different pH with the same catalysts, because different dissolving capacities were obtained at different pH values, so the desirable concentration should be selected for the following experimental section. Moreover, the concentration was different among different catalysts, since the structure of the pigments also determined the dissolving capacities of the pigments.

2.2.2 Calibration curve for brilliant blue

In this procedure, brilliant blue solutions with 11 different concentrations were prepared, at different pH (pH=2, pH=7, and pH=12). The initial pigment stock solution had the concentration of 100mg/L, and the prepared samples are listed in **Table 2-3**. Then, the absorbance of each diluted solution was measured, and a calibration curve was established. The results are presented at **Figures 2-2** to **2-4**.

Table 2-3 Assay conditions for calibration curve calculation using 11 different concentrations of brilliant blue solution.

Entry	concentration (mg/L)	brilliant Blue (mL)	distilled water (mL)
1	75	7.5	2.5
2	50	5	5
3	40	4	6
4	30	3	7
5	20	2	8
6	10	1	9
7	8	0.8	9.2
8	5	0.5	9.5
9	2	0.2	9.8
10	1	0.1	9.9
11	0.5	0.05	9.95

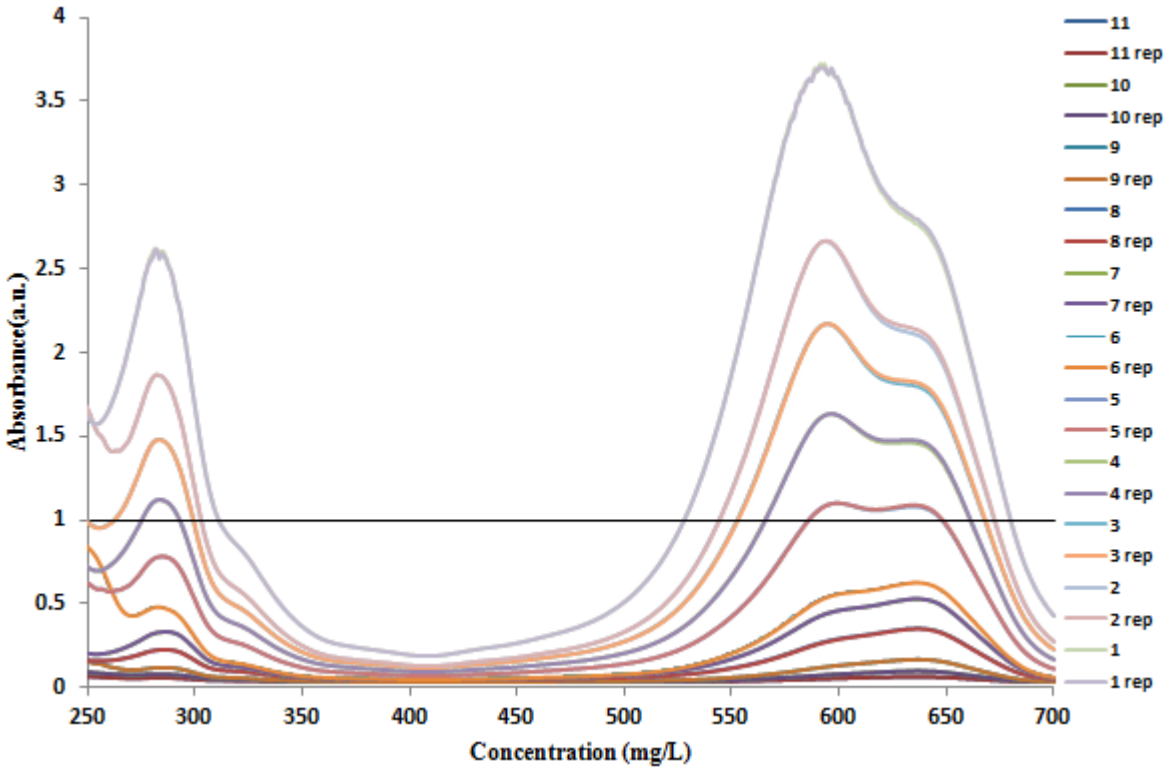

Figure 2-2 UV-Vis spectra with different concentrations of brilliant blue at pH=2. For calculation purposes, only absorbance below 1 a.u. was calculated.

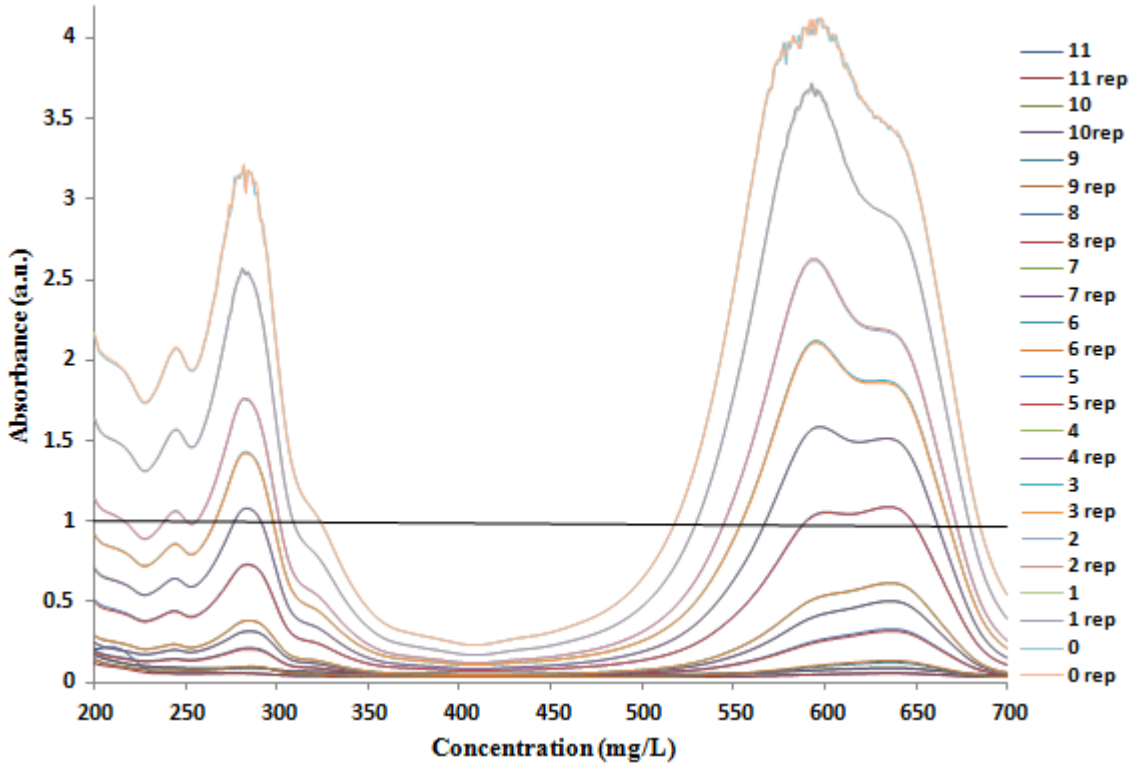

Figure 2-3 UV-Vis spectra with different concentrations of brilliant blue at pH=7. For calculation purposes, only absorbance below 1 a.u. was calculated.

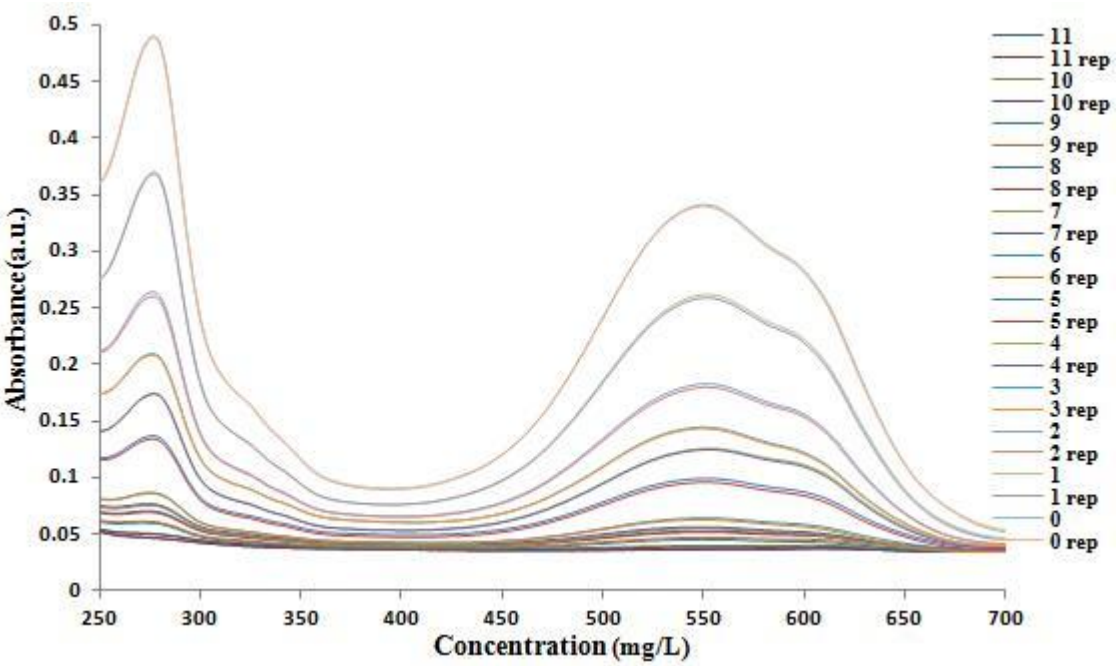

Figure 2-4 UV-Vis spectra with different concentrations of brilliant blue at pH=12. For calculation purposes, only absorbance below 1 a.u. was calculated.

From **Figures 2-2** to **2-4**, the absorbance under different concentrations at

different pH can be observed, and the maximum absorbance wavelength of brilliant blue at studied pH was used to construct the calibration curve, and the results are presented below.

Table 2-4 Maximum absorbance wavelength of brilliant blue at different pH values.

Entry	Con. /(mg/L)	λ(pH=2) /nm	Absorbance (pH=2)	λ(pH=7) /nm	Absorbance (pH=7)	λ(pH=12) /nm	Absorbance (pH=2)
1	75	590	3.70	596	3.68	548	0.26
2	50	594	2.67	598	2.61	550	0.18
3	40	591	2.15	599	2.10	549	0.14
4	30	593	1.63	601	1.58	548	0.12
5	20	593	1.08	642	1.07	548	0.10
6	10	634	0.63	644	0.60	551	0.06
7	8	637	0.53	644	0.49	552	0.06
8	5	638	0.35	644	0.32	542	0.05
9	2	639	0.17	643	0.13	541	0.05
10	1	641	0.10	644	0.09	542	0.04
11	0.5	639	0.98	642	0.06	542	0.04

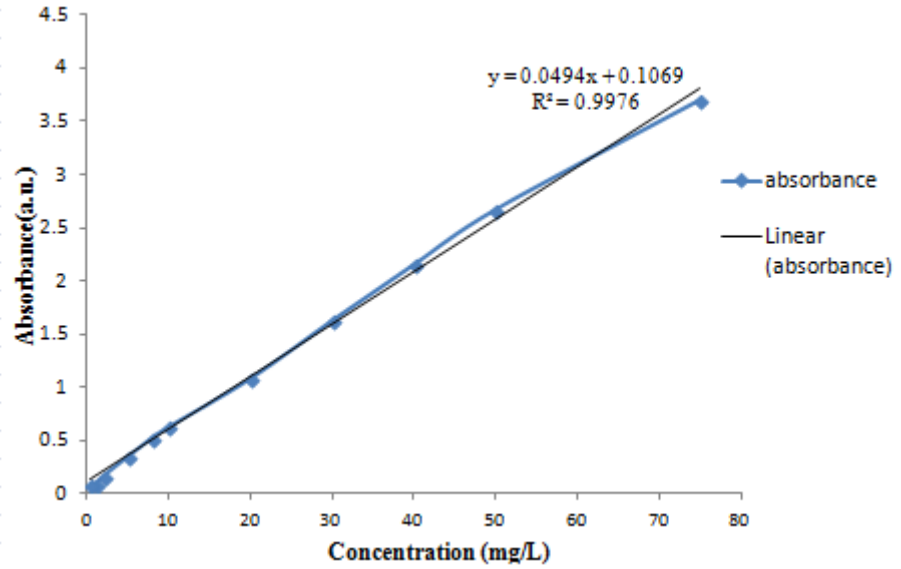

Figure 2-5 Calibration curve of brilliant blue at pH=2.

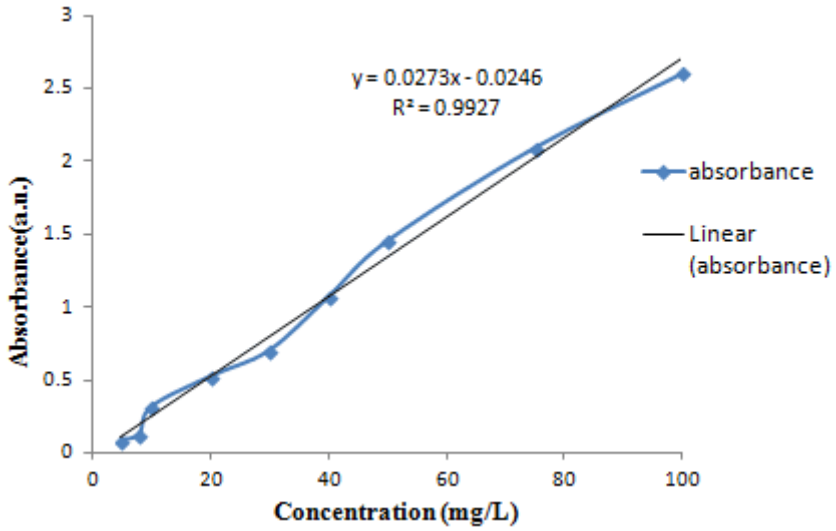

Figure 2-6 Calibration curve of brilliant blue at pH=7.

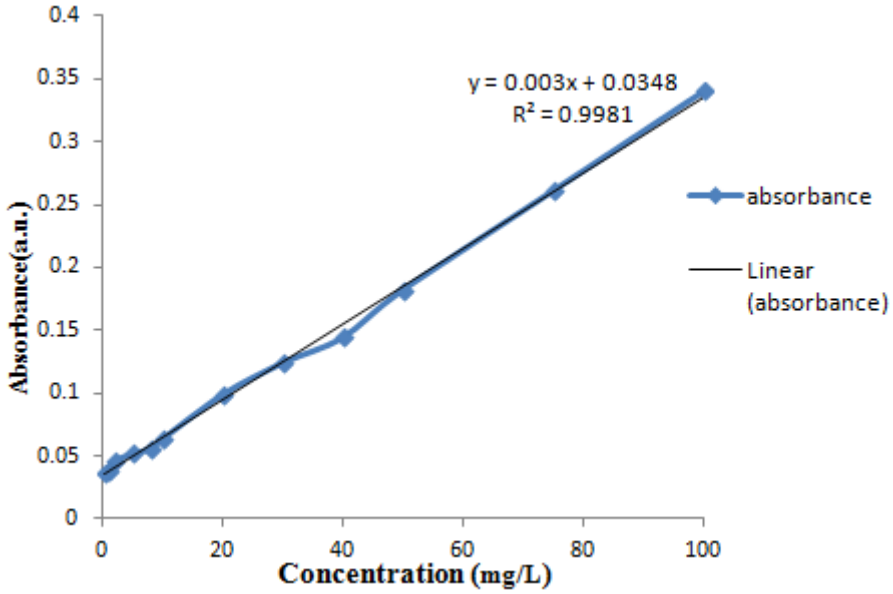

Figure 2-7 Calibration curve of brilliant blue at pH=12.

From **Figures 2-5** to **2-7**, in the case of pH = 2, the coefficient is 0.0494, and R^2 is 0.9976, for pH=7, the coefficient is 0.0273, and R^2 is 0.9927. Moreover, the coefficient is 0.003, and R^2 is 0.9981 at pH=12, and R^2 is a statistical measure that how close the data are to the fitted regression line. The equation of the regression can be achieved to calculate the concentrations of the samples in the working range, by simply plugging X in the equation; in this case, the suitable concentration can be

selected for brilliant blue at different pH in the following work.

2.2.3 Calibration curve for tartrazine

The preparation of tartrazine solution followed the same method as for brilliant blue, which was presented in **Table 2-5**. Therefore, the absorbance of each diluted solution was measured by UV-Visible spectrophotometry, and then the calibration curve was established. The results are shown from **Figures 2-8** to **2-10**.

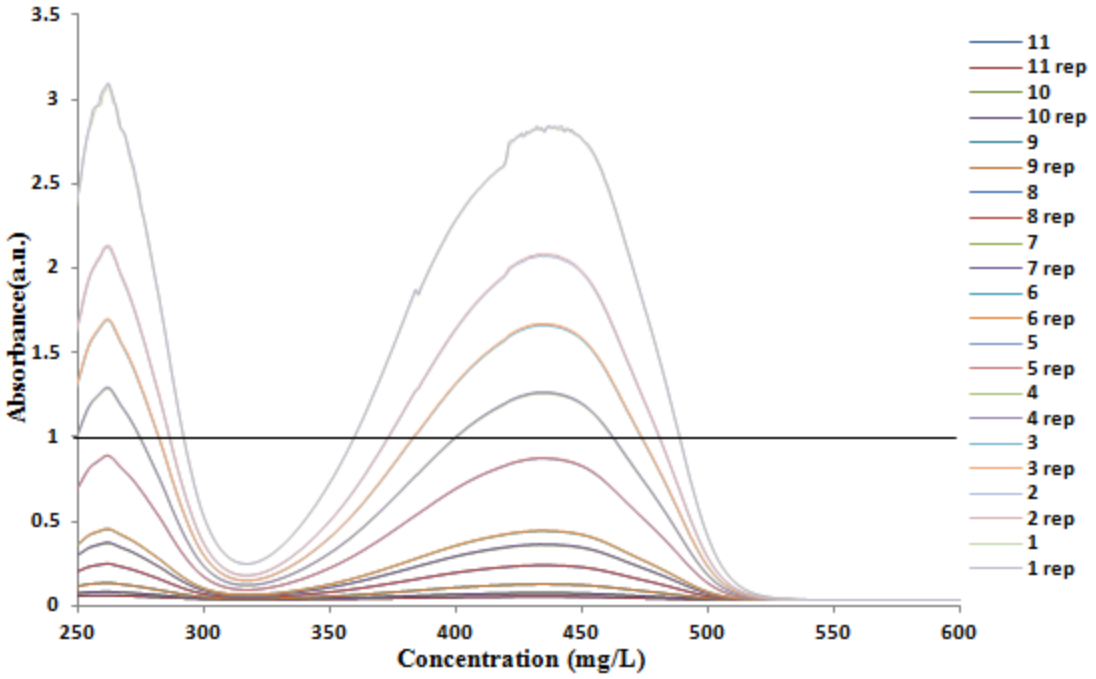

Figure 2-8 UV-Vis spectra with different concentrations of tartrazine at pH=2. For calculation purposes, only absorbance below 1 a.u. was calculated.

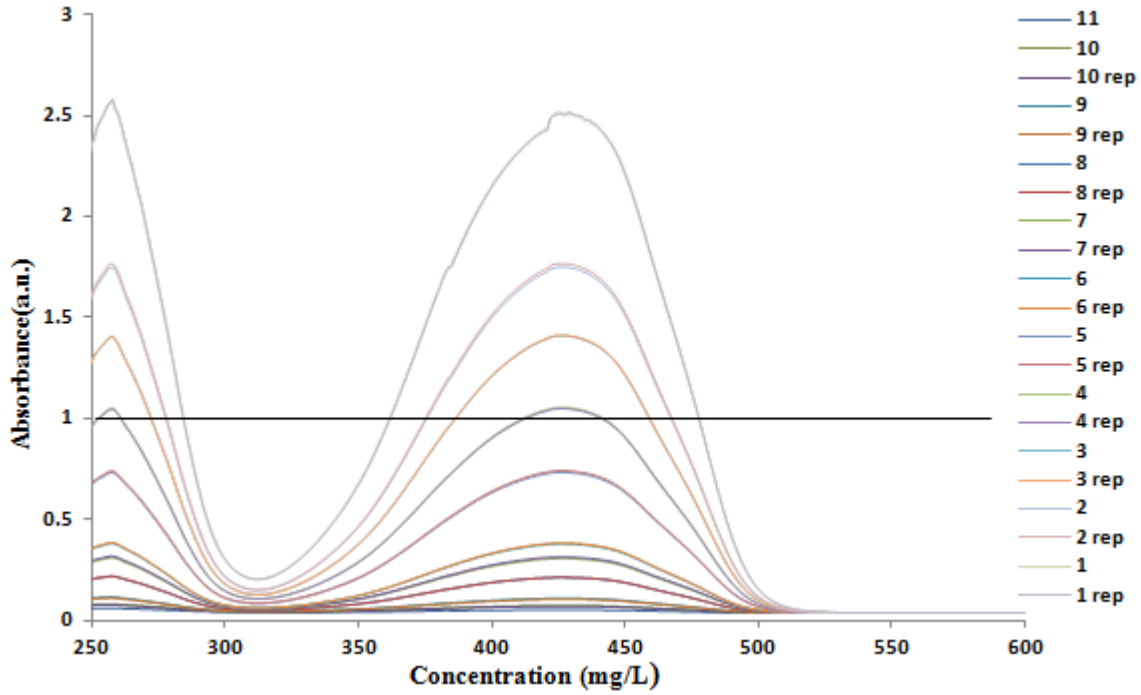

Figure 2-9 UV-Vis spectra with different concentrations of tartrazine at pH=7. For calculation purposes, only absorbance below 1 a.u. was calculated.

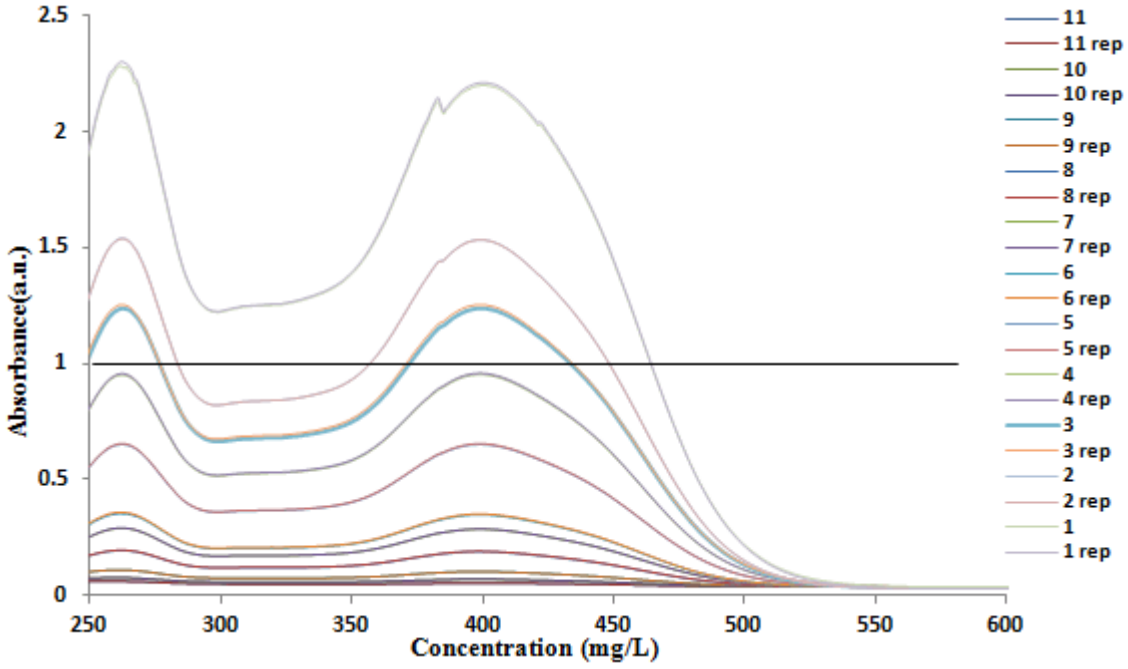

Figure 2-10 UV-Vis spectra with different concentrations of tartrazine at pH=12. For calculation purposes, only absorbance below 1 a.u. was calculated.

From the graphs above, the absorbance of different concentrations at different pH values can be observed, then the maximum absorbance wavelength of tartrazine at

studied pH was used to establish the calibration curve, and the results are shown below.

Table 2-5 Maximum absorbance wavelength of tartrazine at different pH values.

Entry	Con. /(mg/L)	λ(pH=2) /nm	Absorbance (pH=2)	λ(pH=7) /nm	Absorbance (pH=7)	λ(pH=12) /nm	Absorbance (pH=2)
1	75	440	2.84	429	2.52	400	2.21
2	50	434	2.08	425	1.77	401	1.53
3	40	434	1.67	425	1.41	398	1.25
4	30	434	1.26	428	1.05	399	0.96
5	20	435	0.87	427	0.74	398	0.65
6	10	433	0.44	423	0.38	400	0.35
7	8	434	0.36	418	0.30	397	0.28
8	5	437	0.24	422	0.21	399	0.19
9	2	437	0.13	421	0.10	399	0.10
10	1	435	0.08	422	0.07	399	0.07
11	0.5	438	0.05	420	0.05	397	0.05

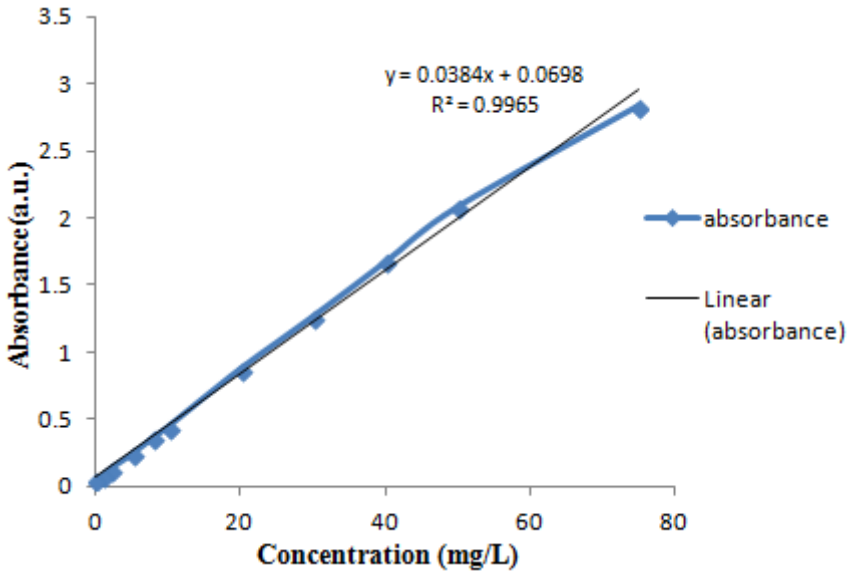

Figure 2-11 Calibration curve of tartrazine at pH=2.

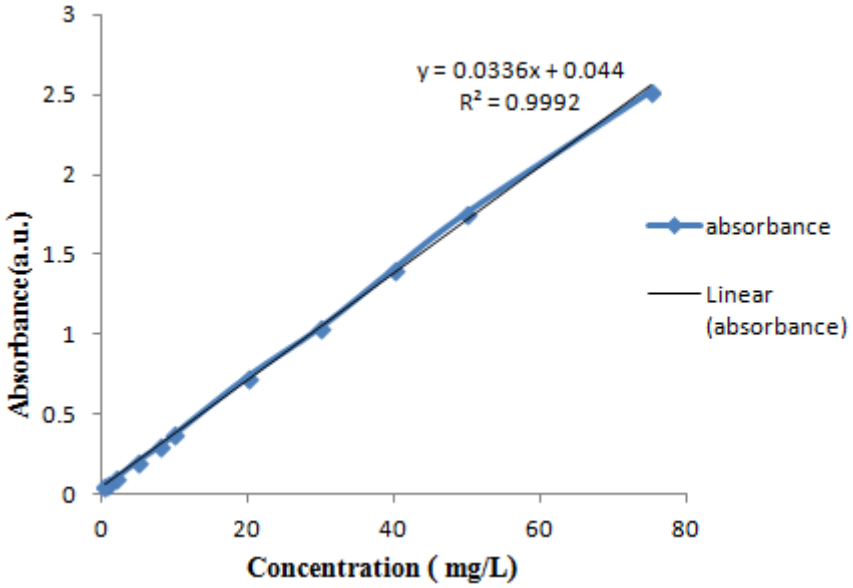

Figure 2-12 Calibration curve of tartrazine at pH=7.

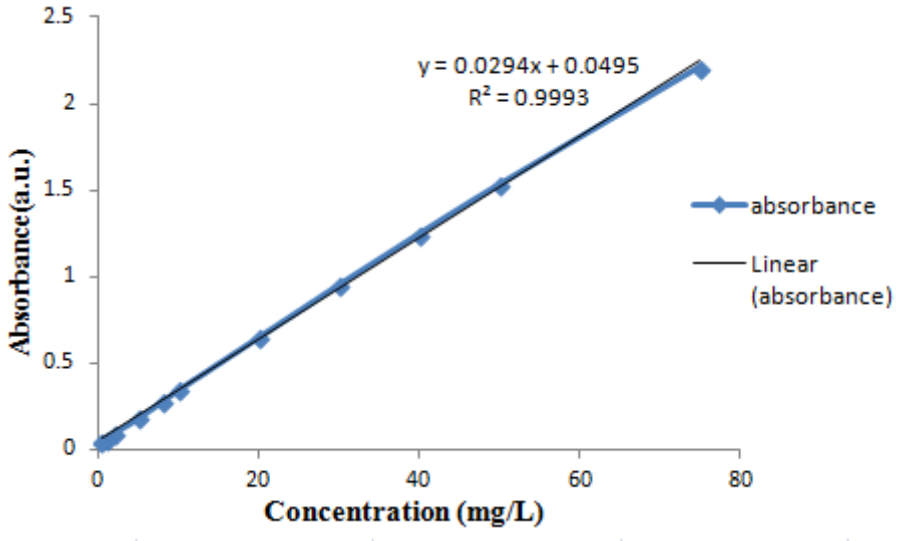

Figure 2-13 Calibration curve of tartrazine at pH=12.

From the graphs above, it can be known that R^2 is 0.9965, and the coefficient is 0.0384 at pH=2, in the presence of pH=7, R^2 and coefficient is 0.992 and 0.0336, respectively. Regarding pH=12, the coefficient is 0.0294, and R^2 is 0.9993. The regression equation is used to calculate the unknown concentration of samples in the working range by the absorbance, and R^2 is the statistical measure that how close the data are to the fitted regression line. In this case, the suitable concentration can be chosen for tartrazine at different pH regarding calibration curve, which is important

for the following work.

2.2.4 Calibration curve for amaranth

The preparation of amaranth solutions uses the method same as for previous pigments (tartrazine and brilliant blue), and is presented in **Table 2-6**. Moreover, the absorbance of each diluted solution was measured by UV-Visible spectrophotometry, thus allowing establishing the calibration curve. The results are presented below.

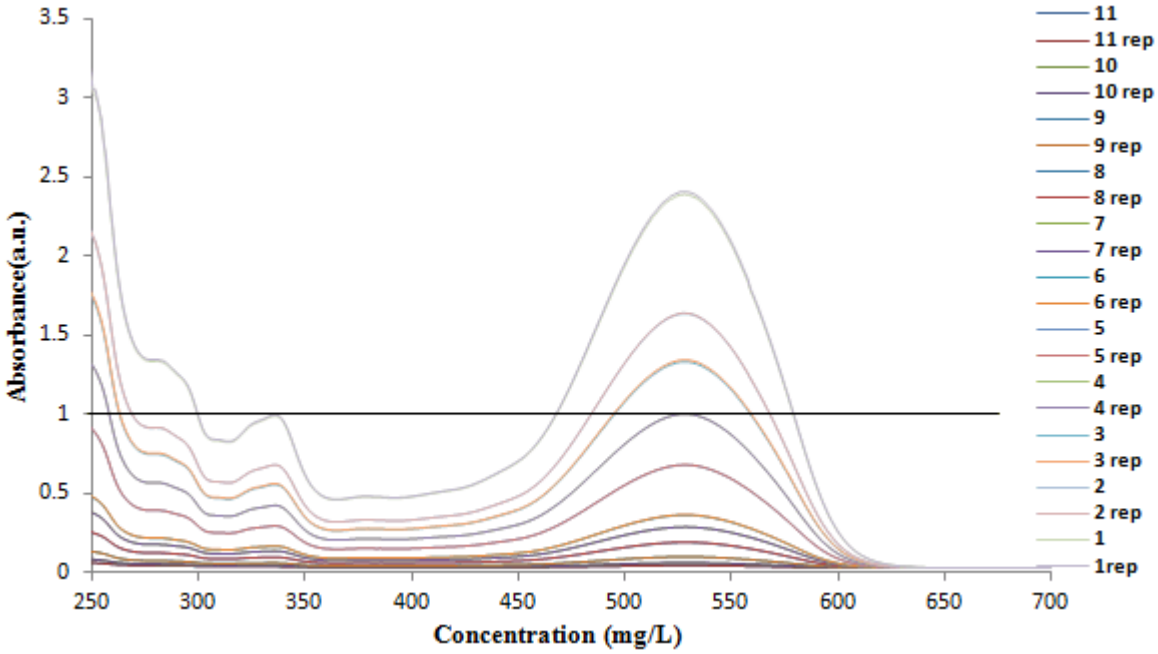

Figure 2-14 UV-Vis spectra with different concentrations of amaranth at pH=2. For calculation purposes, only absorbance below 1 a.u. was calculated.

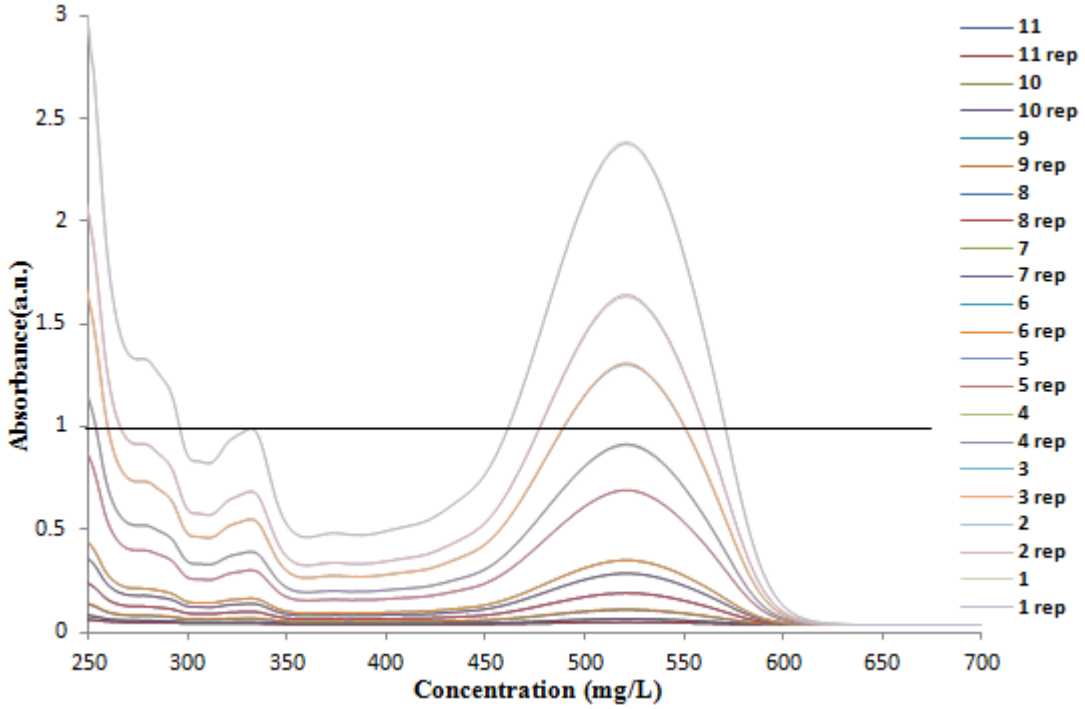

Figure 2-15 UV-Vis spectra with different concentrations of amaranth at pH=7. For calculation purposes, only absorbance below 1 a.u. was calculated.

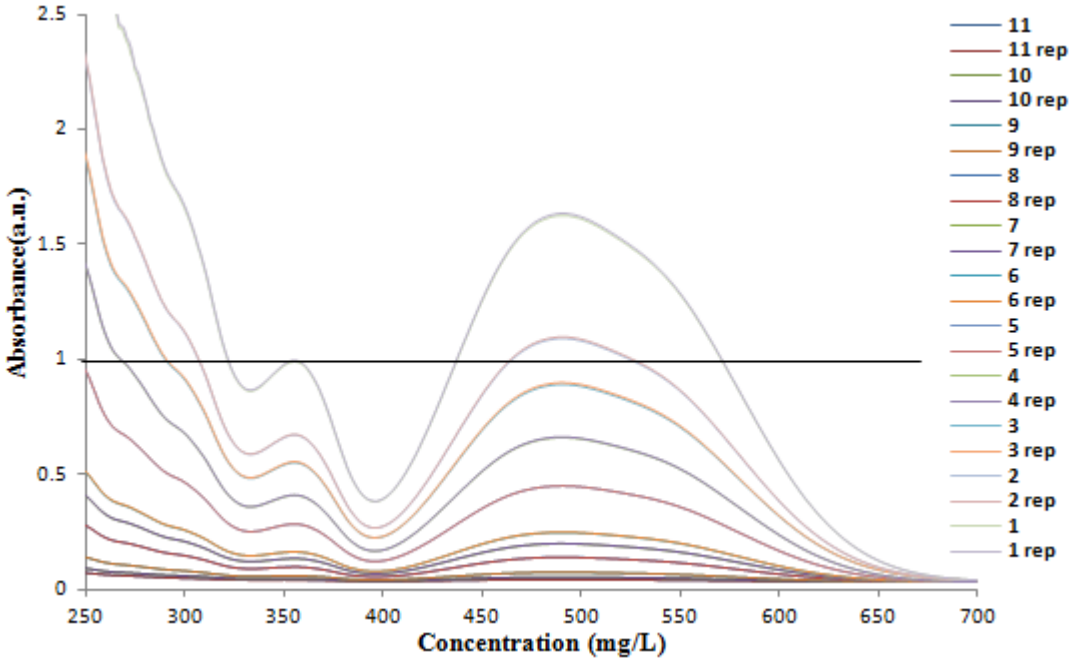

Figure 2-16 UV-Vis spectra with different concentrations of amaranth at pH=12. For calculation purposes, only absorbance below 1 a.u. was calculated.

It can be observed from **Figures 2-14** to **2-16** that, in the case of pigment amaranth, the maximum absorbance wavelength with different concentrations at

studied pH values can be observed, and the results are presented as follows.

Table 2-6 Maximum absorbance wavelength of amaranth at different pH values.

Entry	Con. /(mg/L)	λ(pH=2) /nm	Absorbance (pH=2)	λ(pH=7) /nm	Absorbance (pH=7)	λ(pH=12) /nm	Absorbance (pH=2)
1	75	547	4.31	522	2.39	494	1.63
2	50	557	4.11	524	1.64	492	1.10
3	40	590	3.60	522	1.31	491	0.90
4	30	588	2.96	522	0.91	492	0.67
5	20	588	2.05	524	0.69	491	0.45
6	10	589	1.14	522	0.35	489	0.25
7	8	589	0.82	522	0.29	492	0.20
8	5	589	0.58	522	0.11	490	0.14
9	2	593	0.21	525	0.11	491	0.08
10	1	593	0.11	526	0.07	491	0.06
11	0.5	593	0.07	530	0.07	492	0.04

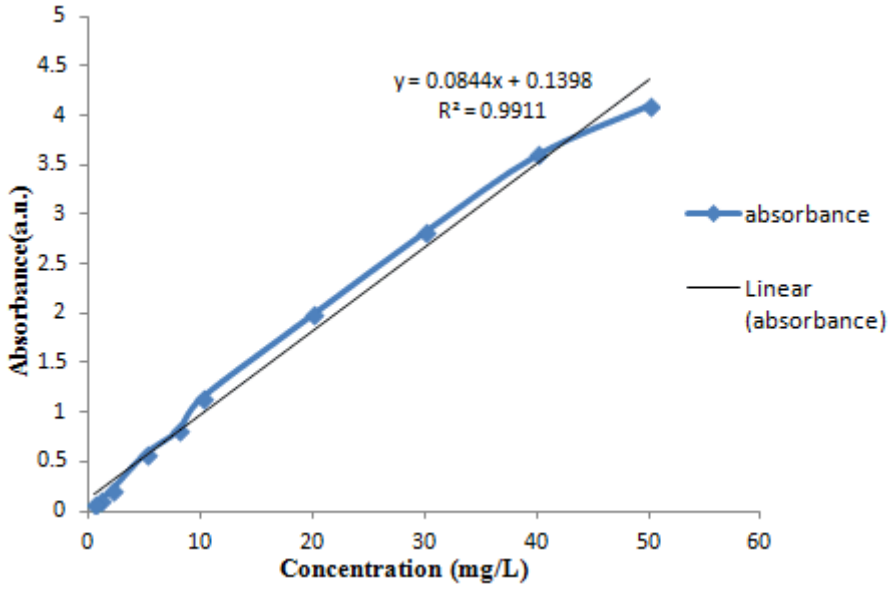

Figure 2-17 Calibration curve of amaranth of pH=2.

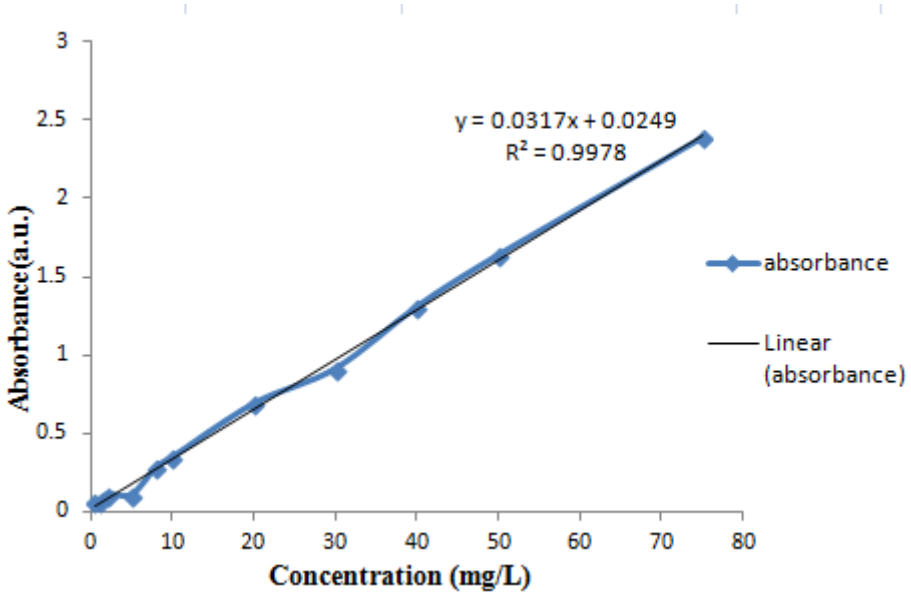

Figure 2-18 Calibration curve of amaranth of pH=7.

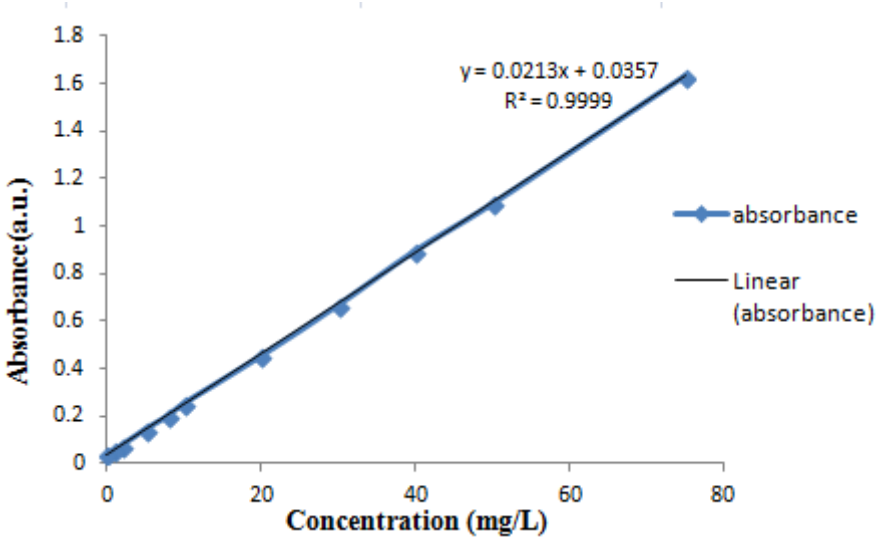

Figure 2-19 Calibration curve of amaranth at pH=12.

From **Figures 2-17** to **2-19**, it can be observed that R^2 is 0.9877, and the coefficient is 0.0851 at pH=2 for amaranth. Regarding pH=7, R^2 and coefficient is 0.9978 and 0.0317, respectively. At pH=12, R^2 is 0.9999, and the coefficient is 0.0213. R^2 is the coefficient of multiple determinations for multiple regressions. Moreover, the regression equation is used to calculate the unknown concentration of the sample in the working ranging by the absorbance. So the suitable concentration can be selected for amaranth regarding calibration curve, and it is important for the following

work.

2.2.5 Calibration curve for methyl violet

The preparation of methyl violet solutions used the same procedure as brilliant blue, which is presented in **Table 2-7**. Then the absorbance of each diluted solution was measured by UV-Vis spectrophotometry, to establish the calibration curve. The results are presented from **Figures 2-20** to **2-21**.

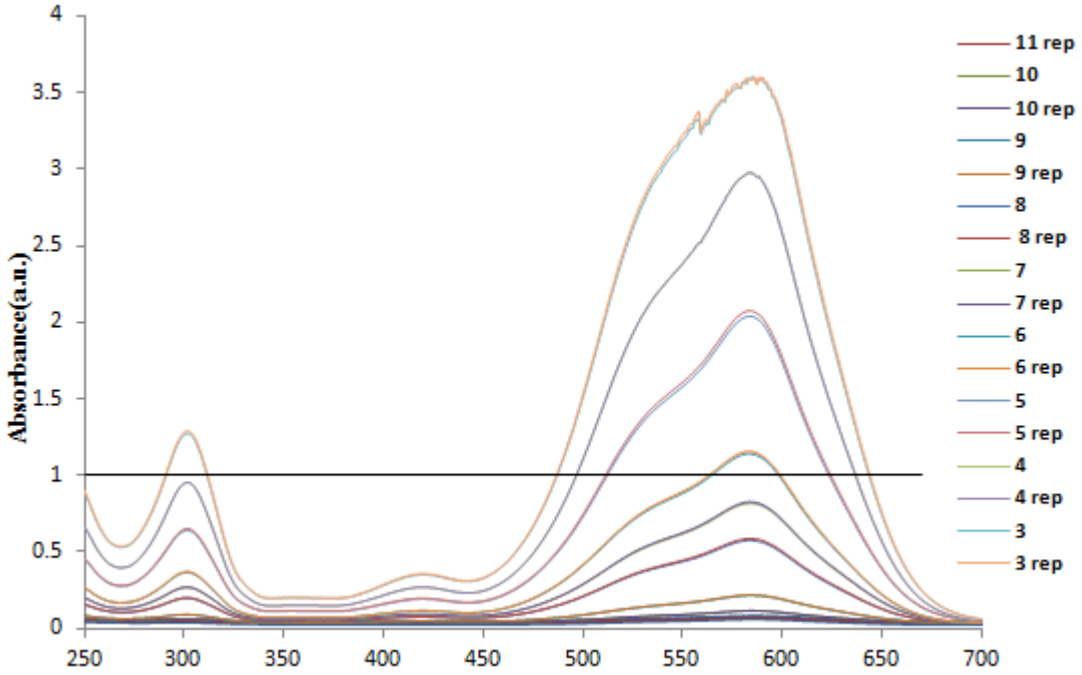

Figure 2-20 UV-Vis spectra with different concentrations of methyl violet at pH=2.

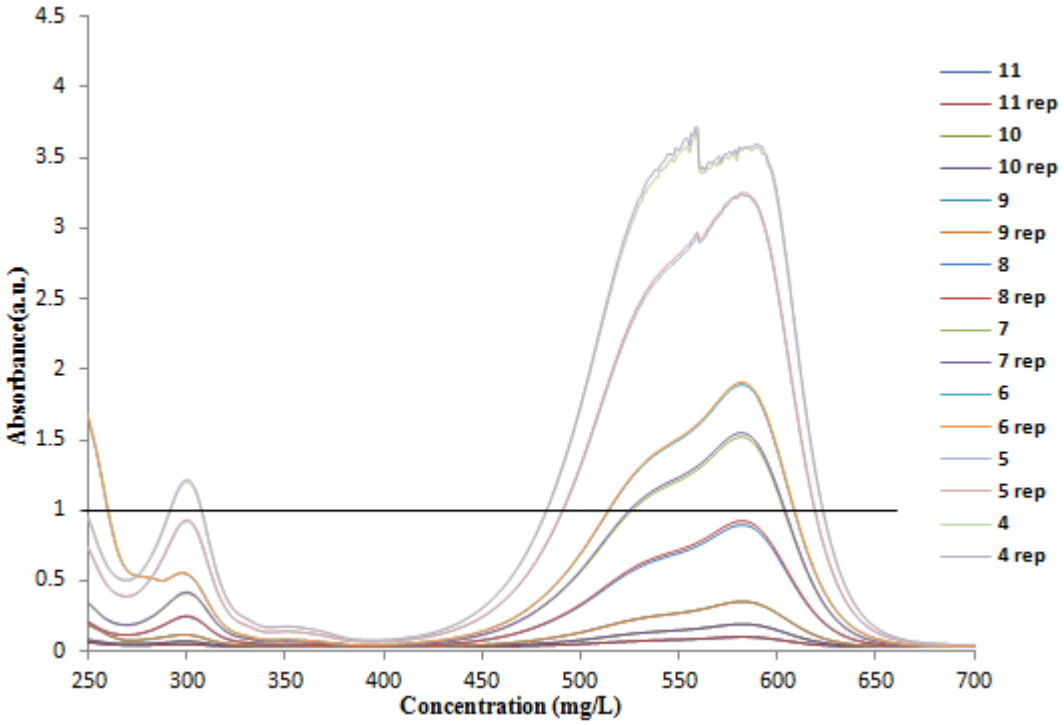

Figure 2-21 UV-Vis spectra with different concentrations of methyl violet at pH=7.

It can be observed from **Figures 2-20** and **21**, in the case of pigment methyl violet, the maximum absorbance wavelength with different concentrations at studied pH values (methyl violet cannot dissolve at pH=12), and the results are shown below.

Table 2-7 Maximum absorbance wavelength of methyl violet at different pH value.

Entry	Con. /(mg/L)	λ(pH=2) /nm	Absorbance (pH=2)	λ(pH=7) /nm	Absorbance (pH=7)
1	75	547	4.31	546	4.23
2	50	557	4.11	550	4.23
3	40	590	3.60	546	4.01
4	30	588	2.96	558	3.71
5	20	588	2.05	586	3.21
6	10	589	1.14	585	1.90
7	8	589	0.82	584	1.54
8	5	589	0.58	586	0.91
9	2	593	0.21	586	0.35
10	1	593	0.11	588	0.10
11	0.5	593	0.07	589	0.10

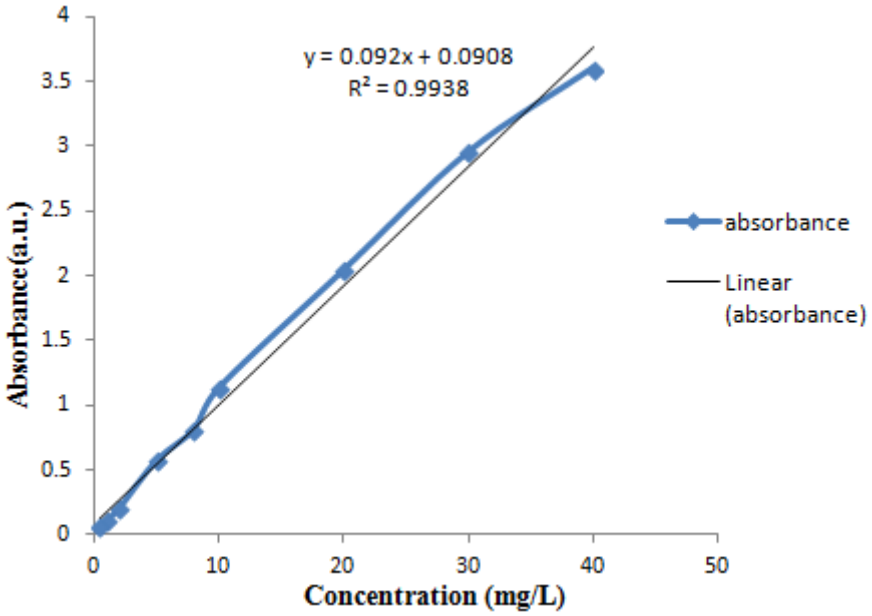

Figure 2-22 Calibration curve of methyl violet at pH=2.

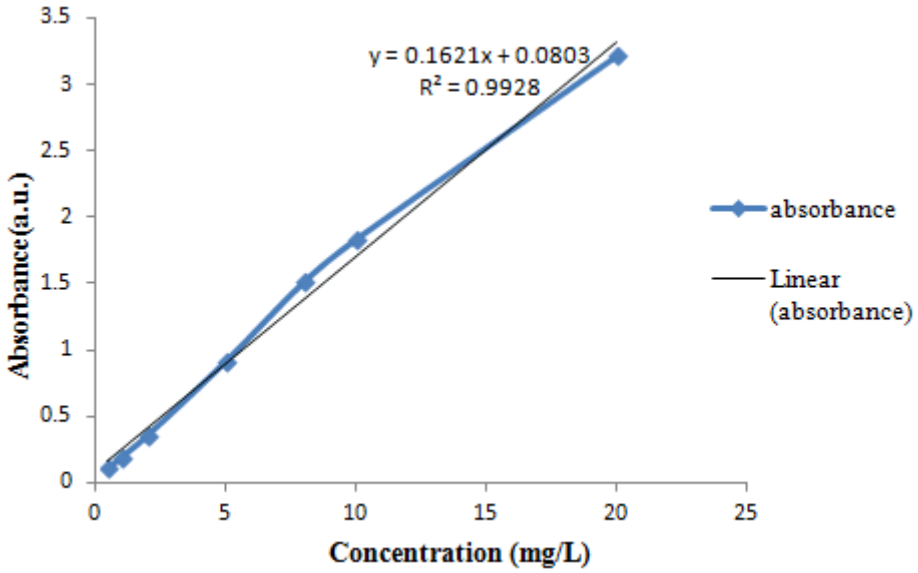

Figure 2-23 Calibration curve of methyl violet at pH=7.

From **Figure 2-22** and **2-23**, regarding with pH=2, R^2 is 0.9938, and the coefficient is 0.092. In the case of pH=7, R^2 and coefficient is 0.9928 and 0.1621, respectively. The suitable concentration for pigment methyl violet in the following work can be calculated from the regression equation, which is very important.

2.3. Pigment analysis

The decoloration of pigment solutions was related to Langmuir Hinshelwood (L-H) kinetic equation, used to describe the heterogeneous reaction for a long time. When possible, the degradation of the pigments was subjected to the first order kinetics, which is given by the equation:

$$\ln\left(\frac{Af}{Ai}\right) = Kapp\ t \qquad (1)$$

where A_f is the initial absorbance of the pigments.

A_i is the absorbance of the pigments at time t.

K_{app} is the reaction rate constant (min^{-1})

The prepared pigment solutions were subjected to UV-Vis detection in the

presence of the catalyst. The absorption spectrum of the pigment solution was changed over a period of time regularly, the absorbance decreased with the irradiation time, therefore indicating the decoloration of the pigment solution, and it can be explained by the equation as follows：

$$decrease\ in\ absorption\ (\%) = \left(1 - \frac{Ai}{Af}\right) \times 100 \qquad (2)$$

where A_f is the initial absorbance of the pigment.

A_i is the absorbance of the pigment at time t.

A set of experiments have been performed to study the catalytic activity of Cu@MWCNT with different pigments at different pH values. The color of the pigments changed with the reaction time (the time varied with different pigments performance). The colors of the pigments are presented in **Table 2-8.**

Table 2-8 Color of the pigments before and after the decoloration catalyzed by Cu@MWCNT component with different pH value.

Pigment	pH=2		pH=7		pH=12	
	Before reaction	After reaction	Before reaction	After reaction	Before reaction	After reaction
brilliant blue						
tartrazine						
amaranth						

methyl violet						

Since we have been constructed a calibration curve for each pigment, we can choose the best concentration for each sample, in the case of the following work, which have been presented in **Table 2-2**. The maximum absorbance wavelength of pigments at different pH values is presented in **Table 2-9**.

Table 2-9 Maximum absorbance wavelength of pigments at studied pH values.

Pigment	λ(pH=2) /nm	λ(pH=7) /nm	λ(pH=12) /nm
Brilliant blue	627	627	627
Tartrazine	431	426	401
Amaranth	521	513	490
Methyl violet	587	583	–

2.3.1 Decoloration of brilliant blue

Brilliant blue FCF is known as a triarylmethane dye. It is a reddish-blue powder; the common application for brilliant blue is the coloring agent for food such as ice cream and packet soups, it also can be used in soaps and mouthwash. In this study, we explored the activity of Cu@MWCNT to catalyze the decoloration of the brilliant blue by the use of H_2O_2 as the oxidant. UV-Vis spectrophotometry was used to track the kinetic study in 120 minutes at different pH values. Since brilliant blue cannot dissolve well at pH=12, we did not test the activity of pigment at pH=12. The UV spectra of the pigment at different pH values are presented in **Figure 2-24**.

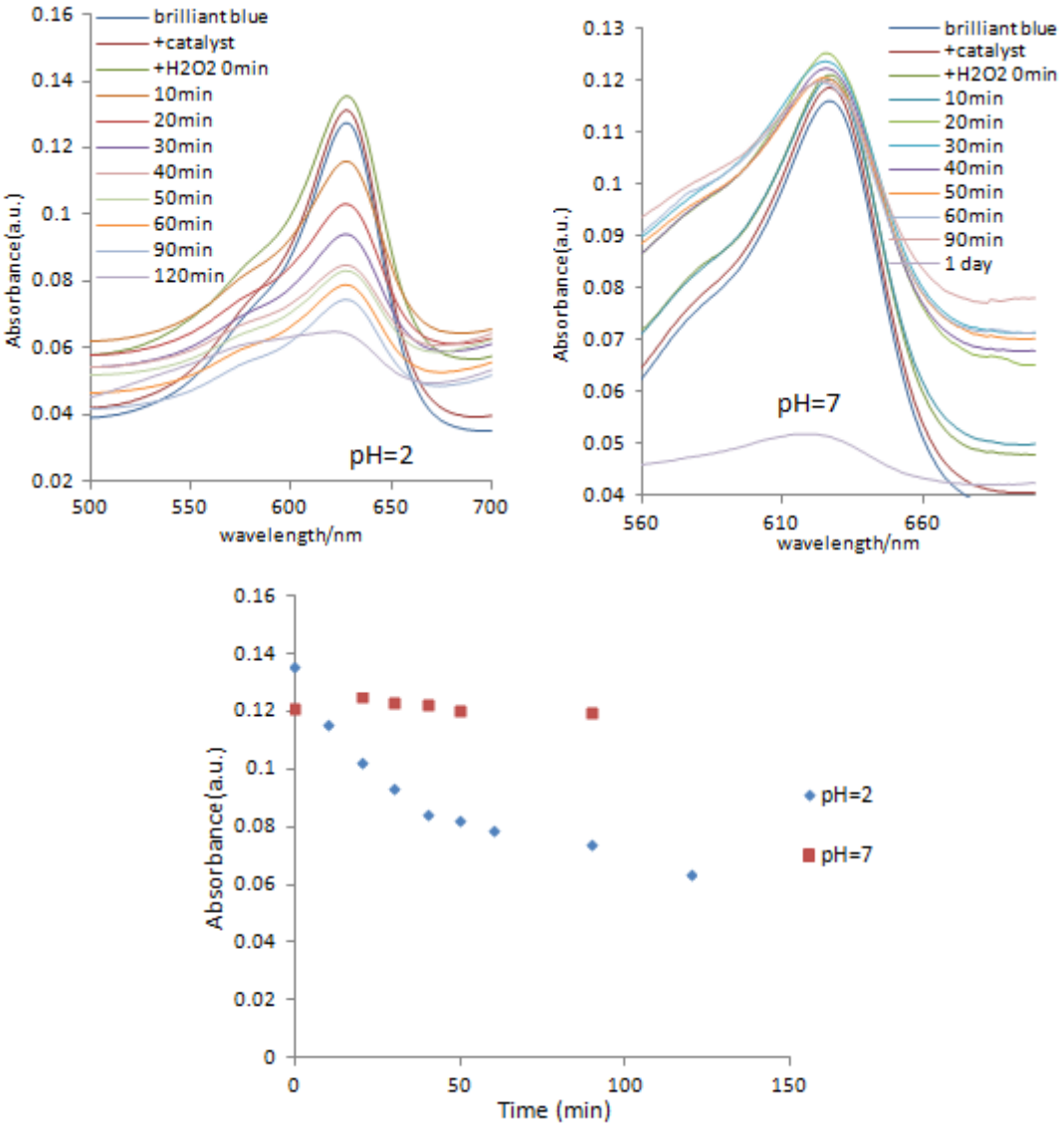

Figure 2-24 The UV-Vis spectrum of brilliant blue catalyzed by Cu@MWCNT in the presence of H_2O_2 as oxidant at pH=2 and 7. Thus the maximum absorption wavelength *vs.* reaction time was plotted at different pH.

It can be observed from **Figure 2-24** that the experimental results are not good enough to use eq. (1) or (2) to determine the constant rate and the decoloration rate, respectively.

2.3.2 Decoloration of Tartrazine

Tartrazine is known as a synthetic lemon yellow azo pigment; it can be used for food coloring. Since it is cheap to produce, and it is more stable than most natural food colorings. Tartrazine is a water-soluble pigment and has a maximum absorbance

at 425 nm. In our study, we use Cu@MWCNT to catalyze the decoloration of pigment tartrazine in the presence of H_2O_2 as an oxidizing agent. UV-Vis spectrophotometer was used to monitor the kinetic study in 36 min at different pH values. The UV spectra of pigment at different pH values are presented in **Figure 2-26**.

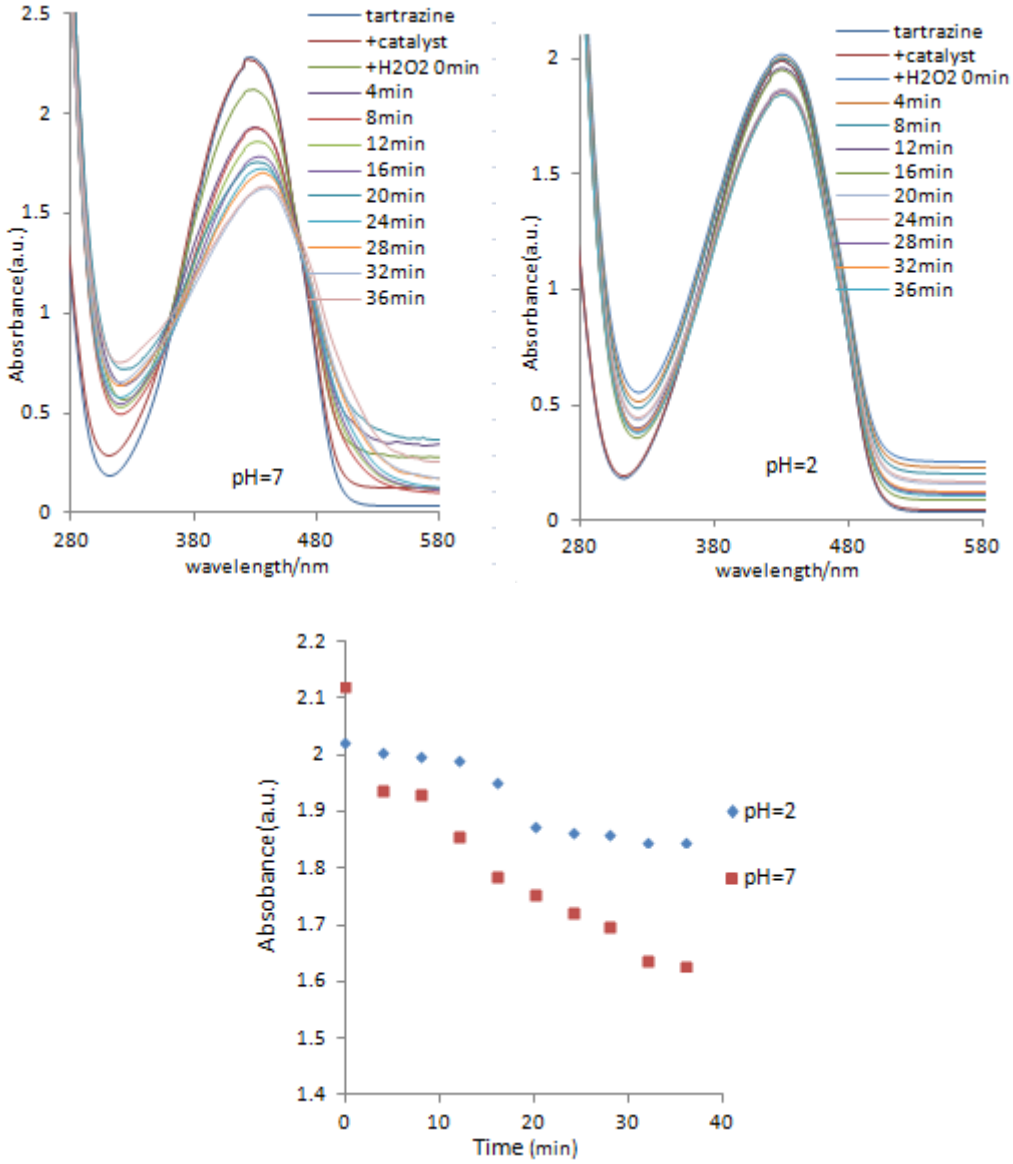

Figure 2-25 The UV-Vis spectrum of tartrazine catalyzed by Cu@MWCNT in the presence of H_2O_2 as oxidant at pH=2 and 7. Thus the maximum absorption wavelength *vs.* reaction time was plotted at different pH.

Figure 2-25 shows the rates for the decoloration of tartrazine using Cu@MWCNT as a catalyst in 36 min reaction at different pH values. The catalyst has good activity at pH=7, and the maximum absorption wavelength shifted from 428 nm to 448 nm, but there is no obvious change in color. While the experimental results are

not good enough to use eq. (1) or (2) to determine the constant rate and the decoloration rate, respectively.

2.3.3 Decoloration of amaranth

Amaranth is a well-known azo pigment, which presented a reddish-rose color from the amaranth plant. It can be used for coloring textile materials, paper and additives for jams. It was used as a hazardous dye since high concentrations of this dye can cause health problems. It is regarded as a water-soluble pigment, and thus hard to remove by using traditional chemical treatment.

In this study, we explored the catalyst Cu@MWCNT to catalyze the decoloration of amaranth by the use of H_2O_2 as the oxidant. UV-Vis spectrophotometry was used to track the kinetic study in 180 minutes at different pH values. The decoloration reaction was carried out directly in 10 mm quartz cell. The UV spectra are shown in **Figure 2-26**.

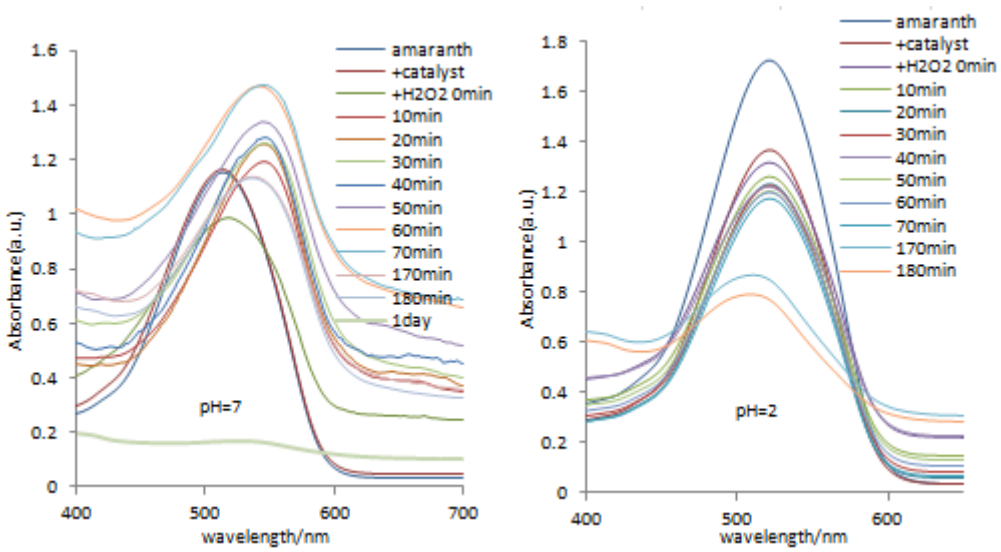

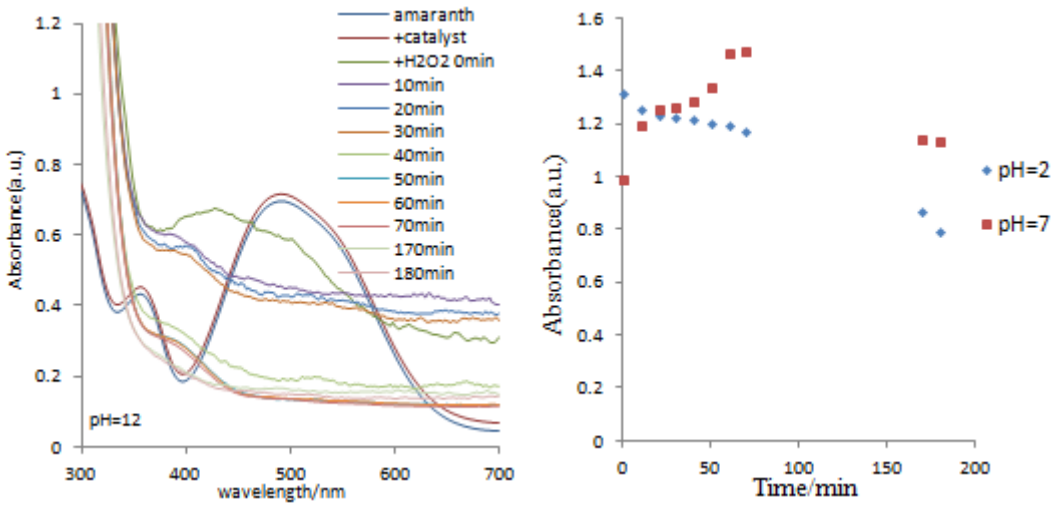

Figure 2-26 The UV-Vis spectrum of amaranth catalyzed by Cu@MWCNT in the presence of H_2O_2 as oxidant at pH=2,7and12. Thus the maximum absorption wavelength *vs.* reaction time was plotted at different pH.

As it can be seen from **Figure 2-26**, the maximum absorption wavelength shifted from 513 nm to 542 nm at pH=2, and the wavelength shifted from 493 nm to 390 nm at pH=12, and slightly shifted from 520 nm to 510 nm at pH=7 after 24 h reaction. In the presence of pH=2, the maximum absorbance decreased from 1.72 to 0.792 after 3 h reaction, while the absorbance decreased to 0.035 after the 24h reaction, and the conversion is 97.9%, the color also changes from reddish to transparent after the 24h reaction, which is presented in **Table 2-13**. In the case of pH=7, the maximum absorbance shifted from 1.15 to 1.13 after the 3h reaction; the conversion is low because the absorbance was increasing from 0 to 70 minutes, and decreasing after 170 min, which means the reagent is not being consumed until 70 minutes. it also can be observed that the absorbance decreased to 0.170 after 24 h reaction, and the conversion is 85.6%, and the color change a lot. For pH=12, a large number of bubbles exists in the quartz cell, in the presence of H_2O_2 in alkaline condition. It is probably the explanation why the curve is not smooth. While the maximum absorbance is decreased from 0.693 to 0.231 after 3 h reaction, and the conversion is 66.8%. While the experimental results are not good enough to use eq. (1) or (2) to determine the constant rate and the decoloration rate, respectively.

2.3.4 Decoloration of methyl violet

Methyl violet is also known as crystal violet. It has six attached methyl groups. The dye is with a blue-violet color when dissolved in water. It is known in medicine, which is the active component in gram stain that used to classify bacteria. It also can be used as a pH indicator, with a range from 0 to 1.6. Methyl violet has been widely used for textile and paper dyeing as well. While more effort is needed to deal with the pollution of the pigment. In this study, we explored the catalyst Cu@MWCNT to catalyze the decoloration of methyl violet with H_2O_2 as the oxidant. UV-Vis spectrophotometer was used to trace the kinetic study in 180 min at different pH values. The UV spectra of the pigment at different pH values are presented in **Figure 2-30**.

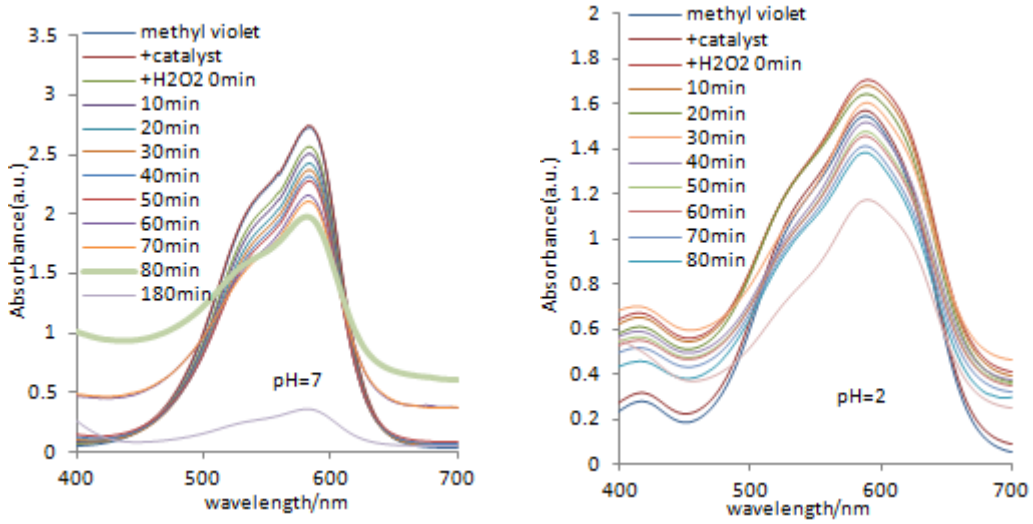

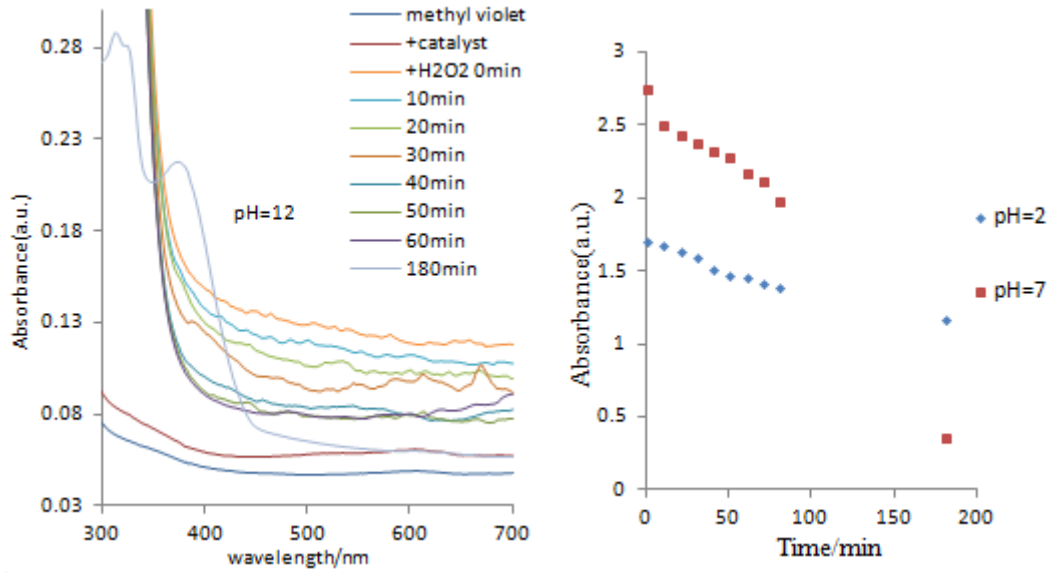

Figure 2-27 The UV-Vis spectrum of amaranth catalyzed by Cu@MWCNT in the presence of H_2O_2 as oxidant at pH=2 ,7 and 12. Thus the maximum absorption wavelength *vs.* reaction time was plotted at different pH.

It can be observed from **Figure 2-27** that the decoloration rate of methyl violet catalyzed by Cu@MWCNT complex. In the presence of pH=12, since the pigment cannot dissolve well in basic condition, so the graph do not have distinct maximum absorption wavelength, and large quantities of bubbles are derived from the decomposition of H_2O_2. Fatema[22] and colleagues have also been found that they cannot check the influence of basic pH on methyl violet pigment decoration in the presence of H_2O_2, the main reason is that crystal violet reacts with OH^- to produce a colorless, non-conjugated form of the pigment. In the case of pH=2, the absorbance decreased from 1.71 to 1.17 after the 3h reaction. Moreover, for pH=7, the absorbance decreased from 2.75 to 0.364. Thus the catalyst has a better activity at pH=7 than at pH=2. However, the experimental results are not good enough to use eq. (1) or (2) to determine the constant rate and the decoloration rate, respectively.

3. Conclusion and future work

Some of the results are reasonable; while most of the results are not acceptable, probably due to non-determined experimental errors, and needed to be repeated in the future work. For example, in the literatures[23-24] the figures regarding the maximum

absorption wavelength *vs.* reaction time that plotted at different pH, mostly they have well linearly coefficient； while in most of the results obtained by me, they did not show acceptable linearly coefficient. Moreover, in my experimental process, the size and the color of Cu-MWCNT component have a significant influence on the absorbance results, which might be the reason why cannot obtain well linearly coefficient； in addition, the results of UV-Vis spectrum of pigments catalyzed by Cu-MWCNT in the presence of H_2O_2 as oxidant at pH=12, all the figures that have been obtained are not good, which appears unsmoothed curve. So more work needs to be done in the future, to solve the problems detected in the presented results.

References

[1]Kang, I.; Heung, Y. Y; Kim, J. H.; et al. Introduction to carbon nanotube and nanofiber smart materials. *Composites Part B.* **2006**, *37*, 382-394.

[2]Nan, C. W.; Liu, G.; Lin, Y.; et al. Interface effect on thermal conductivity of carbon nanotube composites. *Appl. Phys. Lett*. **2004**, *85*, 3549-3551.

[3]Spitalsky, Z.; Tasis, D.; Papagelis, K.; et al. Carbon nanotube–polymer composites: chemistry, processing, mechanical and electrical properties. *Prog. Polym. Sci*. **2010**, *35*, 357-401.

[4]Kim, H. M.; Kim, K.; Lee, C. Y.; et al. Electrical conductivity and electromagnetic interference shielding of multiwalled carbon nanotube composites containing Fe catalyst. *Appl. Phys. Lett*. **2004**, *84*, 589-591.

[5]De, Volder, M. F. L.; Tawfick, S. H.; Baughman, R. H.; et al. Carbon nanotubes: present and future commercial applications. *Science*. **2013**, *339*, 535-539.

[6]Cheng, Z.; Zhong, H.; Xu, J.; et al. Facile fabrication of ultrasmall and uniform copper nanoparticles. *Mater. Lett*. **2011**, *65*, 3005-3008.

[7]Salavati-Niasari, M.; Davar, F. Synthesis of copper and copper (I) oxide nanoparticles by thermal decomposition of a new precursor. *Mater Lett*. **2009**, *63*, 441-443.

[8]Solanki, J. N.; Sengupta, R.; Murthy, Z. V. P. Synthesis of copper sulphide and copper nanoparticles with microemulsion method. *Solid State Sci*. **2010**, *12*, 1560-1566.

[9]Park, B. K.; Jeong, S.; Kim, D.; et al. Synthesis and size control of monodisperse copper nanoparticles by polyol method. *J. Colloid Interface Sci*. **2007**, *311*, 417-424.

[10]Charinpanitkul, T.; Soottitantawat, A.; Tonanon, N.; et al. Single-step synthesis of nanocomposite of copper and carbon nanoparticles using arc discharge in liquid nitrogen. *Mater. Chem. Phys*. **2009**, *116*, 125-128.

[11]Cha, S. I.; Kim, K. T.; Arshad, S. N.; et al. Extraordinary strengthening effect of carbon nanotubes in metal − matrix nanocomposites processed by molecular −

level mixing. *Adv. Mater*. **2005**, *17*, 1377-1381.

[12] Wang, J. Nanocatalysts for sustainable industrial processes. Master thesis in Nanochemistry and Nanomaterials, *University of Madeira*. **2015**.

[13] Wrolstad; R. E. Anthocyanin pigments — Bioactivity and coloring properties. *J. Food Sci*. **2004**, *69*, 419-425.

[14] Yuan, R.; Guan, R.; Shen, W.; et al. Photocatalytic degradation of methylene blue by a combination of TiO_2 and activated carbon fibers. *J. Colloid Interface Sci*. **2005**, *282*, 87-91.

[15] Wang, J.; Sun, W.; Zhang, Z.; et al. Preparation of Fe-doped mixed crystal TiO_2 catalyst and investigation of its sonocatalytic activity during degradation of azo fuchsine under ultrasonic irradiation. *J. Colloid Interface Sci.* **2008**. *320*, 202-209.

[16] Slokar, Y. M.; Le, Marechal, A. M. Methods of decoloration of textile wastewaters. *Dyes and pigments*. **1998**, *37*, 335-356.

[17] Carriazo, J. G.; Centeno, M. A.; Odriozola, J. A.; et al. Effect of Fe and Ce on Al-pillared bentonite and their performance in catalytic oxidation reactions. *Appl. Catal., A*. **2007**, *317*, 120-128.

[18] Singhal, S. K.; Lal, M.; Kabi, S. R.; et al. Synthesis of Cu/CNTs nanocomposites for antimicrobial activity. Adv. Nat. Sci: Nanosci. Nanotechnol. **2012**, *3*, 045011.

[19] Kuo, C. Y. Prevenient dye-degradation mechanisms using UV/TiO_2/carbon nanotubes process. *J. Hazard. Mater*. **2009**, *163*, 239-244.

[20] De, Kreij, A.; Van, den, Burg, B.; Venema, G.; et al. The effects of modifying the surface charge on the catalytic activity of a thermolysin-like protease. *J. Biol. Chem*. **2002**, *277*, 15432-15438.

[21] Al-Degs, Y. S.; El-Barghouthi, M. I.; El-Sheikh, A. H.; et al. Effect of solution pH, ionic strength, and temperature on adsorption behavior of reactive dyes on activated carbon. *Dyes and Pigments*. **2008**, *77*, 16-23.

[22] Alshamsi, F. A.; Albadwawi, A. S.; Alnuaimi, M. M.; et al. Comparative efficiencies of the degradation of Crystal Violet using UV/hydrogen peroxide and Fenton's reagent. *Dyes and Pigments*. **2007**, *74*, 283-287.

[23] Lucas, M. S.; Peres, J. A. Decolorization of the azo dye Reactive Black 5 by Fenton and photo-Fenton oxidation. *Dyes and Pigments*. **2006**, *71*, 236-244.

[24] Sun, J. H.; Sun, S. P.; Wang, G. L.; et al. Degradation of azo dye Amido black 10B in aqueous solution by Fenton oxidation process. *Dyes and Pigments*. **2007**, *74*, 647-652.

UNIVERSIDADE da MADEIRA

ISEL
INSTITUTO SUPERIOR DE ENGENHARIA DE LISBOA

FCT Fundação para a Ciência e a Tecnologia
MINISTÉRIO DA CIÊNCIA, TECNOLOGIA E ENSINO SUPERIOR

União Europeia

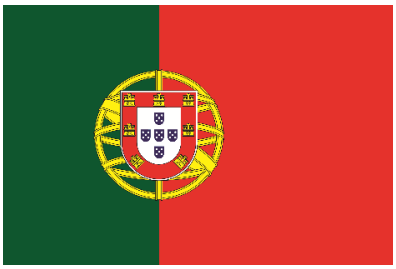

Governo da República Portuguesa

Região Autónoma da Madeira